ADDIS ABABA UNIVERSITY

ADDIS ABABA INSTITUTE OF TECHNOLOGY SCHOOL OF CIVIL AND ENVIRONMENTAL ENGINEERING

Early age thermal cracking tendency assessment on mass concrete (Controlling temperature by pre cooling method)

A thesis submitted to the school of Graduate Studies in Partial fulfillment of the Requirements for the Degree of Master of Science in Civil Engineering (Structures)

By

Elias Aklilu W/Micheal

Advisor: **Dr. Esayas G/Yohannes**

April 2019

ADDIS ABABA UNIVERSITY

ADDIS ABABA INSTITUTE OF TECHNOLOGY SCHOOL OF CIVIL AND ENVIRONMENTAL ENGINEERING

Early age thermal cracking tendency assessment on mass concrete (Controlling temperature by pre cooling method)

A thesis submitted to the school of Graduate Studies in Partial fulfillment of the Requirements for the Degree of Master of Science in Civil Engineering (Structures)

By

Elias Aklilu W/Micheal

April 2019

Esayas G/yohannes (Dr.)	_____	_____
Advisor	Signature	Date
Adil Zakaria (Dr.)	_____	_____
Internal Examiner	Signature	Date
Girma Z/Yohannes (Dr.)	_____	_____
External Examiner	Signature	Date
_____	_____	_____
Chairman	Signature	Date

DECLARATION

I, the undersigned, declare that this thesis is my original work and has not been presented for a degree in any other university and that all sources of material used for the thesis have been duly acknowledged.

Candidate

Name: Elias Aklilu

Signature:

Addis Ababa Institute of technology

(AAiT)

Date of Submission: April, 2019

Acknowledgement

First of all, glory to the almighty God for helping me on every aspect during my stay at the University and for the completion of the thesis. I would like to thank my advisor Dr. Esayas G/Yohannes for his guidance and continuous support during our meetings and discussions. Further, I would like to thank my colleagues in electric power supervision team for their wonderful and substantial assistance during field experiment work. Finally, I would like to express gratitude and sincere thanks to my wife Henon for her unlimited patience, understanding, encouragement, and love during my graduate program study.

Contents

List of Figures

List of Tables

List of Appendix

List of Symbols

a	Rate of hydration
λ	conductivity of concrete
β	the surface conductance
c	specific heat of concrete
ρ	the density of concrete
T	Temperature
θ	Adiabatic temperature rise
t	Time
t_e	equivalent maturity time
Q	Heat emitted by the hydration of cement
R	degree of restraint
V	Poisson′s ratio of concrete
Eo	Elastic modulus of concrete
fto	Tensile strength of concrete
fc	Compressive strength of concrete
W	Weight of concrete materials
PT	placement temperature
CAM	Cylindrical axisymmetric mass concrete structure
MW	Massive wall
RCB	Reference concrete block

ABSTRACT

Thermal dilation and autogenous shrinkage are produced by the continued hydration of cement, this volume changes are partly or wholly restrained, and therefore they induce stress. This is issue for massive concrete especially at early age when concrete is immature. This thesis presents assessment on the tendency of cylindrical axisymmetric strictures and massive wall at early age with multiple thickness and placement temperatures. This master thesis focuses on assessment of cracking tendency of massive concrete structures which are subjected to realistic field temperature boundary conditions at early age. The assessment is based on the analysis results of analytical models. This work also shows the efficiency of precooling method in controlling of temperature differential and cracking tendency structures by comparing with reference placement temperature (placement temperature without introducing pre cooling).

At early age, the core of thin sections of mass concrete structures have high tendency of cracking. The reason is that the high temperature drops of the core during cooling phase. Cracking tendency at cores of thin sections is high at high placement temperature. This susceptibility of cracking of thin section structures are controlled by precooling method. Similarly surface of mass concrete structures are susceptible for cracking at early age in moderately hot weather. The tendency of surface cracks can be significantly minimized by reducing the placement temperature but for thick sections precooling method should combined with other temperature differential controlling methods (e.g. surface insulation) to minimize surface early age cracking tendency.

KEYWORDS: *MASSIVE CONCRETE STRUCTURES, HYDRATION HEAT, SHRINKAGE, THERMAL DILATION, YOUNG CONCRETE, PRE COOLING, PLACEMENT TEMPERATURE, TEMPERATURE REDUCTION, CRACK RISK.*

1. Introduction

Significant tensile stress may develop from the volume change associated with the increase and decrease of temperature within the mass concrete. Measures should be taken where cracking due to thermal behavior may cause loss of structural integrity and monolithic action, or may cause excessive seepage and shortening of the service life of the structure, or may be esthetically objectionable.

Early age cracking originates either from internal restraint (due to temperature gradients inside the young concrete during heating, which may result in surface cracking and deep cracks) or by restraint from the adjacent structure during the contraction phase. They are different principal construction practices used to control temperature gradient with in mass concrete including precooling of materials, post-cooling of in-place concrete by embedded pipes, and surface insulation.

Pre-cooling system mainly consists in reducing the amount of heat generated by cement by cooling concrete component in order to minimize the concrete temperature at casting. Same time cooling concrete materials alone are used to reduce placement temperature if strength of concrete at early age is a concern.

The aim of this study to show early age thermal cracking tendency of mass concrete and evaluating efficiency of cooling concrete components in reduction of temperature differential and cracking tenancy. In this study analytical model of Cylindrical axisymmetric mass concrete (CAM) and massive wall are used. Cylindrical axisymmetric mass concrete structure can be classed as a solid of revolution where geometry, elastic properties, loads, and supports are all axisymmetric and nothing varies with circumferential coordinate, materials point displace only in radial and axially. Thus the analysis problem is mathematically two dimensional. Massive wall (MW) with 4.5 m height and 8 m length is analytically modeled with varying thickness. Models are analyzed using real thermal boundary conditions from experimentally validated field reference block.

Generally, this thesis deals with early age thermal cracking tendency assessment in mass concrete and controlling temperature differentials with precooling method.

1.1 Background

Mass concrete

Mass concrete" is defined in ACI 116R as "any volume of concrete with dimensions large enough to require that measures be taken to cope with generation of heat from hydration of the cement and attendant volume change to minimize cracking." The design of mass concrete structures is generally based on durability, economy, and thermal action, with strength often being a secondary concern. Since the cement-water reaction is exothermic by nature, the temperature rise within a large concrete mass, where the heat is not dissipated, can be quite high. Significant tensile stress may develop from the volume change associated with the increase and decrease of temperature within the mass. [1]

The main difference between mass concrete and all other concrete types is its thermal behavior. Mass concrete is a type of concrete used mainly for incrementally constructed dams. [2]

Early age

There is no precise definition of early age and the term can be used to embrace the first hours, the first days or, in certain cases, even the first week. This is because the mechanical and durability property of concrete dependence on different factors. Generally, the concrete develops measurable strength after t_o as shown in figure 1.1

Thermal cracking

Concrete has volume instability property. The volume instability, in the early-age is mainly caused by temperature dilation and autogenous shrinkage effects, and there are several parameters that affect these two mechanisms. The main phenomenon causing early age cracking is volume change due to the variable moisture and temperature state in the concrete. [3]

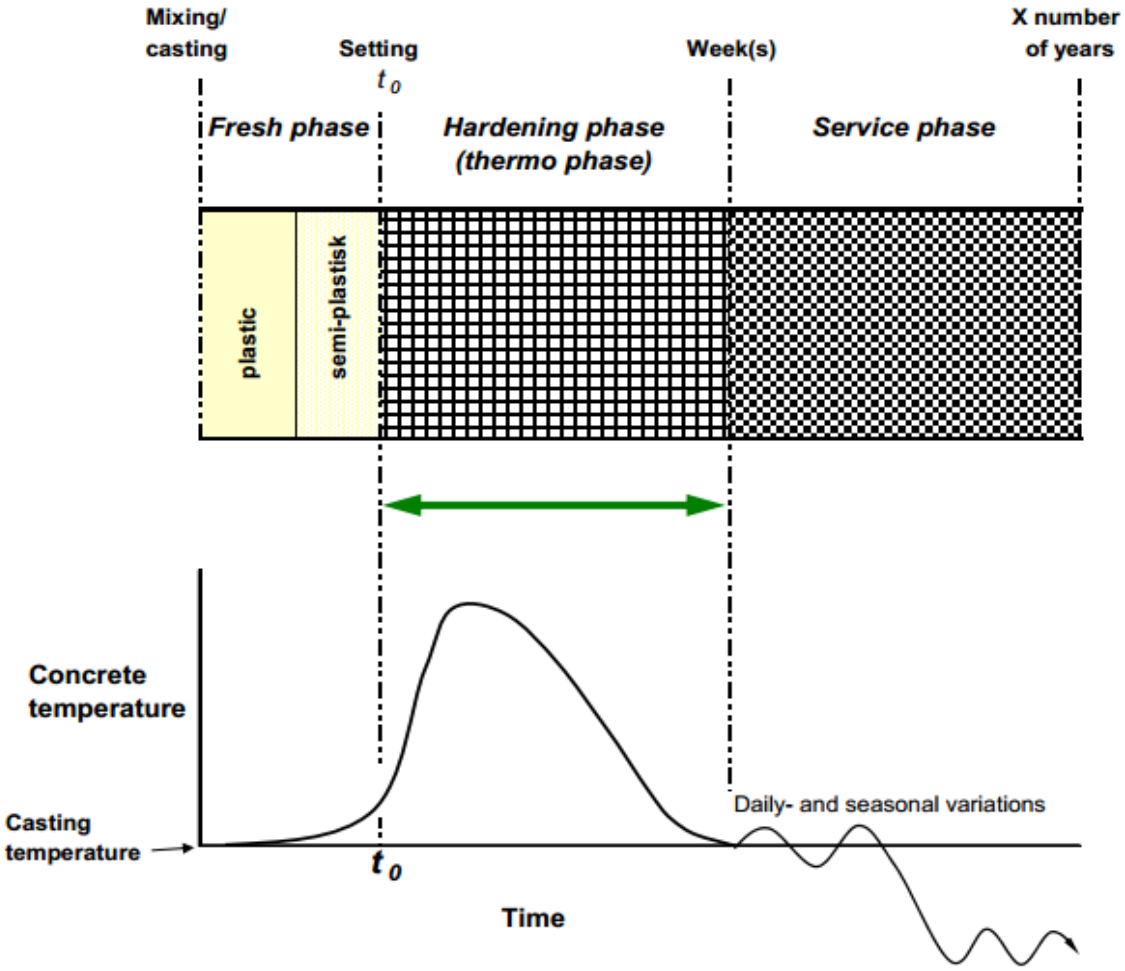

Figure1. 1Different phases of concrete – schematic diagram.

Concrete ingredients pre cooling method

There are various technical measures to prevent cracking of mass concrete, such as choice of raw materials, precooling, pipe cooling, and superficial thermal insulation. Pre-cooling system mainly consists in reducing the amount of heat generated by cooling concrete component in order to minimize the concrete temperature at casting.

1.2 Statement of the problem

Mass concrete is susceptible for cracking at early age which can affect the integrity of structures and aesthetically objectionable. In construction site, materials are not properly placed in shaded area and absorb heat directly from sun and surrounding. This material temperature increases cause the casting temperature to increase. Such scenarios are not considered in design or left

unchecked. Due to this thermal cracking of mass concrete increased. It is important to minimize early age cracking of mass concrete structures by using temperature controlling method to avoid this problem. Therefore, it is very important to carryout assessment on early age thermal cracking tendency of mass concrete structures and controlling the temperature differentials using cost effective way in moderately hot weather.

Figure1. 2 Equipment support foundation (0.8 m thick) cracking at top exposed surface and side surface.

1.3 Objective

1.3.1 *General objective*

The main aim of the study is to make early age thermal cracking tendency assessment in mass concrete and controlling temperature differentials by precooling method to avoid cracking of the core and surface of structures.

Another aim of this thesis is to evaluate the efficiency of concrete ingredient cooling method in reduction of temperature differentials and cracking tendency at early age of mass concrete structure.

1.3.2 Specific objective

Temperature evolution stress history and early age cracking tendency of field concrete will be compares with finite element model with different placement temperature and size. It quantitatively compares the peak temperature with different placement temperature and size for Cylindrical axisymmetric mass

concrete (CAM) and massive wall (MW) model. Efficiency of cooling concrete components in reduction of cracking tendency is evaluated based on temperature placement at field without Appling cooling method.

1.4 Scope of the study

This study is limited to analysis of mass concrete only cylindrical axisymmetric mass concrete and massive wall. The sizes of those structures are limited to maximum of 5.15 m diameter and 2.5 m thick in both types of structures respectively. Keeping the material strength, material property, boundary conditions (temperature, heat, and displacement) and design parameters the same, early age thermal cracking tendency of that structure at early age was study. The efficiency of precooling in controlling of cracking tendency also investigated by comparing with the efficiency reference placement temperature (placement temperature without applying precooling method)

1.5 Methodology

Study on two field reference concrete blocks which are built at multiple placement temperatures and two different ambient temperatures are used to validate thermal analysis of analytical models. Thermal boundary condition of Reference concrete block1 (RCB-1) and placement temperature are taken as real thermal boundary condition for simulation of finite element models of Cylindrical axisymmetric mass concrete (CAM) and massive wall (MW). Experimental study of RCB-1 was done in moderately hot weather. During Simulation reduction of placement temperature to 26 ^{o}C, 20 ^{o}C and 9 ^{o}C was considered. Selection of placement of temperature reduction was done by considering the average air temperature (22 ^{o}C) of field of the study. This means placement temperatures above and below 22 ^{o}C was considered. Assumptions, parameters, modeling procedures are adopted from literatures and presented in chapter 2 to clarify the analysis which is carried out in chapter 4. Geometry of Cylindrical axisymmetric mass concrete (CAM) and massive wall (MW) models used in the analysis are summarized below.

Table1. 1 Summary of simulated analytic models

Structure	DIMENSIONOF STRUCTURE			Placement Temperature(TP-°C)			
	Height	Diameter					
Axi-symmetry mass concrete foundations	1	1.03		33	26	20	9
	2	2.06		33	26	20	9
	3	3.09		33	26	20	9
	4	4.12		33	26	20	9
	5	5.15		33	26	20	9
	Height	Length	Thickness				
Massive wall	4.5	8	0.5	33	26	20	9
	4.5	8	1	33	26	20	9
	4.5	8	1.5	33	26	20	9
	4.5	8	2	33	26	20	9
	4.5	8	2.5	33	26	20	9

2. Literature study

2.1 Kinds of Thermal Stress

The thermal stress is closely related to the type of structure, the weather conditions, the construction process, the properties of material, and the operating conditions. The variation of thermal stress is very complicated. It is more complex to analyze the thermal stress than the stresses caused by water, self-weight, and other external loads.[4]
There are two kinds of thermal stress in mass concrete:

2.1.1. Self-stress

For structures without any external constraint or statically determinate structure, if the internal temperature is linearly distributed, no stress will appear; if the internal temperature is nonlinearly distributed, the stress caused by restraint of the structure itself is called self-stress. For instance, when a concrete wall is cooled in the air, the surface temperature is low and the inner temperature is high. The shrink of the surface is restrained by the inner concrete. The tensile stress appears at the surface, and the compressive stress appears in the interior. At any section, the area of tensile stress must be equal to the area of compressive stress, as shown in figure 2.1

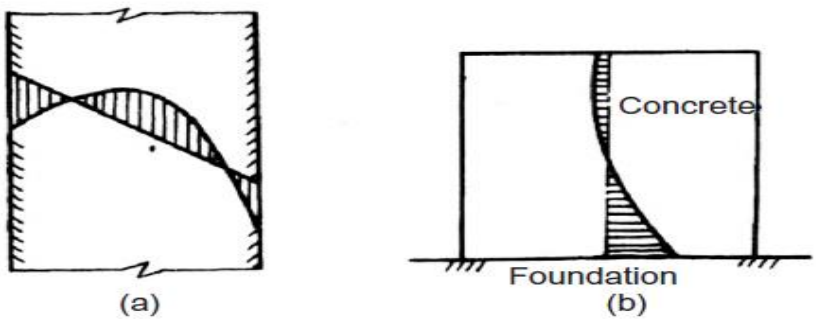

Figure2. 1 Sketch of two types of thermal stress: (a) self-stress and (b) restraint stress.

2.1.2 Restraint stress

When the whole or part of the boundaries of the structure is restrained, the structure cannot deform freely with the change of temperature. The stress

produced by this reason is called restraint stress, for instance, the stress in a concrete block caused by the restraint of the rock foundation when the concrete is cooling as shown in Figure 2.1(b). In the statically determinate structure, only self-stress will appear, but in the statically indeterminate structure, both self-stress and restraint stress will appear. [4]

2.2 Early age thermal cracking of mass concrete

Cracking can occur when the concrete residual stress exceeds the concrete tensile strength. In general the cracks in mass concrete can be classified into three kinds, namely through cracks, deep cracks and surface cracks.

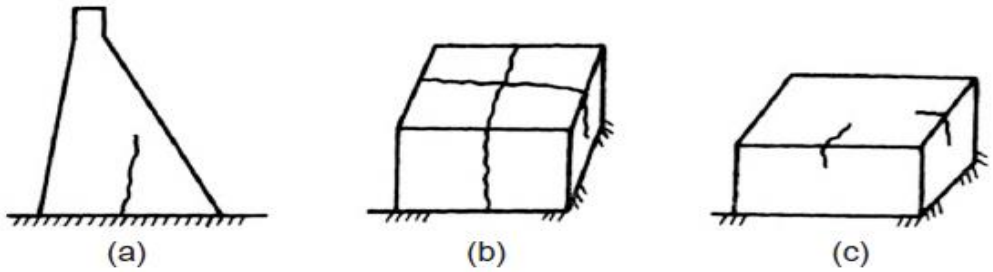

Figure2. 2 Sketch of different kinds of cracks in a massive concrete structure: (a) through crack, (b) deep crack or surface crack, and (c) surface crack. [4]

2.2.1 Surface crack

Stresses in concrete develop when its volume changes are restrained internally and/or externally. Temperature gradients over the concrete cross-section give differential thermal strain and internal restraint. When the formwork is removed from a hot structural element, there is rapid cooling (contraction) of the surface, see Figure 2.3. This contraction is restrained by the core and results in tensile stresses that can result in surface cracks.

Tensile stresses and surface cracks may also occur during the heating phase (even with formwork) if the surface temperature lags behind the core temperature due to heat loss through the formwork. Typical damage due to internal restraint is indicated at the top of the wall in Figure 2.4. (See ‘Expansion phase’). [3]

Surface cracks can also initiate through cracks, which would not develop otherwise. Hence, crack risks concerning early surface cracks are in the

regulations considered equally harmful as later through cracks with respect to the ratio of tensile stress to the momentary tensile strength.[9]

2.2.2 Later through crack and Deep cracks

Through cracks generate over the entire cross section as a result of restraint from the adjacent existing structural concrete or subgrade. Deep cracks partly cut the structure, and they are also dangerous. Surface cracks in a region above foundation or old concrete can develop to deep cracking. Depending on dimensions and other prevailing conditions, the cracks may appear weeks, months and in extreme cases even years after a section has been poured. The critical time period for later through cracks starts from the point of “zero stress” shortly after the temperature maximum in Figure 2.3 (b), and continues until cracking appears or to the maximum tensile stress to tensile strength ratio is reached. Restraint situation plays a significant role for the stress and thereby for the formation of later through cracks. [5]

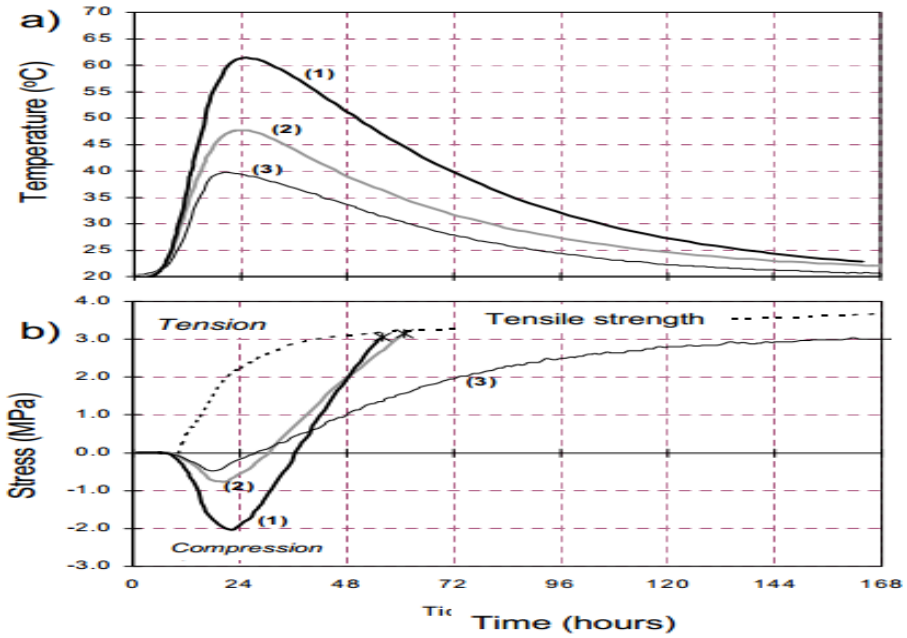

Figure2. 3 (a) Measured (and imposed) temperature, and (b) stress development in laboratory tests on 100% restrained concrete specimens. [3]

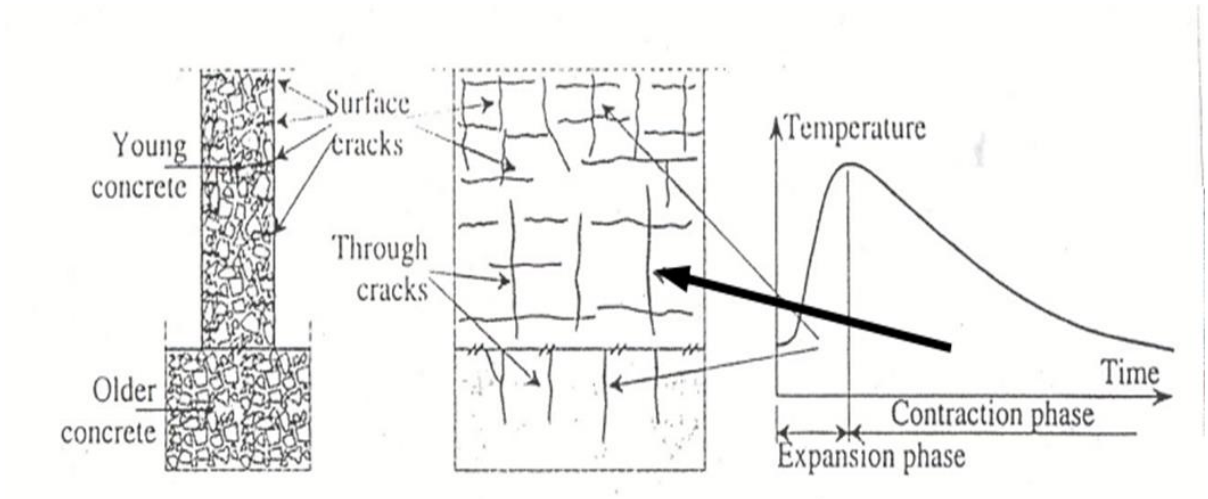

Figure2. 4 Example of cracking in a concrete wall due to internal and external restraint [3]

2.3 Driving force for early age cracking

According to (Bjøntegaard 2011), the main driving forces that create early age cracking are the thermal dilation and autogenous shrinkage. The response of adjacent structures and response of the material itself are another factor for early age cracking of concrete. In practice volume changes due to thermal dilation and autogenous shrinkage are usually partly or wholly restrained, and therefore they induce stresses.

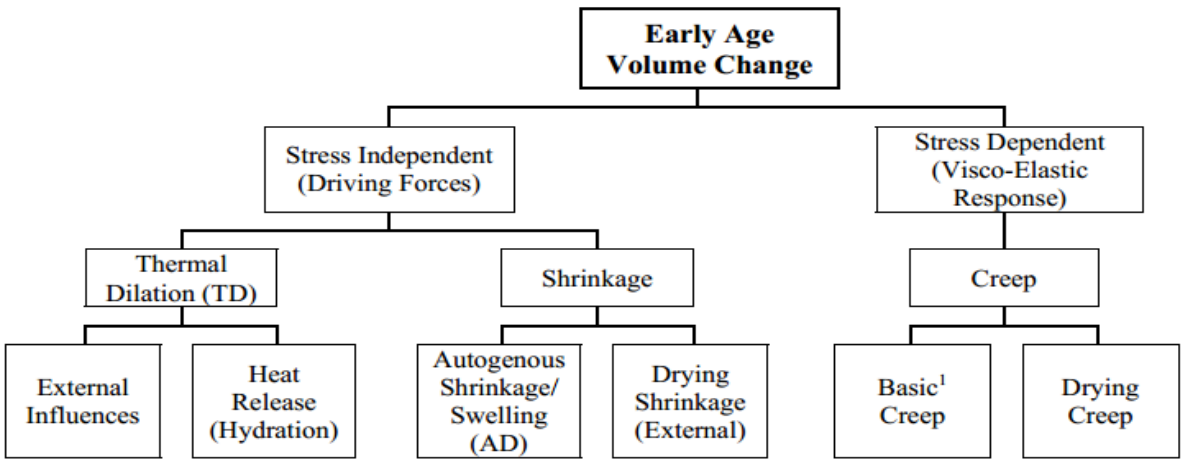

Figure2. 5 Phenomenological summary of early age volume change.

If the temperature of the concrete is constant (isothermal conditions), autogenous shrinkage operates alone, while under normal conditions where the

temperature varies, thermal dilation and autogenous shrinkage operate simultaneously to produce stresses.

2.3.1 Thermal dilation

The thermal dilation is induced by the temperature rise caused by hydration reactions and is proportional to the coefficient of thermal Expansion. The thermal dilation is in most cases the most important factor when it comes to build up of restraint stresses in concrete structures at early ages. [3]

For short-time loading, the ultimate tensile strain is about (0.6-1.0) $x10^{-4}$, which is equal to the strain caused by 6^{o}C-10 ^{o}C temperature drop. For long-time load, the ultimate tensile strain is about (1.2-2.0) $x10^{-4}$. [4]

2.3.2 Autogenous Shrinkage

ACI 116R defines autogenous deformation as “change in volume produced by the continued hydration of cement, exclusive of the effects of applied load and change in either thermal condition or moisture content. Autogenous deformation is a consequence of chemical shrinkage: the absolute volume of hydration products is less than the total volume of the reactants (cement and water).

2.4 Property of Early age concrete

2.4.1 Hydration of cement

Heat generated in the concrete due to the cement hydration. Cement is a manufactured product with lime, gypsum, silica and alumina, where the main chemical component is calcium silicate. Calcium silicate is the unique source of strength during the hydration process. In Portland cement, there are approximately 50 % of tricalcium silicate (Ca_3SiO_5) and 25 % of dicalcium silicate (Ca_2SiO_4), depending on the type of cement that is used. Both tricalcium and dicalcim silicate generate significant heat while reacting with water. The tricalcium silicate and the dicalcium silicate produce about 173.6 kJ/kg and 58.6 kJ/kg of energy respectively.

2.4.2 Degree of hydration

The strength of the concreted develops during the hydration process, which consists of several simultaneous chemical reactions. To obtain measure of how far the reactions have developed, the quantity degree of hydration α is introduced. The degree of hydration has the interval (0,1) where α = 0 implies that no reaction between the cement and water has occurred. For α = 1 theoretically all cement has hydrated, however, in practice full hydration is never achieved as the dense microstructure restricts the water from the cement particles.

Hydration process is dependent on temperature, it is reasonable to introduce the quantity equivalent maturity time t_e which facilitates the comparison of hydration processes during different thermal conditions. The equivalent maturity time t_e is defined by the integral.

$$\text{te} = \int_o^t e^{\theta\left(\frac{1}{T}-\frac{1}{Tref}\right)} dt \qquad (2.1)$$

The maturity is expressed as the equivalent age, which is the actual curing age t [hour] of a concrete cured at any temperatures T [Kelvin] converted to an equivalent curing age t_e [hour] for a specimen cured at a specific reference temperature T_{ref}, normally 293 Kelvin (20 ^{0}C).

Degree of hydration could be expressed as

$$\propto = e^{-\lambda \ln\left(1+\frac{te}{t1}\right)^{-k1}} \qquad (2.2)$$

For various cement types, measurements have been made where the fitting parameters λ_1, t_1 and k_1. For different cement types, the hydration procedure is different and the fitting parameters are therefore unique for each cement type. [6]

2.4.3 *Influencing factors of rate of Hydration process*

The rate of heat generation (Q) is affected by the cementations materials, mixing proportion, curing, and also initial temperature. The amount of heat lost or gained as governed by the size of the member and exposure conditions affects the hydration temperature. Different investigations shows factors affecting hydration temperature affect the development of concrete strength (janByfors).

(A) Influence Cement type (chemical composition of cement and fineness)

C_3S is the clinker component which gives the main contribution to hydration at an early age, the quantity of C_3S in the clinker is 55-65 % ordinary cements. If the hydration sequence for C_3S is affected by the chemical composition of cement the hydration will be affected. For example, the gypsum mixed in to the cement so as to prevent what is known as false setting. This gypsum also affects C_3S. An increase the amount of gypsum mixed in to the cement normally speeds up the process for the early silicate reactions. Although with the amount of gypsum over 2-3% the early reaction rate may decrease. The following factors increase the rate of reaction at an early age. [janbyfors (1980)],

- Increased C_3S content
- Increased C_3A content
- Increased quantity of gypsum (optimum exists)
- Increased alkali content

Fineness of cement also affects the hydration process. The finer the particle sizes the larger the surface which can react simultaneously with water.

(B) Influence of Water-cement ratio

The reason why the degree of hydration increases when the water-cement ration increases for hardening concrete is that low water- cement ratio means a dense cement paste. The denser the cement paste the more difficult it is for the water to penetrate to the point of reaction. The influence of the water-cement ratio at an early age is reversed but small.it should be reasonable to assume that the effect of water-cement ratio does not affect the hydration process at an early age.

(C) Influence of temperature

An Increase in the temperature increases the rate of reaction. The initial rate of reaction is affected by temperature increases [janbyfors(1980)]

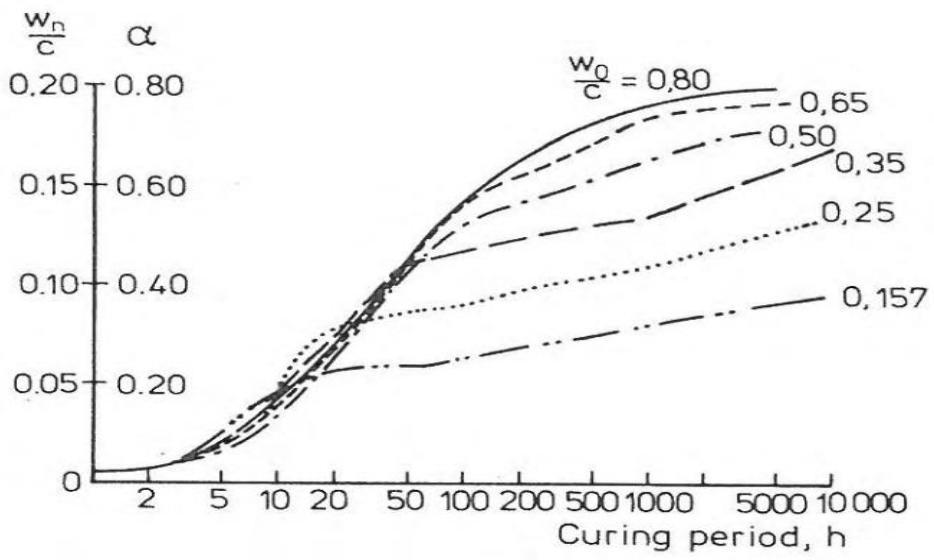

Figure2. 6 Effect of w_o/c on the hydration process [janbyfors(1980)]

2.4.4 Compressive strength

The compressive strength f_{co}, after hardening for a reference time t_r =672 hr (28 d), at a reference temperature T_r=293K (20 ^{0}C), is often used as measure of the quality of the concrete. The strength f_{c0} depends mainly on the water-cement ratio w_0/C.

$$fc = \eta c f_{co} \tag{2.3}$$

Where:-

$$\eta c = \frac{a_{1c}\left(\frac{t_e}{t_r}\right)^{b_{1c}}}{1+\frac{a_{1c}}{a_{2c}}\left(\frac{t_e}{t_r}\right)^{(b_{1c}-b_{2c})}} \tag{2.4}$$

And the parameters a_{1c}, b_{1c}, a_{2c} and b_{2c} depend on the cement type and the concrete composition. In absence of detailed experimental data on the concrete in question, the parameters may, on the basis of experimental data presented by Byfors[5], be chosen as a_{1c} =10 $^{(3.4\ -1.1w0/C)}$, b_{1c} =2.0; a_{2c} =1.0, and b_{2c} =0.14.

Many research show that [Byfors], there is a linear relation between compressive strength and degree of hydration. This means that factors affecting the hydration process will affect the development of the material properties. For example, an increase in temperature will increase the rate of hydration and, consequently, the strength. [6]

2.4.5 Tensile strength

The growth of tensile strength is mainly influenced by the same factors as those, which influences hydration and the compressive strength. The result presented by many researchers' shows that the tensile strength grows faster than the compressive strength.

The development of the tensile strength f_t may be described in analogy with the growth of the compressive strength described above.

$$f_t = \eta t f_{to} \tag{2.5}$$

Where:-

$$\eta t = \frac{a_{1t}\left(\frac{t_e}{t_r}\right)^{b_{1t}}}{1+\frac{a_{1t}}{a_{2t}}\left(\frac{t_e}{t_r}\right)^{(b_{1t}-b_{2t})}} \tag{2.6}$$

And $f_{to}$is the tensile strength at time $t_e = t_r$. An estimation of the value of f_{to} can be obtained by the relation

$$f_{to} = f_{t1}\left(\frac{f_{co}}{f_r}\right)^{\frac{2}{3}} \tag{2.7}$$

and the parameters a_{1t}, b_{1t}, a_{2t} and b_{2t} depend on the cement type and the concrete composition. In absence of detailed experimental data on the concrete in question, the parameters may, on the basis of experimental data presented by Byfors[5], be chosen as $a_{1t} = 10^{(6\ -2.0w0/C)}$, $b_{1t} = 3.0$; $a_{2t} = 1.0$, and $b_{2t} = 0.14$.[6]

2.4.6 Elastic strain

During hardening, the elasticity properties change. The growth of the elastic modulus E during hardening may be described in the same manner as the development of the compressive strength fc has been described by Byfors[5], i.e

$$E = \eta c\ E_o \tag{2.8}$$

Where:-

$$\eta c = \frac{a_{1E}\left(\frac{t_e}{t_r}\right)^{b_{1E}}}{1+\frac{a_{1E}}{a_{2E}}\left(\frac{t_e}{t_r}\right)^{(b_{1E}-b_{2E})}} \tag{2.9}$$

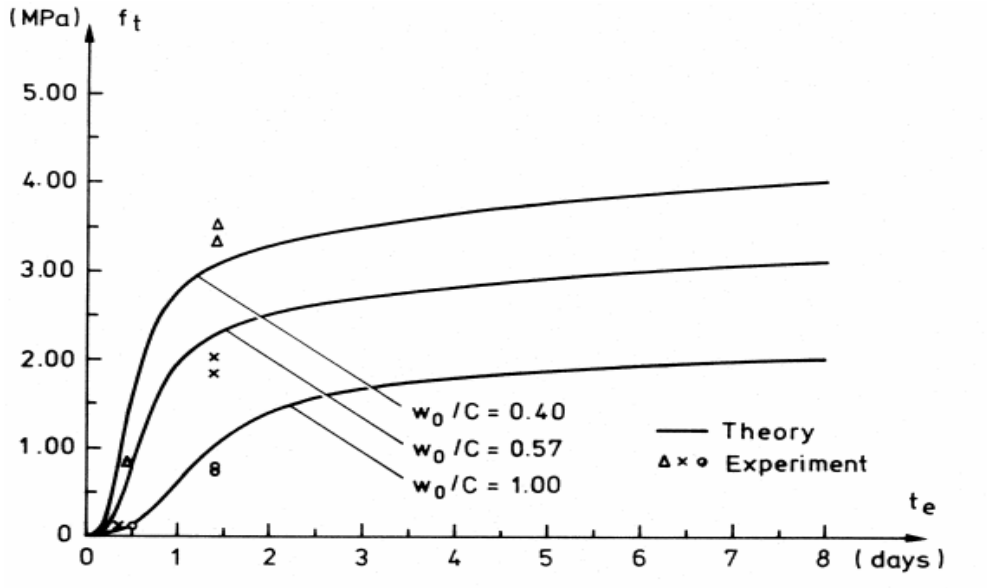

Figure2. 7 comparison between Eq (2.14) and experimental data.[Byfors]

E_o is the elastic modulus at time $t_e = t_r$. the parameters a_{1E}, b_{1E}, a_{2E} and b_{2E} depend on the cement type and the concrete composition. With parameters chosen as $a_{1E} = 10^{(6 - 2.0 w0/C)}$, $b_{1E} = 4.0$; $a_{2E} = 1.0$, and $b_{2E} = 0.1$, is compared with experimental data by Byfors [5] in Fig. 2.8.

To get an estimation of the value of E_0 in Eq. (2.15) one may use the relation

$$E_o = E_1 \sqrt{\frac{f_{co}}{f_r}}$$

(2.10)

Where E_1 =6:0GPa and f_r is a reference value, chosen as f_r=1:0MPa

The value of Poisson's ratio decreases rapidly at a very early age, and then increases. This behavior may be described by the relation

$$V = V_1 e^{-\alpha_{1v}\left(\frac{t_e}{t_r}\right)} + V_2\left(1 - e^{-\alpha_{2v}\left(\frac{t_e}{t_r}\right)}\right) \qquad (2.11)$$

Where v_1 and v_2 are the initial and final values of v, respectively, and α_{1v} and α_{2v} ($\alpha_{1v} > \alpha_{2v}$) are parameters which express the influence of hardening.in figure 2.16 Eq.(2.18), with v_1 = 0:5, v_2 = 0:25, α_{1v} = 150, and α_{2v} = 40, is illustrated and compared with experimental data according to Byfors [5].

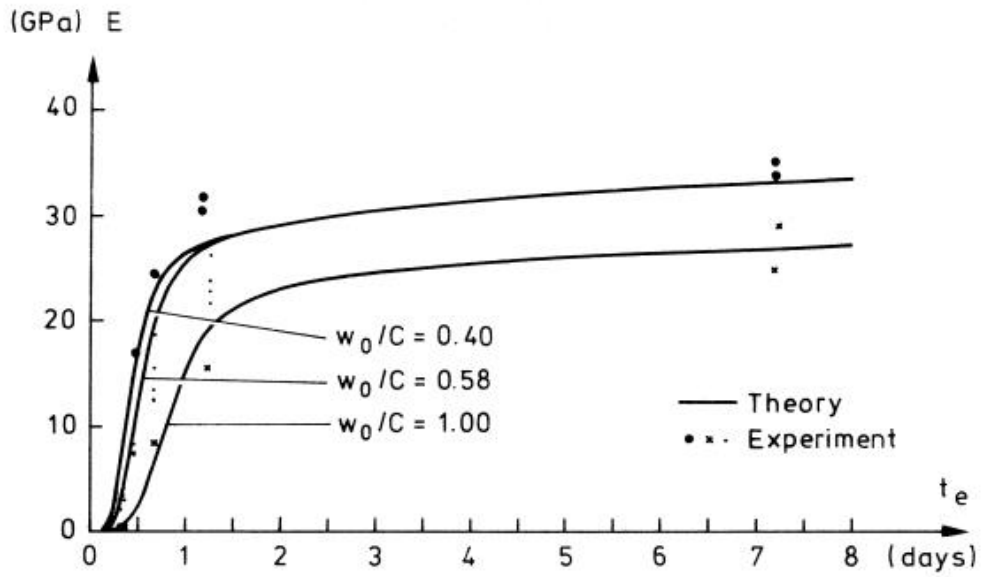

Figure2. 8 Comparison between Eq. (2.19) and experimental data according to [5]

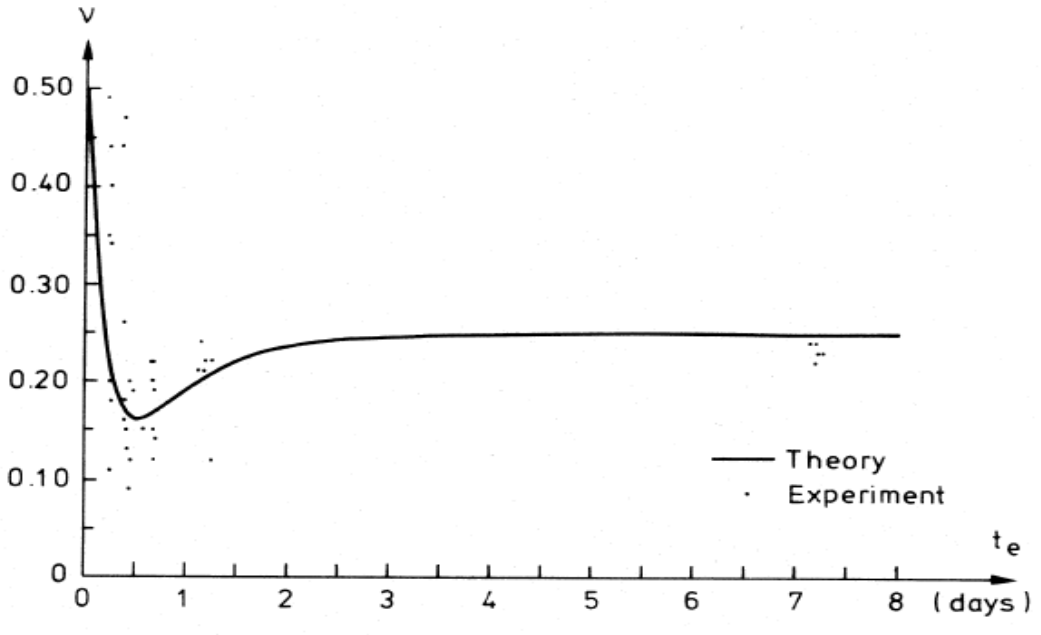

Figure2. 9 Comparison between Eq. (2.18) and experimental data according to Byfors[5].

2.5 Pre cooling System

2.5.1 Need for temperature control

The main aim of controlling temperature is to avoid crack or preventing structures from cracking. To prevent cracks, we must control the thermal stress so that it does not exceed the allowable tensile stress. To prevent crack, the following three aspects should be considered:

1. Control temperature difference ΔT
2. Minimize the restraint coefficient R
3. Enhance the tensile strength (f_{ct}).

Cooling and insulating systems are used to control the temperature changes (ΔT) which occur in concrete structures. The principal construction practices used to control maximum temperature and temperature difference are precooling of materials, post-cooling of in-place concrete by embedded pipes, and surface insulation. Supplementary cementious materials are also used to control maximum temperature.

2.5.2 Thermal shock.

The interior of most concrete structures, with a minimum dimension greater than about 2 ft (0.6 m) will be at a temperature above the ambient air temperature at the time forms are removed. At the boundary between the concrete and the forms, the concrete temperature will be but above that of the air. When the forms are removed in that instance the concrete is subjected to a sudden steepening of the thermal gradient immediately behind the concrete surface.[8]

2.5.3 Precooling of concrete materials

Temperature control method for concrete dams based on cooling pipes and dividing the dam into concrete blocks which are grouted after complete cooling of concrete. This method had been successfully used to build the Hoover Dam in the 1930s. However, this method also has some disadvantages: formwork, cooling pipes, and joint grouting required more man power and increase the cost.[4]

Precooling and post-cooling have been used in combination in the construction of some massive structures such as Glen Canyon Dam, completed in 1963, Dworshak Dam, completed in 1975.[8]

Concrete components can be precooled in several ways. The batch water can be chilled or ice can be substituted for part of the batch water. Aggregate stockpiles can be shaded. Aggregates can be processed and stockpiled during cold weather. Fine aggregates can be processed in a classifier using chilled water. Methods for cooling coarse aggregates, which provide the greatest Potential for removing heat from the mixture, can range from sprinkling stockpiles with water to provide for evaporative cooling, spraying chilled water on aggregates on slow-moving transfer belts, immersing coarse aggregates in tanks of chilled water, blowing chilled air through the batching bins, to forcing evaporative chilling of coarse aggregate by vacuum. While the most common use of nitrogen is to cool the concrete in the mixer, successful mixture cooling has resulted from nitrogen cooling of aggregates and cooling at concrete transfer points.[8]

Chilled batch water

One kg of water absorbs 4.18 kJ when its temperature is raised 1 ^{o} C. A unit change in the temperature of the batch water has approximately five times the effect on the temperature of the concrete as a unit change in the temperature of the cement or aggregates. This is due to the higher specific heat of water with respect to the other materials.[8]

Using ice as batch water

One kg of ice absorbs 334 kJ when it changes from ice to water; thus, the use of ice is one of the basic and most efficient methods to lower concrete placing temperatures. It is important that all of the ice melts prior to the conclusion of mixing and that sufficient mixing time is allowed to adequately blend the last of the melted ice into the mix. Where aggregates are processed dry, this may mean adding no more than 3/4 of the batch water as ice. Where aggregates are processed wet, there will normally be enough moisture on the aggregates to permit almost all of the batch water to be added as ice with just enough water to effectively introduce any admixtures. [8]

Aggregate Cooling

The temperature of the mixed concrete is influenced by each component of the mixture and the degree of influence depends upon the individual component's temperature, specific heat, and proportion of the mixture. Because aggregates comprise the greatest part of a concrete mixture, a change in the temperature of the aggregates will affect the greatest change (except where ice is used). Under the most severe temperature conditions of construction, the objectives of a comprehensive temperature control program cannot be achieved without some cooling of the concrete aggregates.[8]

Liquid nitrogen

To promote greater cooling of the concrete, liquid nitrogen is injected into the water in a specially designed mixer just prior to the water entering the concrete mixer, whereby the liquid nitrogen causes a portion of the water to freeze. The amount of ice produced can be varied to meet different temperature requirements.[8]

Cooling cement

Cement is relatively small portion of mass concrete mixtures, its initial temperature has little effect on the concrete temperature. Also, cooling the cement is not very practical or economical.[8]

2.5.3 Mixing Temperature of Concrete—T0

The mixing temperature is the temperature of concrete at the exit of mixer after mixing which is computed by. [4]

$$To = \left(\frac{(C_s+C_w q_s)W_s T_s+\left(C_g+C_w q_g\right)W_g T_g +C_c W_c T_c \ +C_w\left(W_w-q_s W_s-q_g W_g\right)T_w+H_c}{C_s W_s+C_g W_g+C_c W_c+C_w W_w}\right) \qquad (2.12)$$

Where

To —the mixing temperature of concrete

c_s, c_g, c_c, c_w—the specific heat of sand, gravel, cement, and water

q_s, q_g—the water content (%) of sand and gravel

W_s, W_g, W_c, W_w—the weight of sand, gravel, cement, and water in 1 m^3 of concrete

T_s, T_g, T_c, T_w—the temperature of sand, gravel, cement, and water

H_c—the mechanical heat (kJ/m^3) produced in the mixing process.

The mechanical heat H_c is given by the following formula:

$H_c = 542Pt/V$

Where

P =the power of motor of the concrete mixer, kW

t =the time of mixing, min

V =the effective volume of the concrete mixer, m^3.

2.6 Boundary Conditions and Initial Condition

2.6.1 Initial Condition

The initial temperature of the structure is given as follows: when T = 0

$$T(x, y, z,0)= T_o (x, y, z,0) \quad \text{or} \quad T(x, y, z,0) = T_o \tag{2.13}$$

Where, $T_o (x, y, z,0)$ is a continuous function of x,y,z and T_o is a constant.

On the contact surface between the concrete and the rock or between the new and the old concrete, the initial temperature may be discontinuous; in this case, two numbers relating to different initial temperatures must be given to one point on the contact surface.

2.6.2 Boundary Conditions

There are four kinds of boundary conditions.

1. First kind of boundary condition: prescribed surface temperature. The surface temperature is prescribed as follows: on the surface,

$$T_s(\tau)= f_1(\tau) \tag{2.14}$$

Where $f_1(\tau)$ is a function of τ.

2. Second kind of boundary condition: prescribed heat flux across the surface.

The flux of heat across the surface is a known function of time, namely on the surface,

$$-\lambda \frac{\delta T}{\delta n} = \mathrm{f}_2(\tau) \tag{2.15}$$

Where

n—the outward normal of the surface

λ —the conductivity of concrete

$\mathrm{f}_2(\tau)$—a known function of time τ.

When there is no flux across the surface, Eq. (2.15) will become: on the surface

$$\frac{\delta T}{\delta n} = 0 \tag{2.16}$$

3. Third kind of boundary condition: linear heat transfer on the surface. The flux across the surface is proportional to the temperature difference between the surface and the surrounding medium, namely on the surface

$$-\lambda \frac{\delta T}{\delta n} = \beta(Ts - T\mathrm{a}) \tag{2.17}$$

Where

β —the surface conductance, kJ/(m^2 h _C)

Ts —surface temperature

Ta —the air temperature.

4. Fourth kind of boundary condition: contact surface between two different solids. If the contact is good, the temperature will be continuous on the surface, the boundary condition is on the contact surface:

$$T1 = T2$$

$$\lambda 1 \frac{\delta T1}{\delta n} = \lambda 2 \frac{\delta T2}{\delta n} \tag{2.18}$$

Where: - λ1 and λ2—the conductivities of the two solids. If the contact is imperfect, the temperature will be discontinuous and the boundary conditions will be

$$\lambda 1 \frac{\delta T1}{\delta n} = \frac{1}{Rc}(T2 - T1)$$

$$\lambda 1 \frac{\delta T1}{\delta n} = \lambda 2 \frac{\delta T2}{\delta n} \tag{2.19}$$

2.7 Hacon [3] 2D Simulating software.

From experimental study on design parameters of mass concrete [9], one concrete block is selected to validate simulation results of Hcaon3. Since Hacon[3] is only capable of analyzing 2D and axisymmetric problems. Only For validation purposes it is possible to simulate core thermal load by consider the block as solid cylindrical axisymmetric problem.

*Figure2. 10 (A) Top and quarter section view of 1.1m*1.1m*1.1m concrete block and (B) 1.1 m diameter cylindrical Axisymmetric mass concrete quarter section (simulation by Hacon 3)*

Temperature results of 1.07m *1.07m*1.07m concrete block from study report [9] are compared with approximate solid cylinder concrete by Hacon [3]. Simulation is done based on information presented in the report [9]. The concrete block which is taken for validation purpose was built with Mix 1. The following information is used in simulating process.

Table 2. 1 concrete mix proportion report [9].

Material	Mix 1 100% Portland Cement (lb/yd^3)	Mix 2 50% Portland - 50% Slag (lb/yd^3)	Mix 3 65% Portland - 35% Fly Ash (lb/yd^3)	Mix 4 50% Portland - 30% Slag - 20% Fly Ash (lb/yd^3)
Cement	681	341	443	341
GGBF slag	0	341	0	204
Fly ash	0	0	238	136
Water	341	341	341	341
Fine aggregate	1095	1088	1036	1050
Course aggregate	1650	1668	1660	1650

(A)

(B)

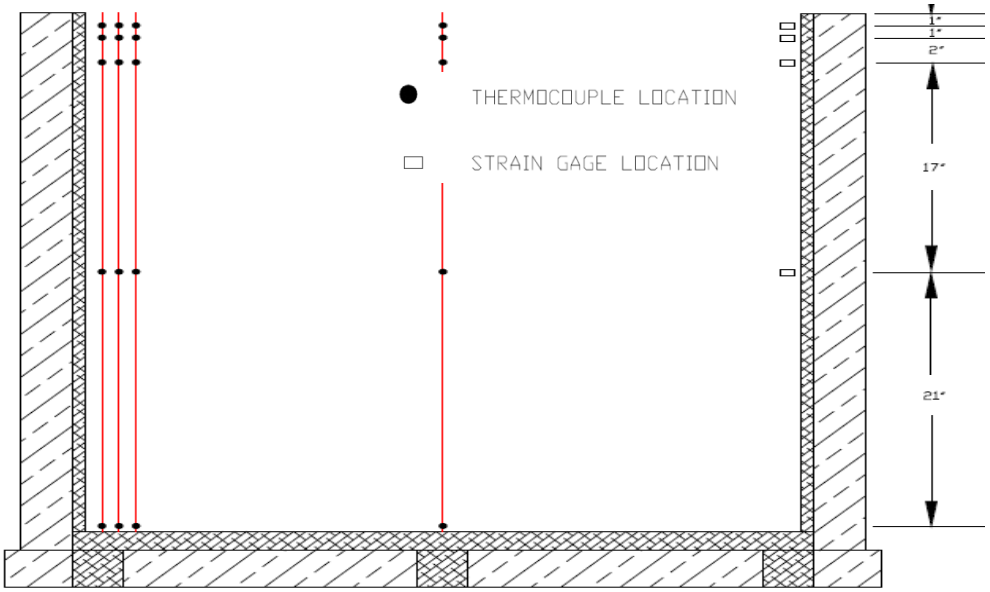

Figure2. 11 (A) uninsulated and insulated mass concrete blocks, (B) location of thermocouple [9]

Table 2. 2 Thermal properties of Materials used in experiment.[9]

	Conductivity (J/m-hr-°C)	Heat Capacity (J/m^3-°C)	Activation Energy (J/mol)
Mixture 1	7920	2675596	34235

	Conductivity (J/m-hr-°C)	Heat Capacity (J/m^3-°C)
Plywood	540	85440
Polystyrene	224.85	20824

Table 2. 3 Modules of Elasticity and Tensile strength of concrete [9]

	Time (Days)	Modulus of Elasticity (MPa)	Tensile Strength (MPa)
Block 1 (100% Portland cement)	1	13445	1.25
	2	16892	1.66
	3	18064	1.93
	7	20236	2.206
	14	22248	2.972
	28	25213	3.303

Poisson ration 0.19 and coefficient of thermal expansion 9.16 E-06 in / in.^{o}C. The average temperature history of the laboratory during the monitoring of the experiment blocks was approximately 23 ^{o}c. The boundary conditions imposed for structural analysis of quarter block consisted of restriction of displacement along the Z direction. [9]

2.7.1 Core and surface temperature comparison of Dian and Hacon 3

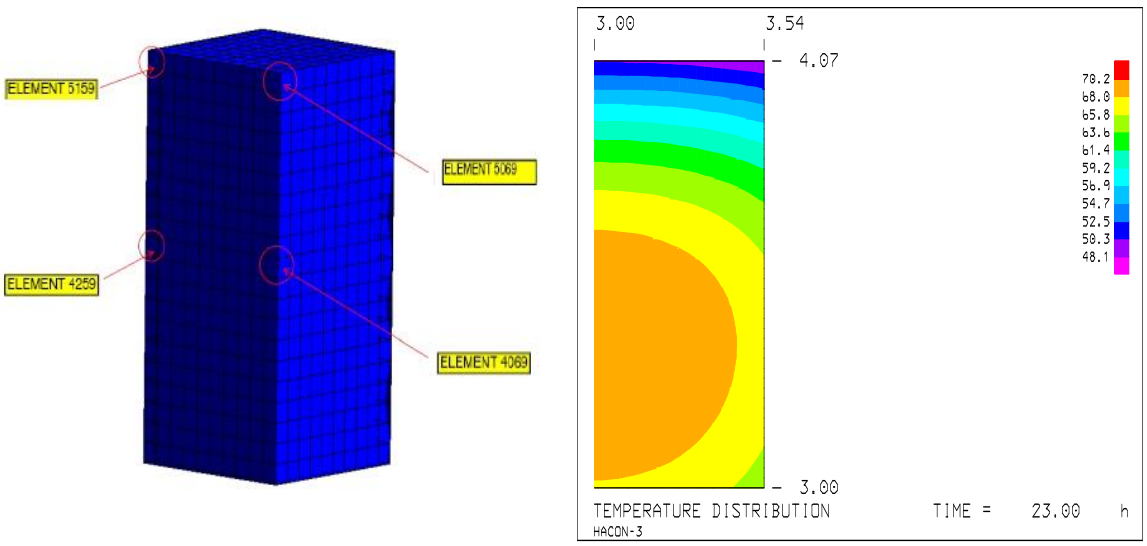

Figure2. 12 (A) Quarter concrete block of Mix-1[9] (B) Axisymmetric solid cylindrical concrete temperature distribution 23 after concrete casting.

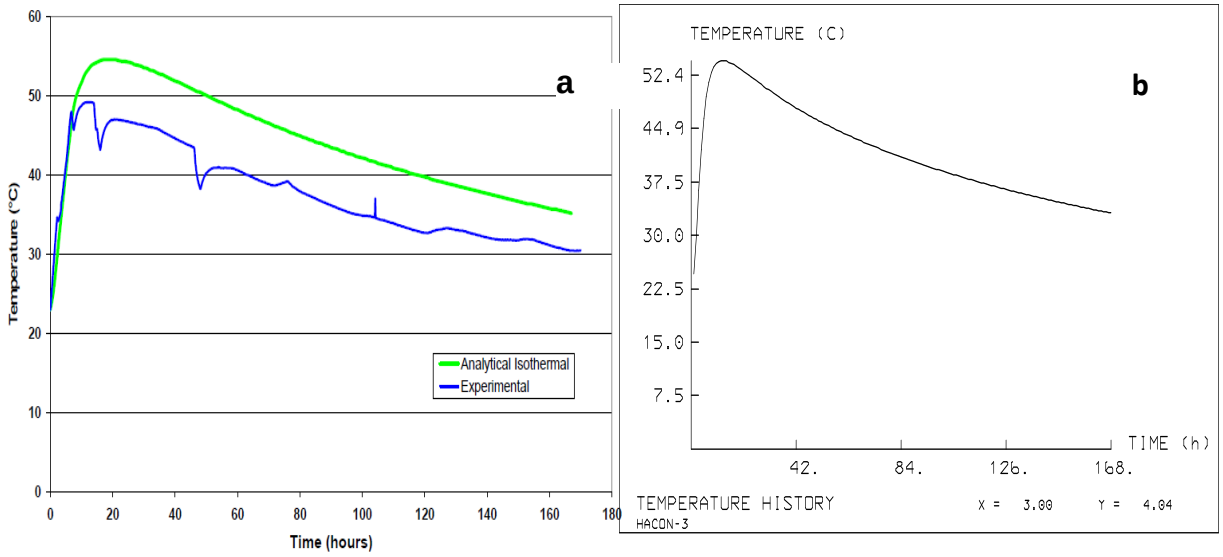

Figure2. 13 (A) semi adiabatic and experimentally measured temperature-time history at the center of the block 4 in. below the exposed top surface of Mixture 1 simulated by Diana .(B) temperature-time history at the center of the solid cylinder concrete 4 in. below.

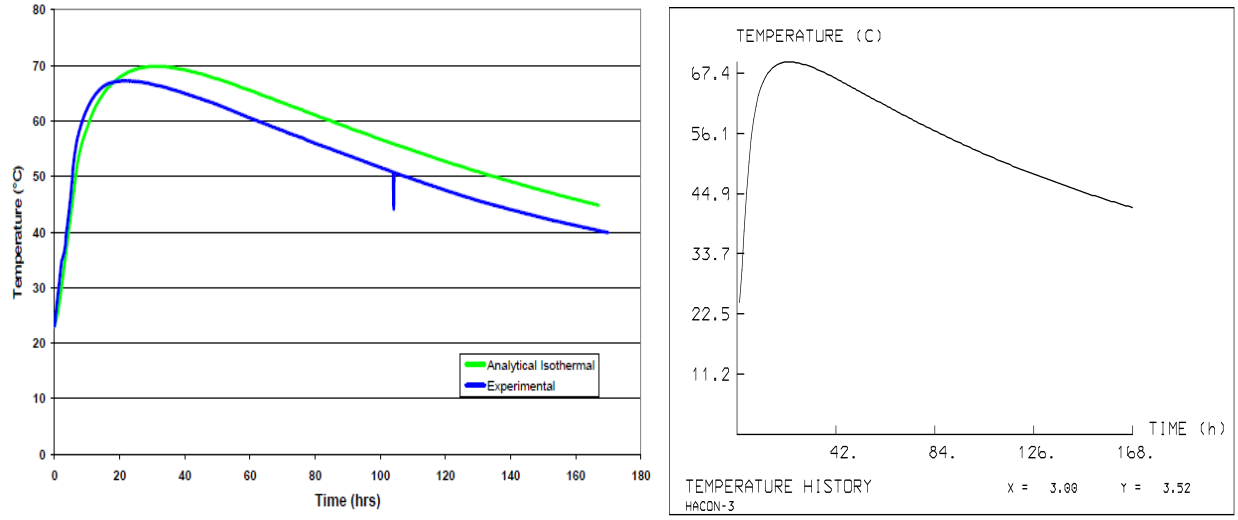

Figure2. 14 (A) semi adiabatic and experimentally measured temperature-time history at the center of the block 21in. below the exposed top surface of Mixture 1 by Diana [9].(B) temperature-time history at the center of the solid cylinder concrete 21 in. below top exposed surface of Mix 1, simulated by Hacon 3

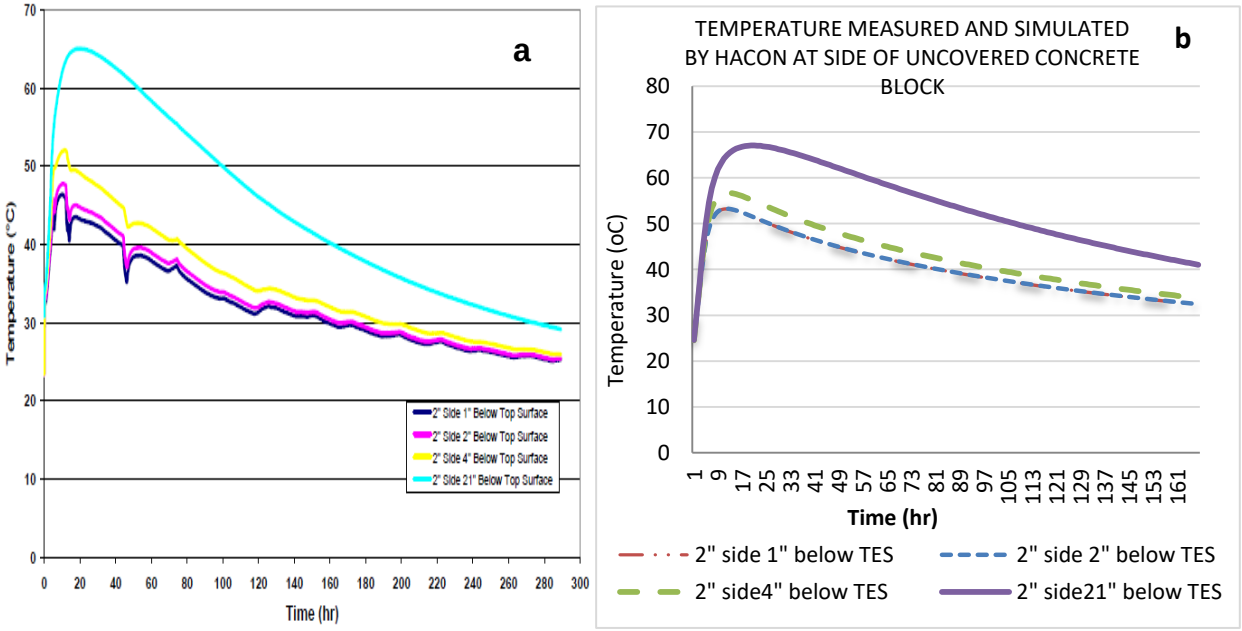

Figure2. 15 (a) Measured Temperatures 2in.From the side of uncovered block in Mix 1 simulated by Diana [9]. (b) Temperatures Simulated by Hacon3 2 in from the side of the uncovered block in Mix 1simulated by Hacon [3].

Table 2. 4 comparison summery of maximum temperature history reported [9] and simulated by Hacon 3.

Location below top exposed surface	Measured[9] (^{o}C)	Simulated by TNO Dian [9] (Hydrated reaction from Semi adiabatic calorimetric test) (^{o}C)	Simulated by TNO Dian [9] (Hydrated reaction from Isothermal calorimetric test) (^{o}C)	Simulated for validation purpose by Hacon[3]-(^{o}C)
2 in.	49.5	49.3	54.6	52.34
4 in.	52	53.34	57	55.37
21 in.	67.2	61.2	69	68.4

The result in table 2.4 shows that Hacon [3] can simulate very well the temperature history of concrete at early age, if necessary execution parameters are properly used.

3. Experimental- Materials and methods

3.1 Reference field concrete blocks

Four reference concrete blocks were built to study temperature evolution of field concrete. Based on their dimension and temperature exposure they are grouped as reference 1 and 2 and consist of a cubical dimension of 1.1m x 1.1m x 1.1m and 0.5m x 0.5m x 0.5m respectively. The purpose those reference field concrete was to study evolution of temperature and to validate the temperature evolution of reference field concrete predicted by the computer program Hacon [3] which is developed to simulate the temperature and stress in hardening concrete. Field boundary condition and design parameters of reference concrete block-1 casted with placement temperature-33 ^{o}C are used for study of CAM and MW.

Blocks of which are grouped as reference 1(RCB-1) and 2 (RCB-2) was built at kombolcha (wollo) and Addis Ababa on July 2018 with different ambient temperature respectively. The same concrete ingredients and mix proportions were used. Bellow, general information of reference concrete blocks is presented.

3.1.1 Geometry

Two concrete blocks for each RCB were built to study the temperature history for 168 hrs. In the case of RCB-1, one block was casted without cooling concrete ingredients while pre cooling method (cooled water) was applied to lower the placing temperature for the second mass concrete block. See, Figure 3.1 (A) and 3.2 (A).

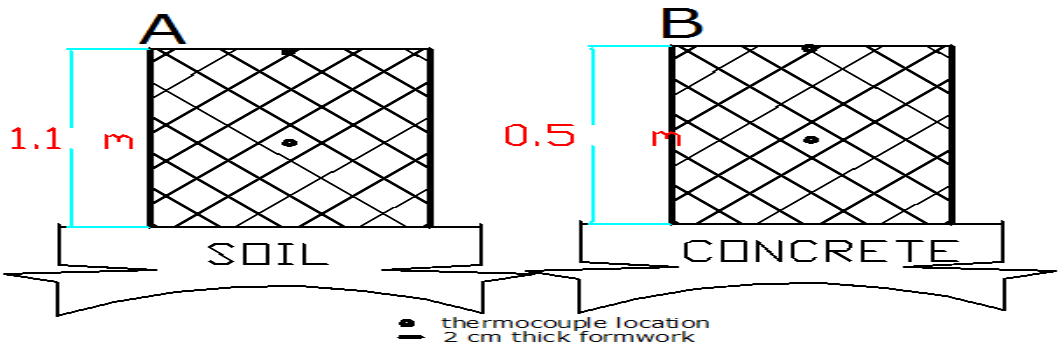

Figure3. 1 (A) Geometry of mass concrete and Thermocouple location for RCB-1 and (B) RCB- 2.

(A)

(B)

Figure3. 2 (A), Experiment 1 RCB -1, and RCB -2 , (B) Experiment 2 RCB -1 and RCB -2.

In the case of RCB-2, one block was casted by heating concrete ingredients while pre cooling method (mixes of cooled water and ice were introduce in to mixer) was applied to lower the placing temperature for the second mass concrete block. See, Figure 3.1 (B) and 3.2 (B).

3.1.2 Materials

Concrete grade C 20/25 was used to build the RCB 1 and 2 with the following materials mix proportion. The same material cement, sand, aggregate and mix ratio was used for both reference models. The concrete is composition of Ordinary Portland cement (ZHONGSHO), river sand and basaltic coarse aggregates. No admixtures were used in both RCB-1 and RCB-1 mix proportion. See, Table 3.1.

Table3. 1 Mix proportions and material property.

Cement (OPC-ZHONGSHU CEMENT)	350 kg/m^3
Water	125 Liters
Fine aggregate 0-8mm	793 kg
Coarse aggregate 10-25mm	1178 kg
Coarse Aggregate (density)	1561 kg/m^3
Fine aggregate density (bulk density)	1534 kg/m^3
Unit weight of concrete	2400 kg/,m^3

3.1.3 Method of cooling concrete ingredients.

Experiment -1

Two concrete blocks were built in field experment-1 in Kombolcha(wollo). The concrete blocks were casted by intentionally precooled concrete materials using cooled water. Cooled water (8^{o}c) was used for concrete mixing and Sprinkling of coarse and fine aggregate in a controlled manner. Aggregate temperature reduced from 28 ^{o}C to 22 ^{o}C and sand from 22 ^{o} C to 19 ^{o}C. The second block is normally casted without applying ingredient pre cooling method. The ambient temperature during concrete pouring of block 1 and 2 of RCB -1 was 25 ^{o}C and 28 ^{o}C respectively. Daily ambient temperature variation affects materials temperature and placing temperature. Temperature of materials before Concreting for field experment-1 was recorded and presented below. See, Table 3.2.

Experiment -2

The same as RCB 1, two blocks are casted at different placing temperature as RCB-2. Concrete ingredients water, and sand were intentionally heated to be at temperature 27, 36 and 36 respectively to cast the first block. Chilled water and ice was introduced in to mixer for the second block of RCB 2. See Table 3.3, and Figure3.3

Table3. 2 Experment 1, RCB-1 concrete ingredients temperature history. (July -10-2018, Kombolcha)

Time	3.30 PM	Time	9:30 AM
Material	Temp(^{o}C)	Material	Temp(^{o}C)
Aggregate	37	Aggregate	28
Sand	34	Sand	22
Water	27	Water	23
cement	23	cement	22
Model-1/normal		Model-2/pre cooled	
Material	Temp(^{o}C)	Material	Temp(^{o}C)
Aggregate	37	Aggregate	22
Sand	34	Sand	19
Water	28	Water	8
cement	23	cement	22
Concrete temperature at casting	33	Concrete temperature at casting	30
Ambient temperature at casting	28	Ambient temperature at casting	25
Casting started on	4:30PM	Casting started on	4.30AM
Casting end on	5:00 PM	Casting end on	11:00 AM

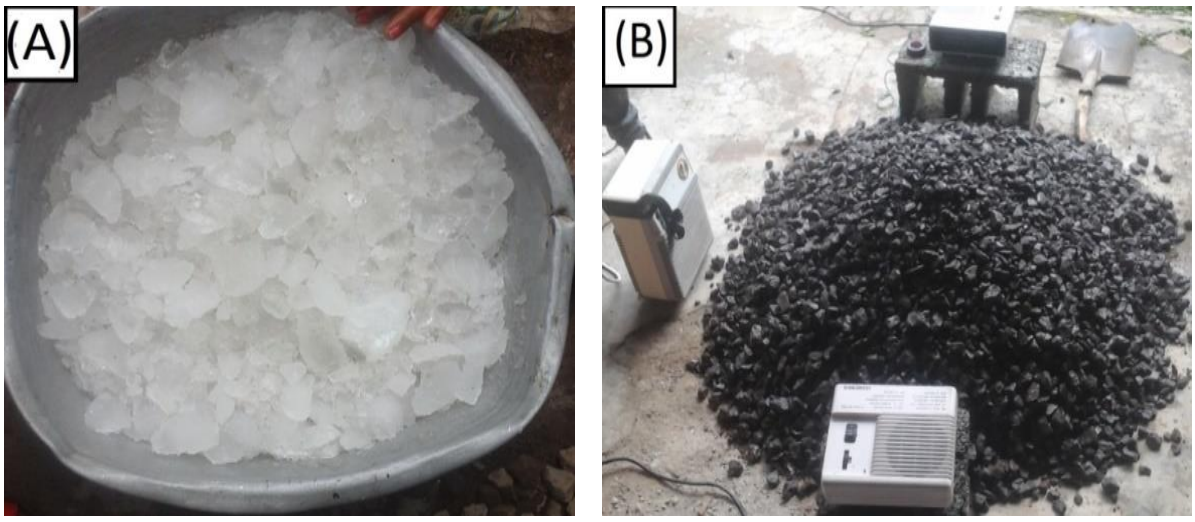

Figure3. 3 (A) chipped Ice, (B), heating aggregate, (C) heating sand,and (D) heating aggregate.

Table3. 3 Experiment 2- RCB-2 concrete ingredients temperature history. (July-27-2018, Addis Ababa).

11.00 AM	
Material	Temp(^{o}C)
Aggregate	14
Sand	14
Water	13
Model-2/pre cooled	
Material	Temp(^{o}C)
Aggregate	14
Sand	14
cement	14
Water	4.5 Liter Ice and 17.5 Liter chilled water
Concrete temperature at casting	9
Ambient temperature at casting	15
Casting started on	12:00 PM
Casting end on	12:15 PM
11.00 AM	
Material	Temp(^{o}C)
Aggregate	14
Sand	14
Water	13
cement	14

Model-1/Heated	
Material	Temp(^{o}C)
Aggregate	36
Sand	36
Water	27
cement	14
Concrete temperature at casting	31
Ambient temperature at casting	15
Casting started on	12:00 PM
Casting end on	12:15 PM

3.1.4 Instrumentation for data collection

Thermocouple Cx 100 series was used to measure temperature history every hour, two points are selected to measure temperature history of the reference model as shown in the figure 3.1. The sensors were placed carefully in a manner that they couldn't move during concrete placement.

Figure3. 4 Cx100 series Thermocouple with sensor

3.2 Simulation of cylindrical axisymmetric mass concrete (CAM) and massive walls (MW)

3.2.1 Modeling Software

The simulations have been performed in computer program HACON [3] which is developed to simulate temperature and stress in hardening concrete. The simulated case consists of mass concrete block and massive wall which is

assumed supported by soil and rigid foundation (externally restraints) respectively.

3.2.2 General Considerations

During the process of field concrete temperature prediction, the following factors are considered: heat transfer inside concrete, rate of heat generation, thermal properties of concrete, boundary conditions, and initial soil conditions.

3.2.3 Thermal Properties of Concrete

Thermal properties to be used for field concrete temperature modeling include the specific heat of concrete and thermal conductivity.

Specific Heat of Concrete

The specific heat is the amount of heat per unit mass required to raise the temperature by one degree Celsius. The specific heat of concrete depends on the specific heat of the constituent materials. Concrete specific heat is not a constant during the process of hydration. Several Researchers found that the specific heat of concrete decreases with time. The typical value of concrete specific heat is between 800 and 1200 J/Kg ° C, and a value of 1000 J/Kg ° C was used in modeling of field concrete in this study.

Thermal Conductivity

Thermal conductivity represents the ability of a material to transfer heat. It is defined as the ratio of the rate of heat flow to the temperature gradient. Thermal conductivity of the concrete governs the rate at which heat flows into, though, or out of a concrete structure. For normal weight concrete, the thermal conductivity is widely influenced by the mineralogical character of the aggregates, water content, temperature, and unit weight in dry condition. For concrete with basaltic aggregate thermal conductivity vary from 1.9 up to 2.2 w/m ^{o} C, and a value of 2.1 w/m ^{o} C was used in modeling of field concrete in this study.

3.2.4 Geometry

Any massive wall needs to be modeled twice, one cross section model and one plane section of the structure. To model the cross section and plane section nodes, curves and surface need to be assigned.

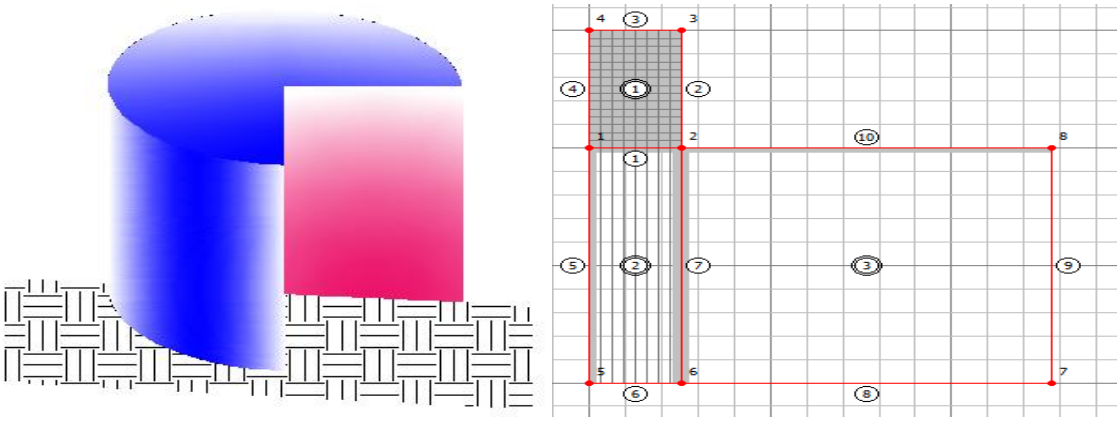

Figure3. 5Cylindrical axisymmetric mass concrete and quarter section model in Hacon 3.

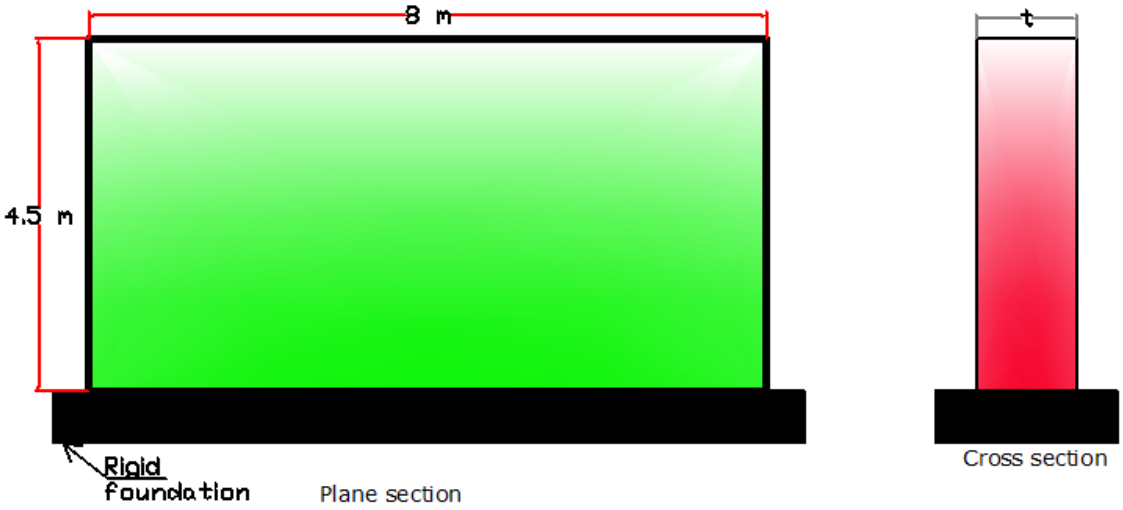

Figure3. 6 plane section and cross section of massive wall

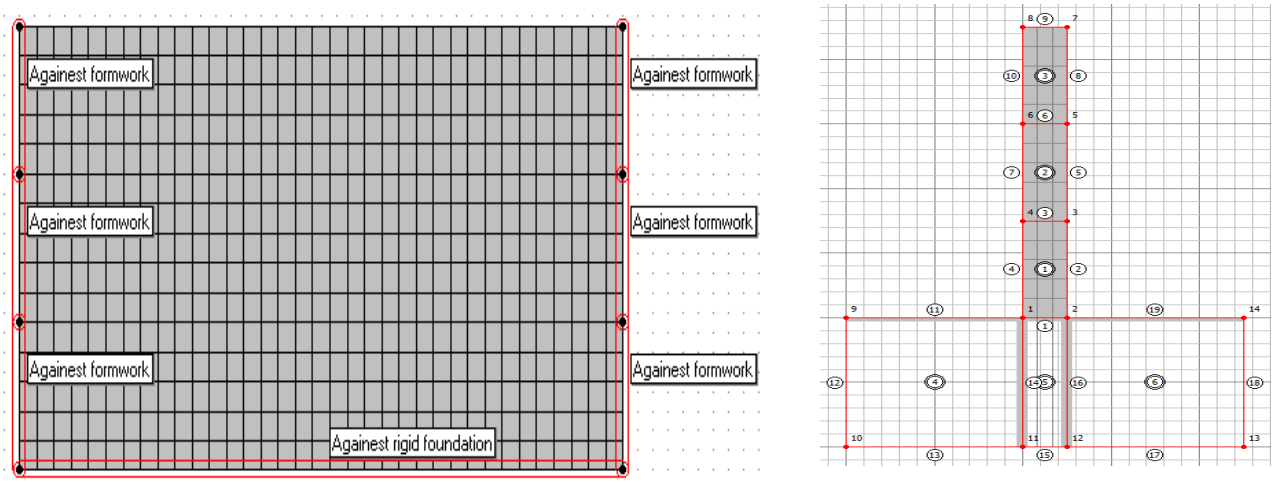

Figure3. 7 plane section and cross section of massive wall model in Hacon 3

Node, curves and surfaces

The first step in modeling is to place nodes. This was done for each structure cross section and plane section properly to have a more realistic simulation. When the nodes are place, they are connected by curves or lines. These curves are presenting the exterior of the structure and will be used to assign a surface. The third step to assign the surface to each part of the structure. The surface should enclose four curves which are placed in counter clockwise way. When the surface defined, it needs to be assigned 8 node elements for concrete and 3 and 5 node element for semi-infinite element in proper orientation. The orientation of nodes indicates the dissipation of heat from the structure.

3.2.5 Material

After the geometry has been determined, the materials are assigned to the surface. Pre-defined and new material can be defined. In this study concrete grade C 20/25 was used.

3.2.6 Boundary Conditions

There are six type of boundary condition in HACON^3:-Temperature, heat flow, displacement, pipe flow, loading and spring. For the simulation, the temperature, heat flows, spring and displacement were used.

Heat flow

Boundary heat transfer conditions, which are time or temperature dependent, are important for solving the differential Heat balance equation. The four major boundary heat transfer mechanisms are conduction, convention, solar absorption, and irradiation. Figure 3.8 illustrates these four major heat transfer mechanisms.

Conduction

Thermal conduction is defined as "heat transport in a material by transfer of heat between portions of the material that are in direct contact with each other. As long as a temperature gradient exists, the transfer of heat will flow from the high temperature region to the low-temperature region. Heat conduction happens inside the concrete. The heat exchange due to the temperature gradient

between the concrete and the soil in contact with concrete happens in the form of conduction. The heat flow through the insulation layer can be estimated by the following equation. Heat conduction happens inside the concrete. The heat exchange due to the temperature gradient between the concrete and the soil in contact with concrete happens in the form of conduction. The heat flow through the insulation layer can be estimated by the following equation.

$$q = (\frac{Ts-Ta}{Rth}) \quad (4.1)$$

Where,

q = Heat flow, (w)

T_s = Surface temperature, (°C)

T_a = Air temperature, (°C)

R_{th} = Thermal resistance, (°C/w), R_{th} =d/k.,

d=Thickness, k=Thermal conductivity.

The boundary condition type one, initial condition, is assumed that the soil will have the same temperature as the ambient temperature.

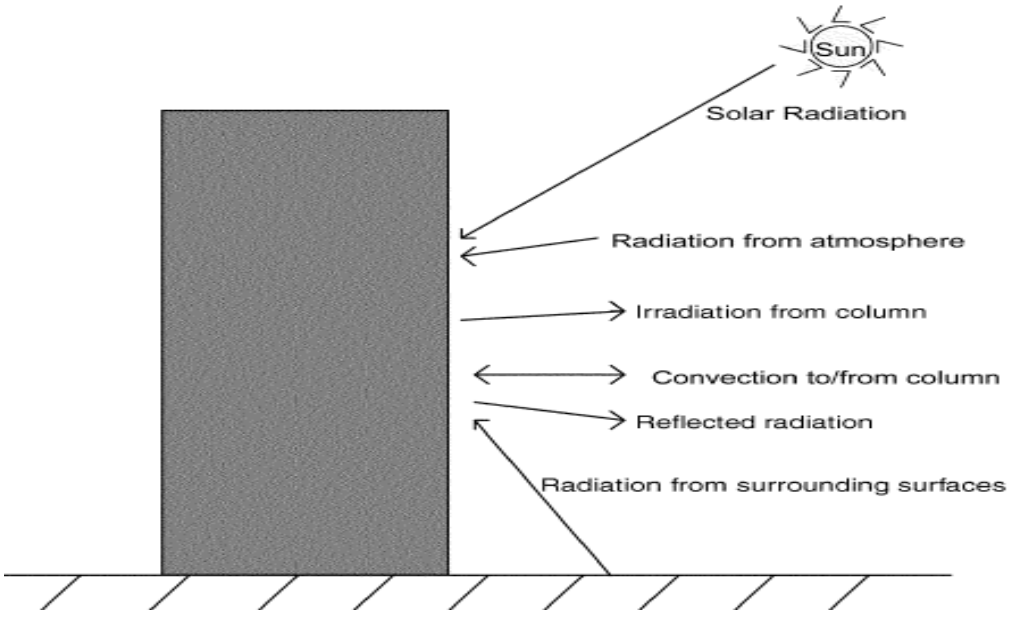

Figure3. 8 Boundary heat transfer condition

Convection

Convection is heat transfer by mass motion of a fluid such as air or water when the heated fluid is caused to move away from the source of heat, carrying energy

with it. In this study, convection heat transfer caused by air motion is considered. The rate of heat flow from a horizontal surface is mainly controlled by the magnitude of the temperature difference, the wind speed, and the surface texture of the member. The following formulations have been used to calculate the Convection heat transfer coefficient (w/m^2 ^{o}C). This approach does not include the effect of surface and air temperature.

$h = 5.6 + 4.0 * v_{wind}$ *for* $v_{wind} \leq 5m/s$

$h = 7.2 * v^{0.78}_{wind}$ *for* $v_{wind} > 5m/s$

For no insulation case Convection heat transfer coefficient

h=5.6+4.0* *(3) =17.6* w/m°C

It is necessary to calculate the overall convection heat transfer coefficient (ho), including the effects of the convection and insulation, because the heat transfer caused by surface convection can simultaneously occur in the presence of surface insulation. (K1 (wood formwork) 0.14 w/m °C)

$$ho = (\frac{1}{h} + \frac{d1}{k1} + \frac{d2}{k2} + \cdots + \frac{dn}{kn})^{-1} \quad (4.2)$$

h =5.6+4(3)=17.6 w/m° C

ho =(1/17.6 +0.02/0.14)= 4.96 w/m° C

Solar Absorption

Solar absorption is solar radiation absorbed by pavement surfaces during their exposure to incoming solar radiation. McCullough and Rasmussen (1999) proposed the following equation to account for the solar absorption of concrete pavement.

$$q_{sol} = \gamma_{abs} * I_f * q_{solar} \quad (4.3)$$

Where,

q_{sol} - Solar absorption of concrete, (W/m^2)

y_{abs} - Solar absorptivity of the concrete

I_f - Intensity factor to account for angle of sun during a 24-hour day

q_{solar} - Instantaneous solar radiation, (W/m^2) as defined in Table 3.4

Solar radiation is a form of thermal radiation. The intensity of solar radiation strongly depends on atmospheric conditions (Table 3.4), time of the year, and

angle of incidence of the sun's ray on the surface of the earth (Holman 1990). The incidence angle is indicated by I_f, the intensity of solar radiation. During the nighttime, the solar radiation is negligible. During the daytime, I_f is assumed to be a sinusoidal distribution (Schindler 2002).

Table3. 4 Solar Radiation Values (McCullough and Rasmussen 1999)

Sky Conditions	Solar Radiation, (W/m^2)
Sunny	1000
Partly Cloudy	700
Cloudy	300

Solar absorptivity is the ratio between how much solar radiation is absorbed by material to that absorbed by a standard black surface. The solar absorptivity of a material is mostly dependent on its color. The solar absorptivity of concrete is a function of the surface color. The typical values range from 0.5 to 0.6. In this study 0.55 has been taken.

Intensity factor (If)

The intensity of solar radiation strongly depends on atmospheric conditions, time of the year, and angle of incidence of the sun's ray on the surface of the earth (Holman 1990). During the daytime, I_f is assumed to be a sinusoidal distribution (Schindler 2002) and during the nighttime, the solar radiation is negligible. Intensity factor (If) is assumed in this paper based on the change in ambient temperature. See, figure 3.9

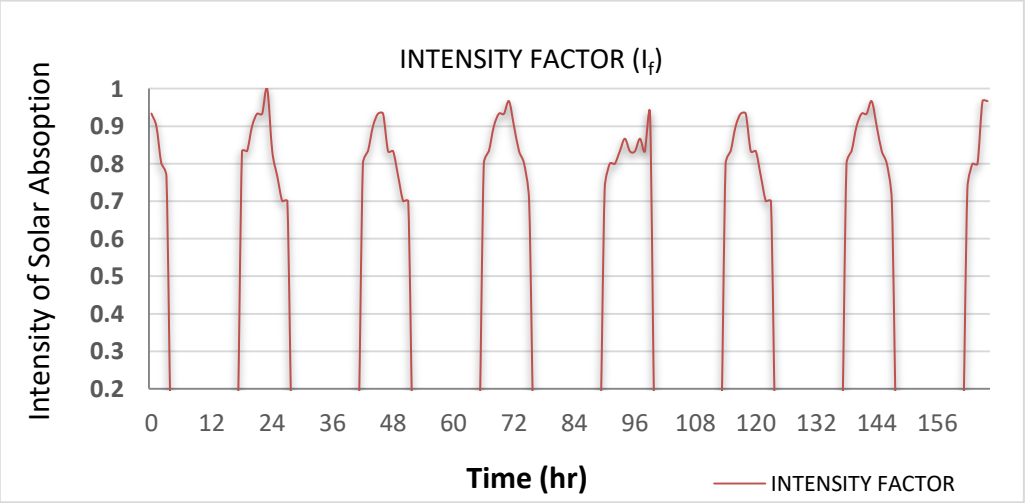

Figure3. 9 Solar absorption intensity factors.

Item	Unit	value
Thermal conductivity of concrete	W/m°C	2.1
Specific heat	J/kg°C	1000
Thermal conductivity of formwork	W/m°C	0.14
Thickness of formwork	m	0.02
Stiffness of soil	kn/m^3	35000
Solar radiation(partly cloudy)	W/m^2	700
Solar absorption coefficient	-	0.55
Heat transfer coefficient thorough formwork	W/m°C	4.96
Heat transfer coefficient at exposed surface	W/m°C	*17.45*
Average wind speed	m/s	*5*

Table3. 5 Execution parameters used for both thermal analysis and stress analysis

Temperature

The casting of the structure was done in month of July. The ambient temperature recorded for 168 hours. Since the simulation was done for this time period. Different Boundary heat transfer condition which are time or temperature dependent, are important for solving boundary conditions for temperature were; formwork, removal of formwork and exposed surface.

(A)

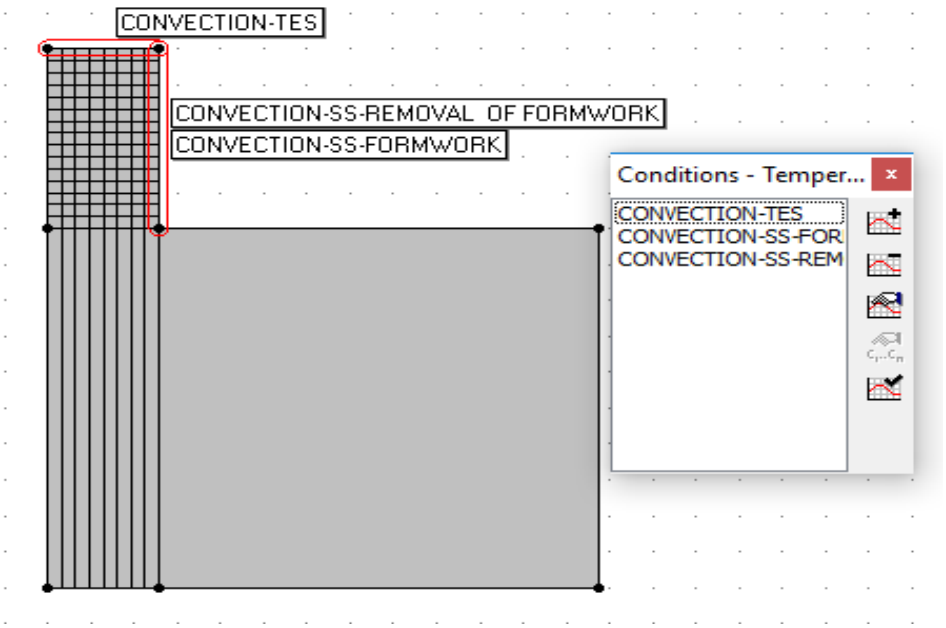

(B)

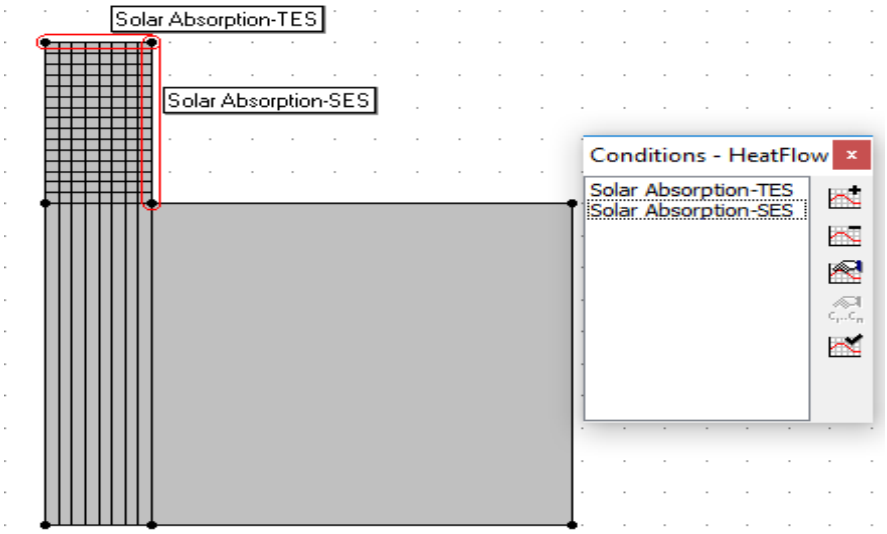

(C)

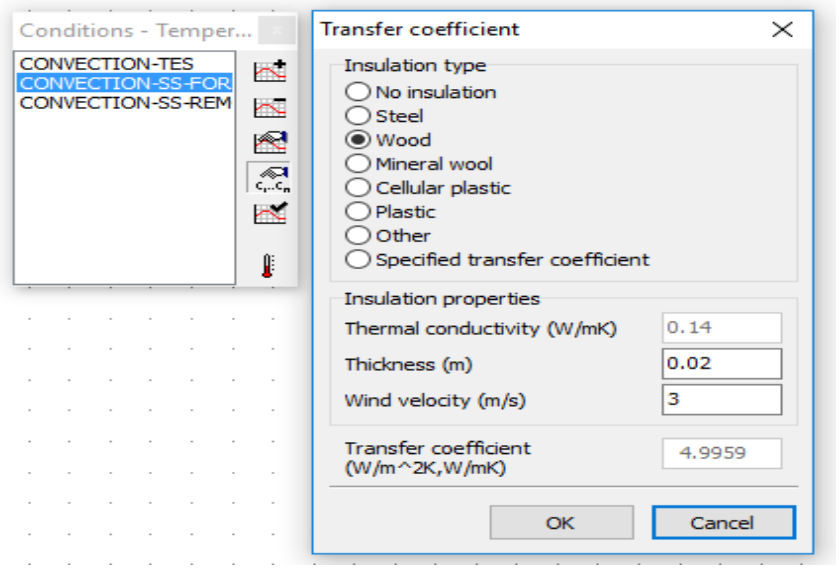

(D)

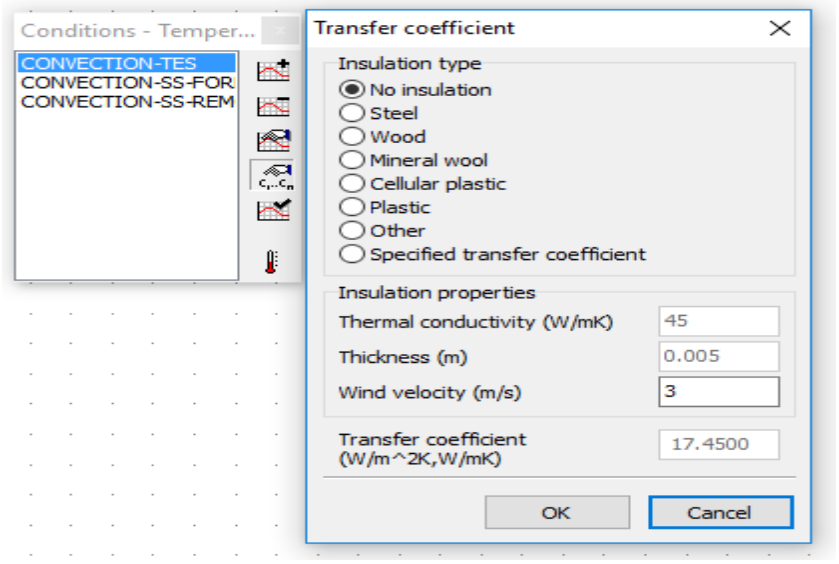

Figure3. 10 (A) and (B) Temperature Boundary condition, (C) and (D) heat transfer coefficient with insulation (formwork) and without insulation

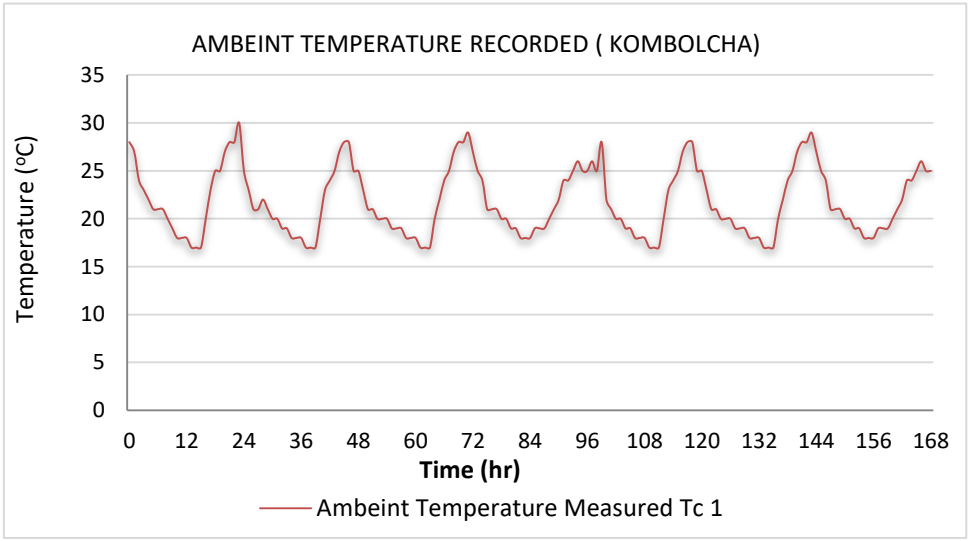

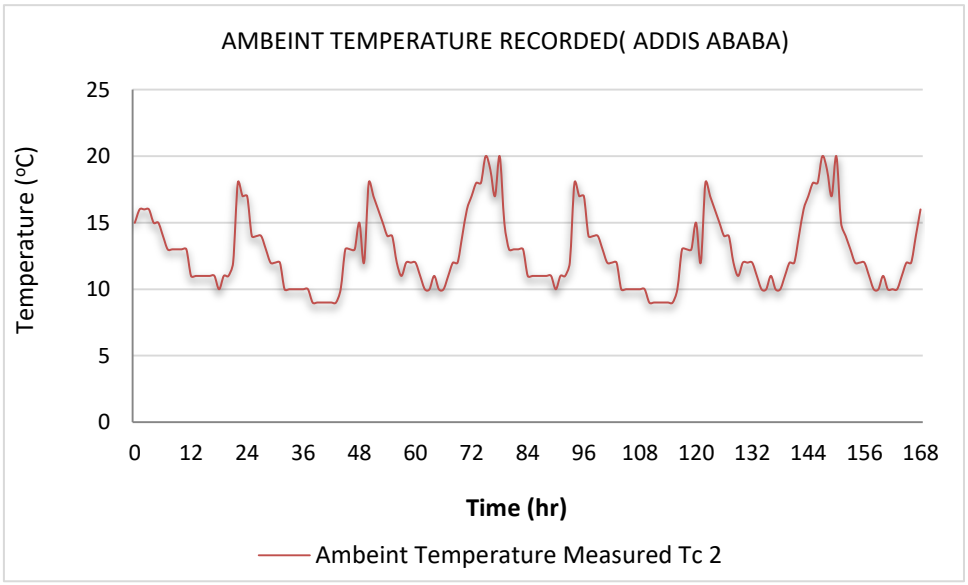

Figure3. 11 ambient temperature recorded for 168 hr. (A) KOMBOLCHA and (B) ADDIS ABABA

Displacement

The restraint can be applied in either x-direction, y-direction, or in x- and y-direction. For Axisymmetric problems at axis of Axisymmetric the displacement in radial (x) direction is zero. Displacement restraint was defined at side in x-direction due to mechanical support for 24 hr for early form removal case. The bottom of the structure against soil is model as spring by assuming stiffness of soil 3500 kn/m^3 as shown below. For massive wall the bottom of the wall is assumed as fixed support condition.

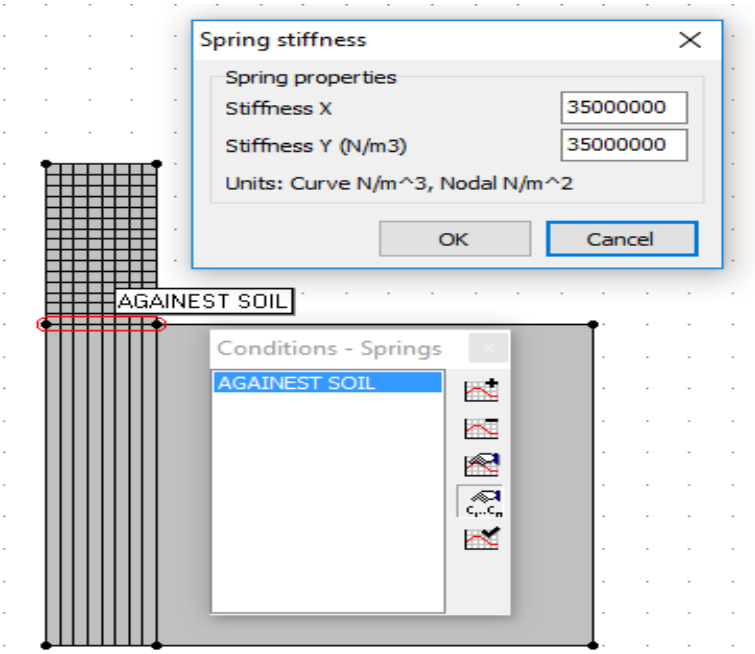

Figure3. 12 Spring Boundary condition in Hacon 3

3.2.7 Calculation of the cross section

The calculation for the cross section is only a temperature and maturity simulation in plane section of massive walls. The time step for the calculations, of temperature and maturity were set to 1 hour, starting from time of casting. In case of axisymmetric problem only cross section modeled and the calculation includes stress and displacement. The total time of simulation was 168 hours. See cross section and general settings for plane strain and axi-symmetry problem in the figure below.

3.2.8 Plane section

The calculations of the plane section were performed in the same manner as for the cross section. However, the difference here was that the geometry for the plane section was defined without any rock or soil in the bottom. The amount of rows needs to be the same as the amount of rows in the cross section. Only additional displacement boundary condition for wall was defined and general setting change to plane stress problem. The temperature and maturity were imported from the cross section to the plane before executing the analysis.

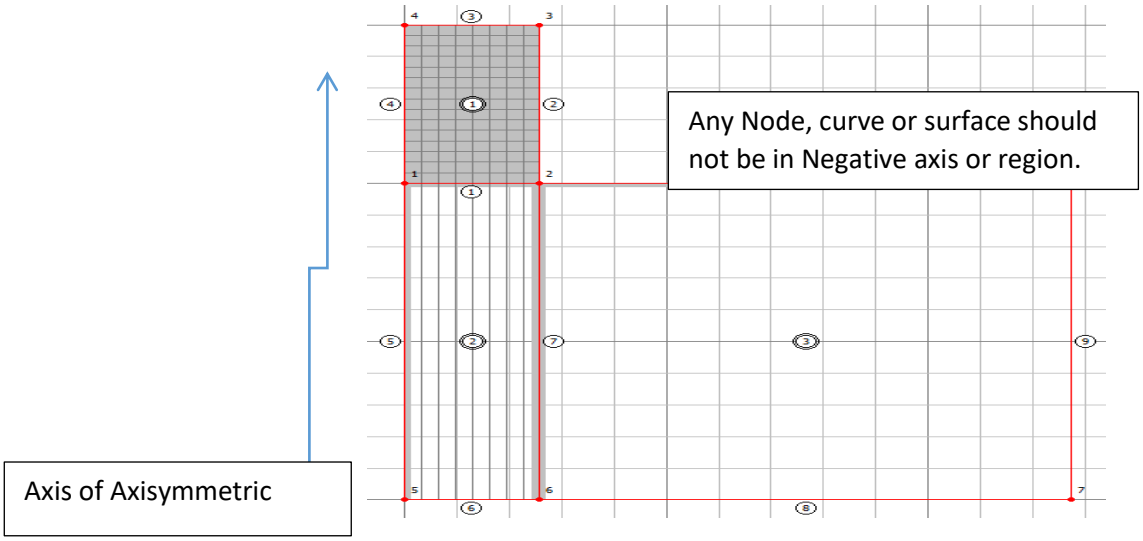

Figure3. 13 Cross section of Cylindrical axisymmetric

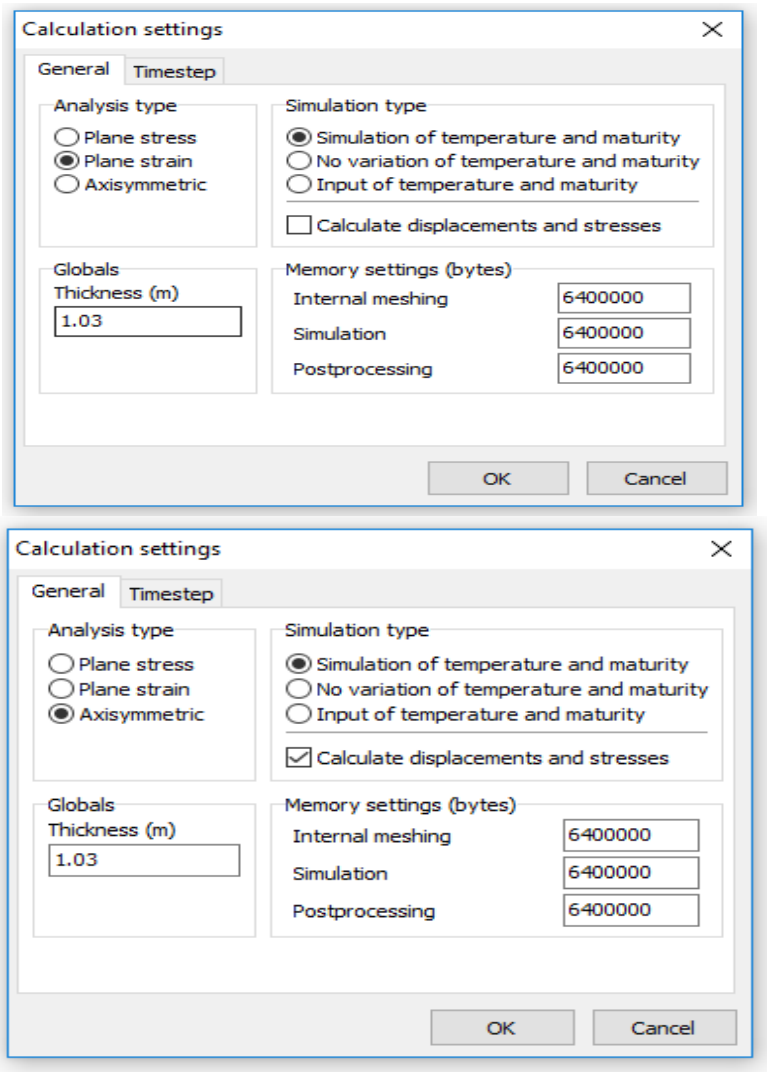

Figure3. 14 General setting of calculation for plane strain and Axi-symmetry problems

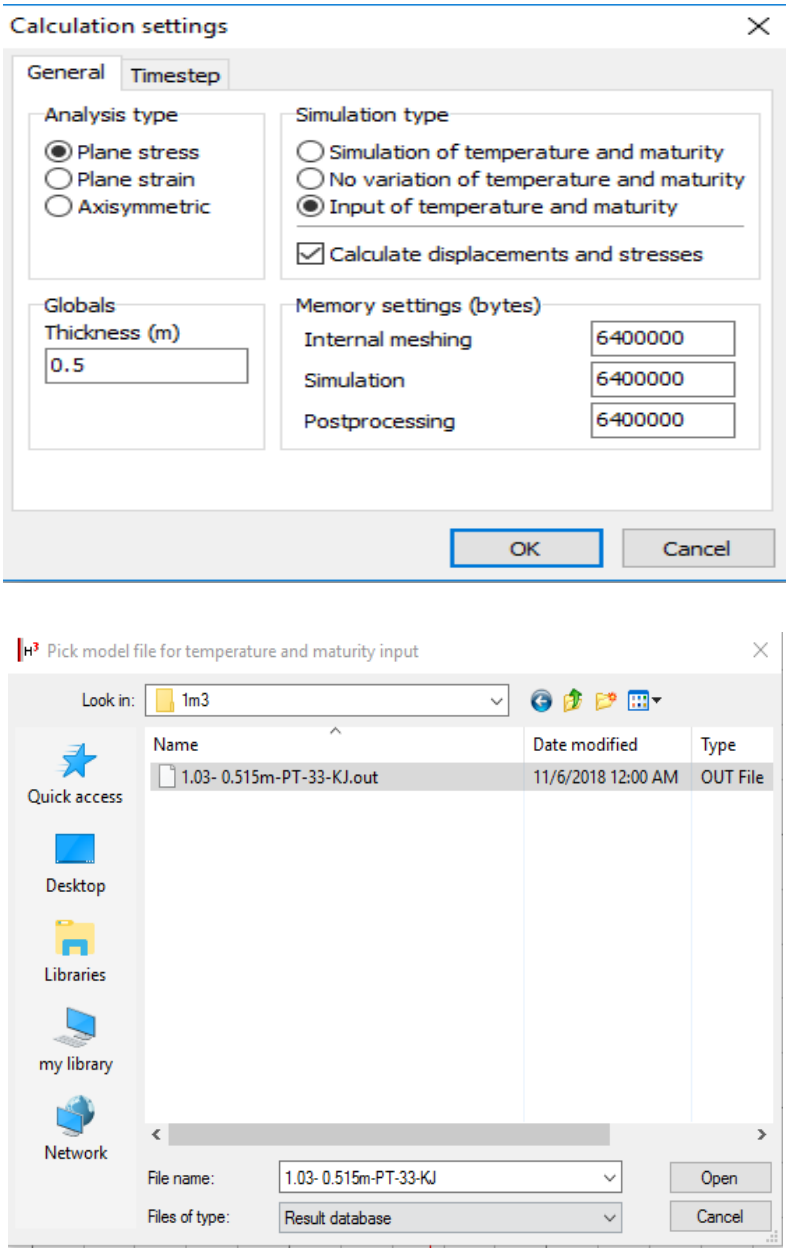

Figure3. 15 General setting for plane stress case , importing Temperature and maturity from cross section in Hacon 3.

3.2.9 Summary of modeling parameters and assumptions for CAM and MW.

The table shown below summarized modeling and assumption used in modeling of axisymmetric mass concrete structure and massive wall.

Table3. 6 Summary of modeling parameters and assumptions for CAM and MW

Modeling parameters and assumption	**Values**
Execution parameters used for both thermal analysis and stress analysis	Table 3.5
Solar absorption intensity factors	Figure 3.9
Ambient temperature recorded	Kombolcha Recorded
Material properties	Table 3.1
Average soil /Rigid foundation/ temperature (^{o}C)	22
Depth of soil modeled (m)	2
Time of casting (hr)	0
Initial maturity at casting(hr)	0
Formwork removal time (hr)	24 hr. and delayed Form removal
Support condition for CAM	soil
Support condition for MW	Rigid foundation

4. Results and Discussion.

4.1 Results and discussion of RCB.

The most important results of reference concrete blocks and analysis results of analytical models are presented and discussed in this section. Other relevant analysis results are presented in Appendix B.

1. *Measured and simulated temperature History of RCB-1 (PT-33 ^{o}C and PT-30 ^{o}C)*

Maximum measured and simulated temperatures history result of reference blocks in experiment-1 program are presented in the figure 4.1. Maximum peak temperatures at core of concrete blocks were 71 ^{o}C and 69 ^{o}C respectively for PT-33 ^{o}C and 30 ^{o}C. The Peak temperatures predicted by Hacon were lower by maximum value of 6 ^{o}C, from the value of measured; the reason for peak temperature difference was that the concrete absorbed heat from the sounding during casting. Heating rate difference between measured and simulated was expected because the heat absorbed by the concrete was not considered in thermal analysis.

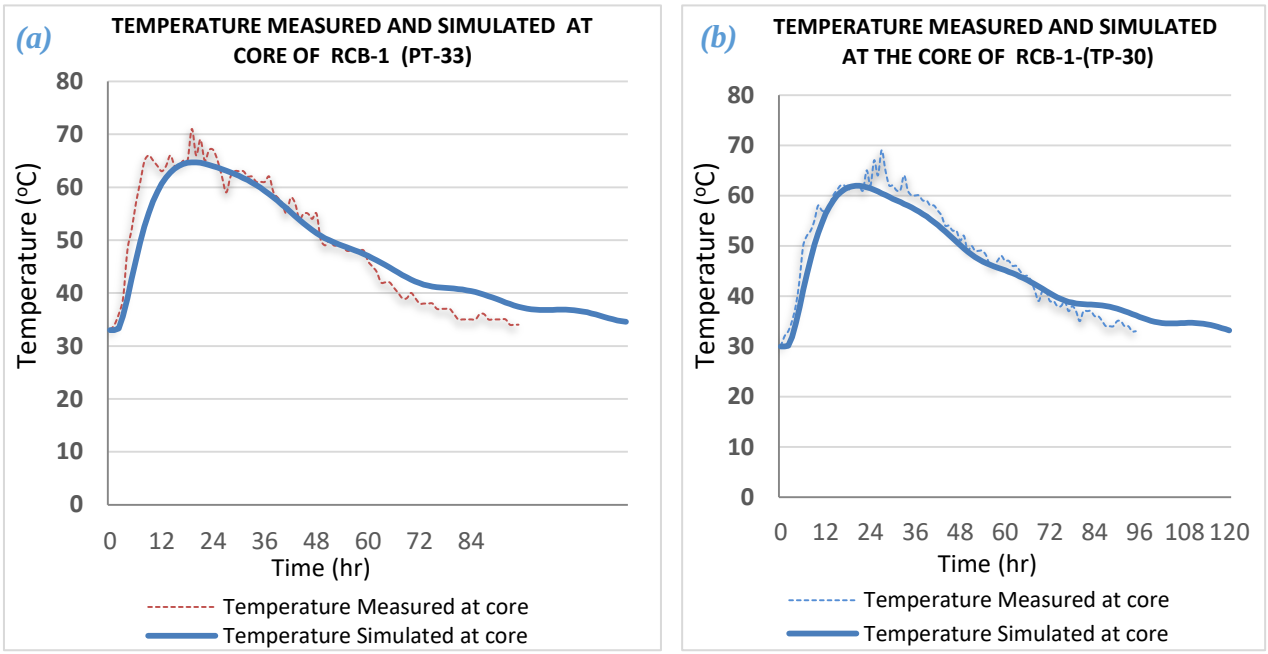

Figure4. 1 Temperature measured and simulated at the core of RCB-1-(a) PT-33 and (b) PT-30

The core of concrete blocks was cool to the placement temperature after 5 days while the surface cools faster as expected. Temperature history of RCB-1 at center of top exposed surface is presented in figure 4.2. The result shows that the surface temperature history was the same fashion as ambient temperature. Center of top exposed surface of RCB-1 experienced 51.84 ^{o}C and 49 ^{o}C temperature respectively for PT-33 ^{o}C, and PT-30 ^{o}C case, this shows that surface lags behind the core and thermal gradient created with in the same sections of the blocks. Temperature above 70 ^{o}C may prevent the normal ettringite formation and result delayed ettrigite, which can cause expansion and cracking in hardened concrete, this means blocks larger than RCB-1 in section are susceptible to the risk of delayed ettrigite formation.

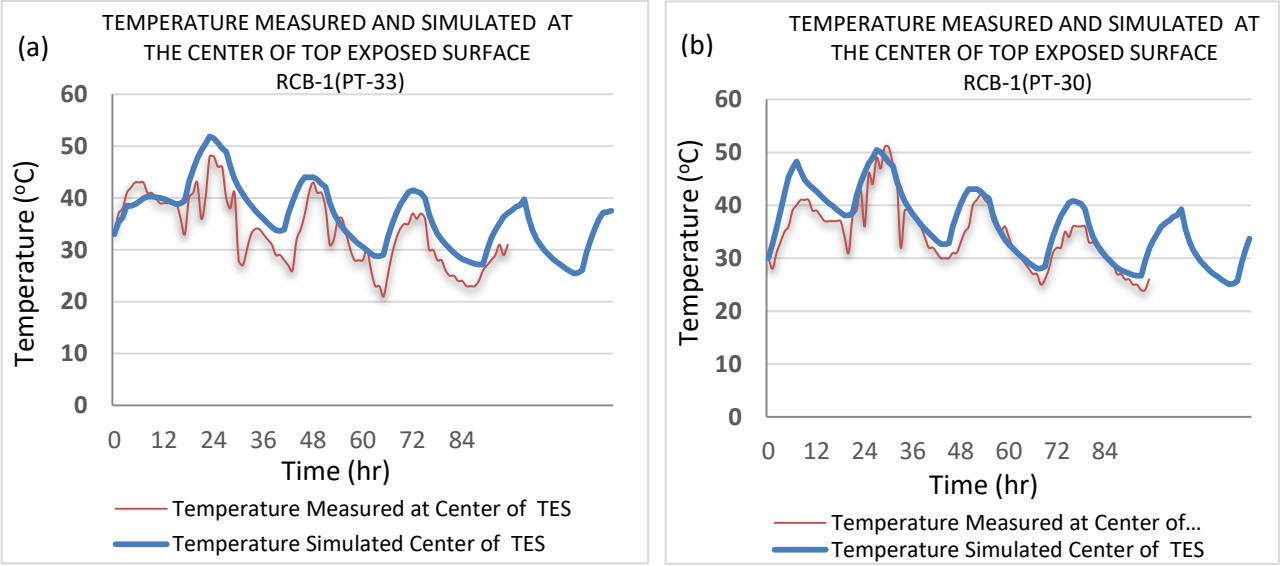

Figure4. 2 Temperature measured and simulated at the center of top exposed surface of RCB-1 (a) for PT 33 , (b) 30 ^{o}C

Figure 4.3 presents comparatively results of temperature deferential which are measured and simulated of RCB-1 for PT-33 ^{o}C. The temperature deferential was high at early age; measured temperature differential of the block was almost similar with simulation result. The temperature differential of top exposed surface was exceeds 20 ^{o}C on the maximum temperature occurrence time of the block and diminished after 43 hour. Finally the value of temperature differential reduced in cooling phase.

In experiment 2, measured and predicted surface temperature history at core and top exposed of RCB-2 for placement temperature 30 °C and 9 °C case are

presented in figure 4.4. To evaluate sensitivity of Hacon for temperature simulation, one concrete block was casted with 30 ^{o}C placement temperatures.

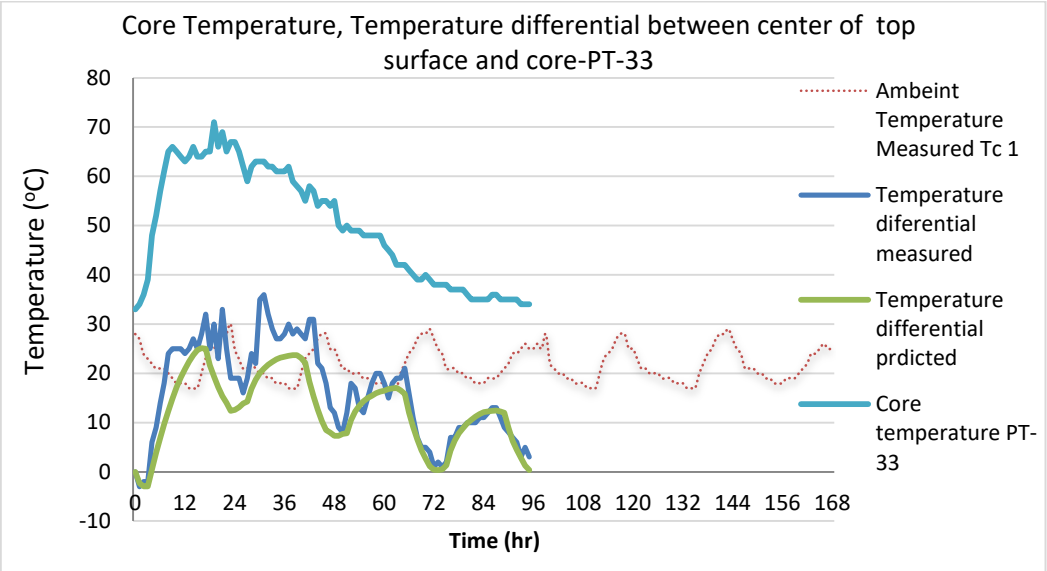

Figure4. 3 temperature differential between top surface and core of RCB-1-PT-33

As shown in the figure 4.4 the peak temperatures of the core reached soon after casting because the blocks are thin in sections. The temperature history result shows that, the core temperature was affected by the air temperature variation and this was high in low placement temperature case. Generally, Measured and simulated results had good agreement at core and surface with maximum temperature difference of 1.5 °C.

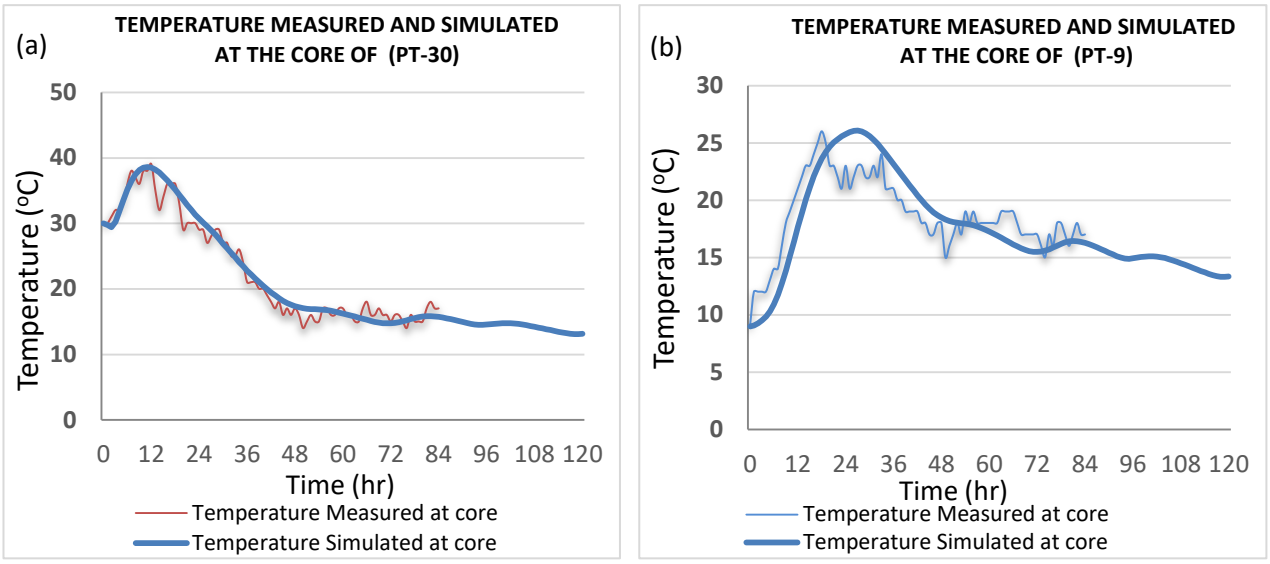

Figure4. 4 Temperature measured and simulated at the center of RCB-2, (a) PT-30, (b) PT-9

In a case of 30 °C placement temperature, the core was reached to 38 °C after 10 hours. While in a case of 9 °C placement temperature, the core reached 26 °C after 19 hours. Heating rate of concrete was affected by placement temperature, because initial rate of reaction of cement was affected by temperature. The result reveals that, If Concrete temperature is below ambient temperature, it demands more heat from hydration to reach the peak. As it can be seen in figure 4.4, about 8.5 °C temperature rise was observed at the core of concrete block which was casted with 30 °C temperature. The temperature of the block gradual diminished to 15°C at 90 hours after casting. Similarly, in the case of PT-9 (a case of precooled), 17 °C temperature rise was measured. This indicates cement hydration is not the only source of heat in thin sections, and the reason behind this was concrete heat absorption from the surrounding. The results show that, dissipation and absorbation of temperature depends on ambient temperature and the section of mass concrete structure. Heat was quickly dissipated from center of surface and cools faster than the core. Temperatures measured and predicted at center of top exposed surface were satisfactory agreed with maximum 4 ^{o}C differences. Generally, temperature histories of analytic models have shown good agreement with measured temperature values at core and center of top exposed surface of reference concrete blocks.

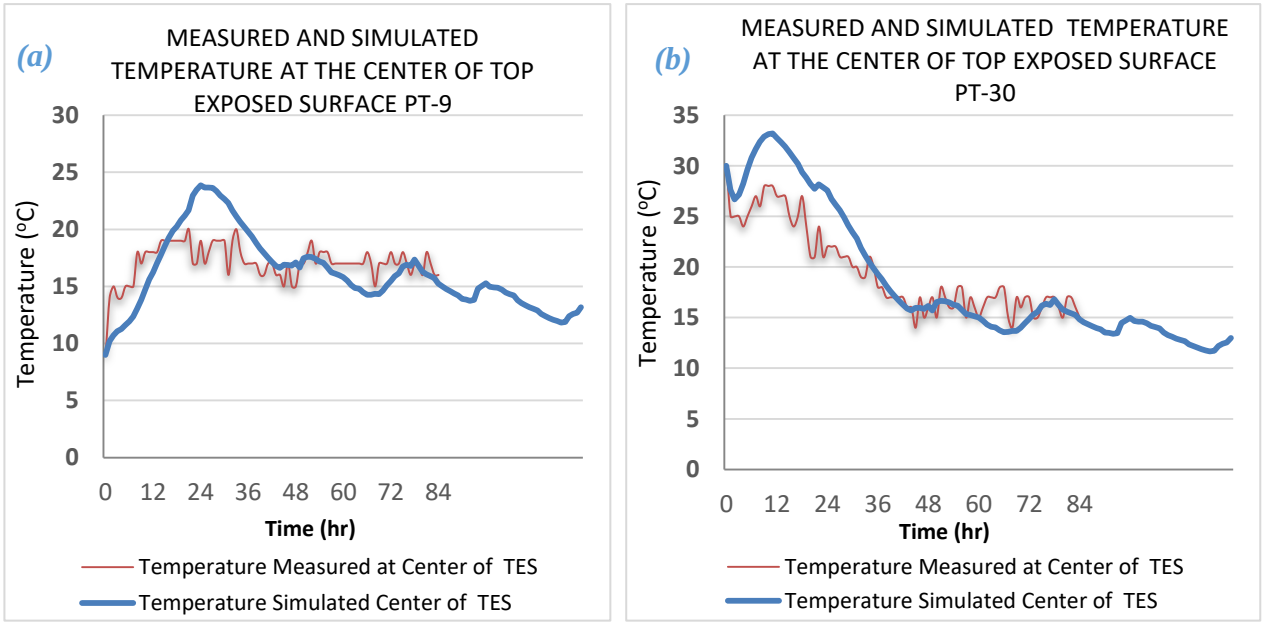

Figure4. 5 temperature measured and simulated at the center of top exposed surface-(a) PT-9, (b) PT-30

2. *Stress history result of RCB-1*

The core of RCB-1 was in compression for a day as per the result of maximum principal stress history. Tensile stress appeared due to internal restraint caused by cooling of the core at higher rate. This stress exceeds the strength 72 hours after casting and the crack tendency reached 101.38 %. This implies cracks were initiated in the core during cooling phase when the core temperature reached 44.38 ^{o}C. Crack initiated at center of top exposed surface early in heating phase when the temperature deferential reached 20.8 ^{o} C as shown in figure 4.7. The temperature deferential at surface during crack initiation exceeds the temperature deferential limitation (20 ^{o} C) provided by codes.

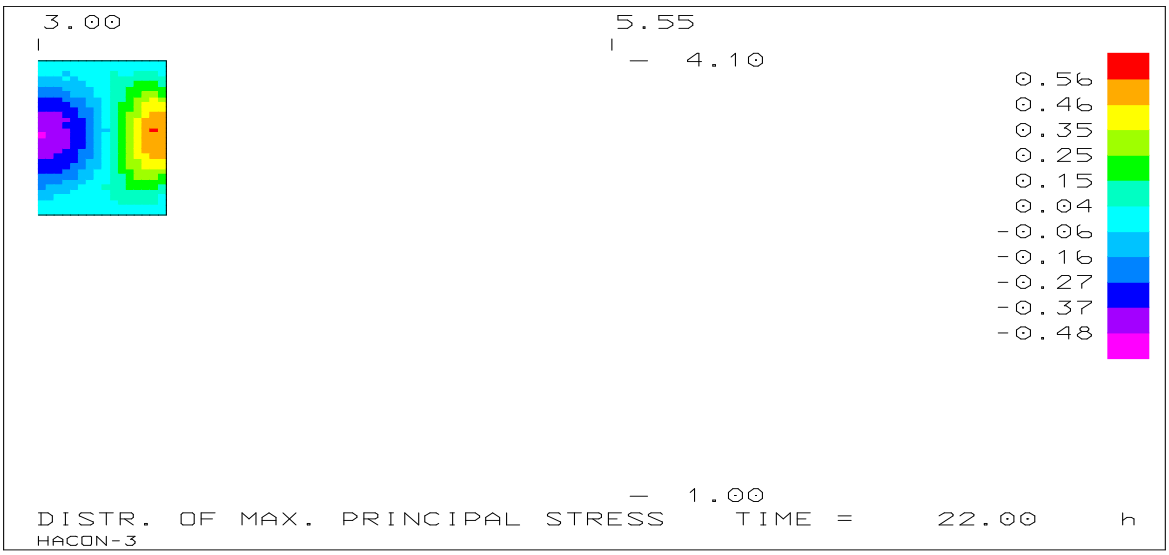

Figure4. 6 (a), Distribution of maximum principal stress at 22 hr. [RCB-1(PT-33)]

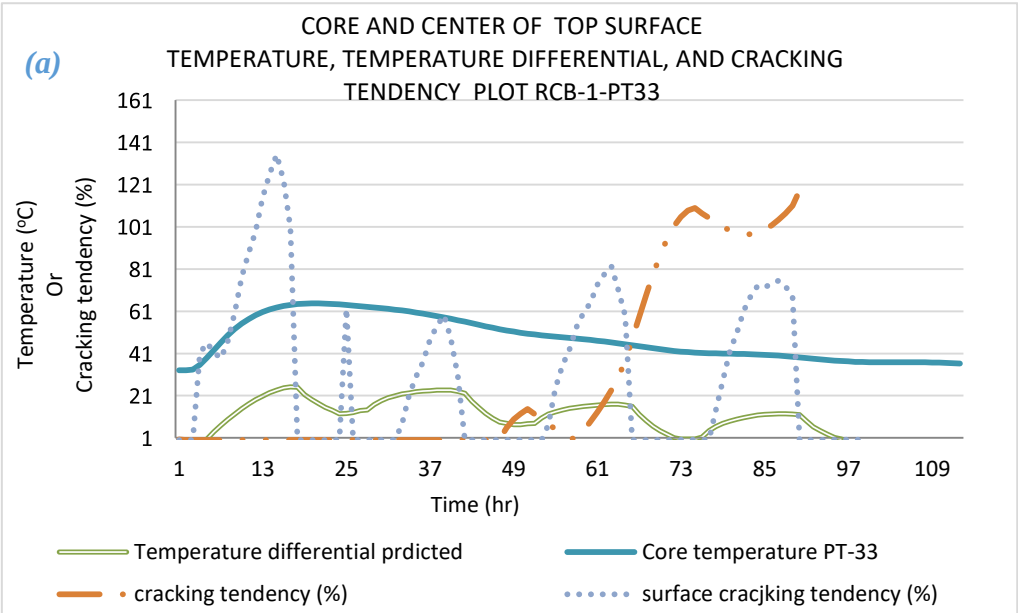

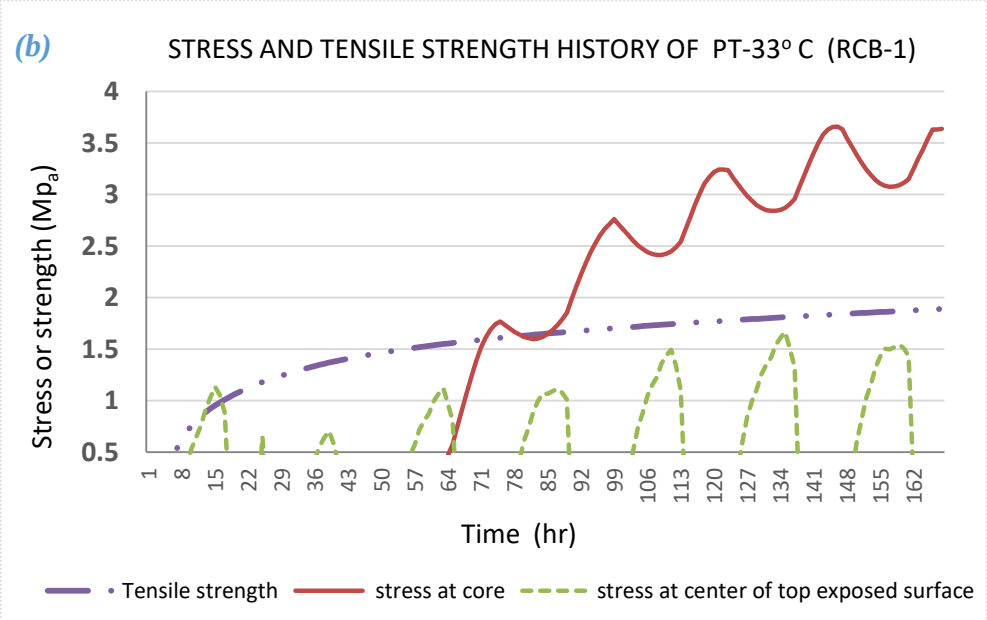

Figure4. 7 core and center of top surface of RCB-1- PT 33 ^{o} c (a) temperature, temperature differential, and cracking tendency (b) stress and tensile strength history .

Temperature differential was high during the night time; during the day time the temperature deferential become minimized due to the reason that the surface absorbs heat from surrounding and directly from sun. Generally, the results show that, the core, center of top exposed surface and side surface was cracked in the case of reference placement (33 ^{o}C). In the next section, analysis results of analytical models of mass concrete with similar material, thermal boundary conditions are presented and discussed.

4.2 Results and discussion of analytic models of CAM and MW.

Thermal and structural Analysis result of analytic models of CAM and MW are presented and discussed in this section. The important results which are not included in this section are presented in Appendix B.

4.2.1 Temperature history of CAM and MW.

The maximum temperature at core, side surface, and top exposed surface of CAM increases with size and placement of temperature. This sensitivity of structure for temperature related to heat of hydration and boundary conditions that the structure was exposed. This also related with strength and stress development. This means, the temperature increased or decreased affects the strength of concrete as reveled in many researches [6]. The effect of casting with

low placement temperature on development of tensile strength is presented in appendix B.

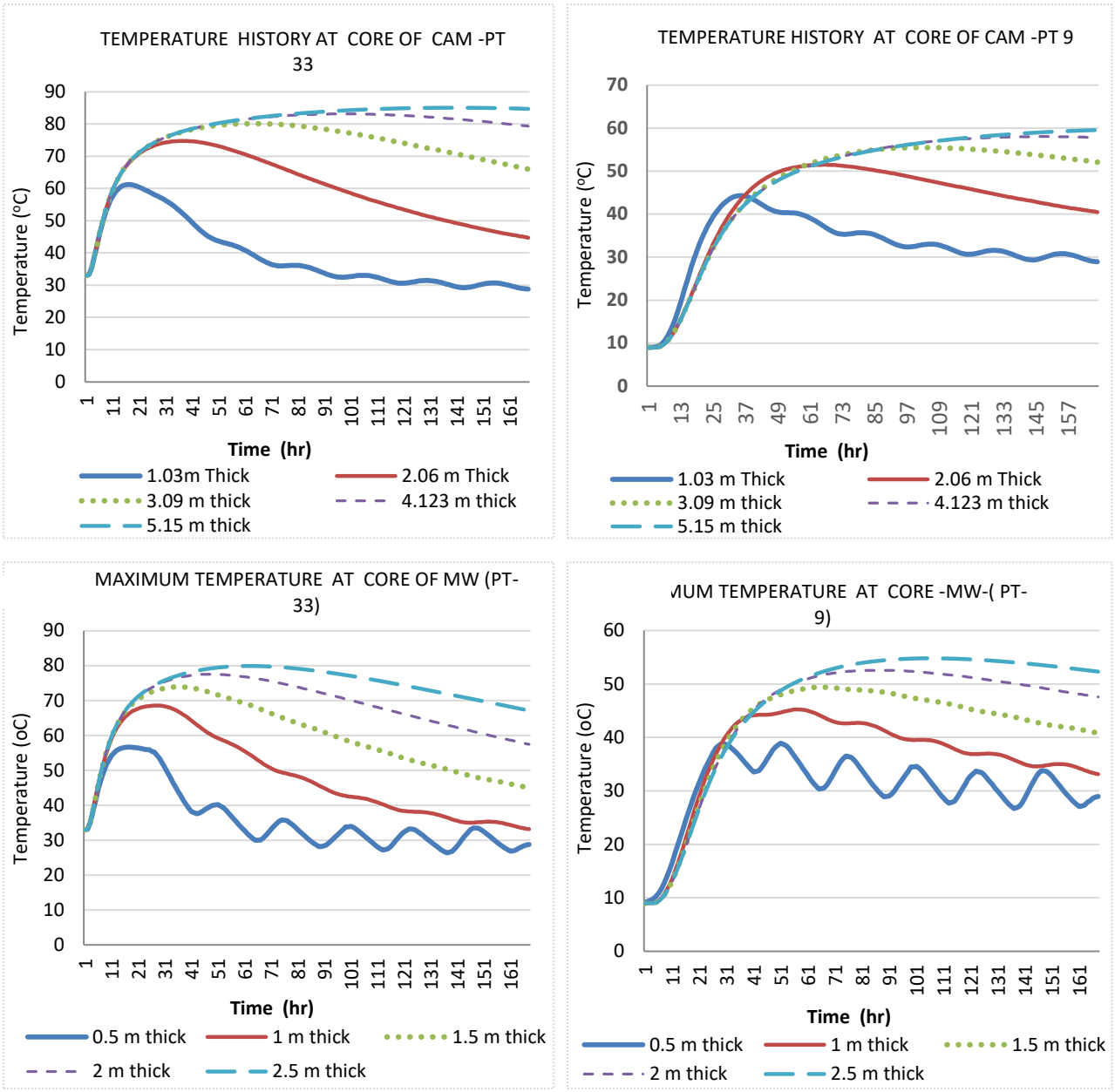

Figure4. 8 Temperature history for early form removal case at core of CAM and MW for PT 33 and 9.

As it can be seen in figure 4.8, the cores of thin sections are more sensitive to ambient temperature than thick sections and this sensitivity is higher in low placement temperature. Thin sections of CAM and MW were not experienced the adiabatic condition at the core because heat was dissipating with form and without form. Core of all size were not in adiabatic condition for 9 ^{o}C placement

temperature case and all sections core maximum temperature were below 60 ^{o}C. This peak temperature controlling was achieved by minimizing the placement temperature from 33 ^{o}C to 20 ^{o}C. Generally, after the peak temperature, heat generation has been moderate after around 1-3 days and heat loss to the surrounding dominated until the concrete reached thermal equilibrium. Refer maximum temperature of CAM and MW in Appendix- B.

4.2.2 Maximum temperature

The rate of heating behavior was affected by placement temperature; rate heating was high at high placement temperature as shown in figure 4.8. This result agrees with the theory that high curing temperature experience high rate of hydration. High rate of heating has been seen in thin sections while blocks were casting with low temperature concrete. This also happened because that thin sections were sensitive to ambient temperature and low surface area to volume ratio will experience high rate of heating by absorb heat from surrounding (ACI 207.1R-96). Significant rate of heating change was not seen when casting concrete at temperature higher than 20 ^{o}C.

It has been observed by many researchers [10] that, mass concrete structures with peak temperatures higher than 70°C are expected to experience an undesirable phenomenon known as delayed ettrigite formation. ACI 301 limits the maximum temperature 158 ^{o} F (70 °C) without mitigation. To avoid delayed ettrigite formation, the maximum temperature has to be reduced below 70 °C. Avoiding this risk of delayed ettrigite formation was achieved by reducing the placement temperature below average air temperature (22 ^{o} C) for both CAM and MW. The temperature history result at center of surface temperature shows that surface temperature was influenced by air temperature immediately after casting. Surface of all sizes are very sensitive for daily air temperature variation. The results also reveal that the temperature rise was high at low PT. Surface maximum temperature was constant for multiple placement of concrete in all sizes except 1.03 m of CAM and 0.5 m thick MW (Refer appendix B surface temperature history of massive wall).

There was no significant maximum surface and core temperature difference between CAM 3.06 m diameter and MW 2.5 m thick. In those sections, reduction of PT from 33 ^{o}C to 9 ^{o}C reduced the maximum surface temperature about 12 ^{o}C and the core by 25 ^{o}C. Precooling the concrete before mix has advantage to shift the core temperature occurrence time forward and this gives time for concrete to develop tensile strength. For example in the case of CAM 3 diameter and 2.5 m thick MW, the cooling of the concrete and reducing PT from 33 ^{o}C to 9 ^{o}C shifts the peak temperature occurrence time by 42 hr.

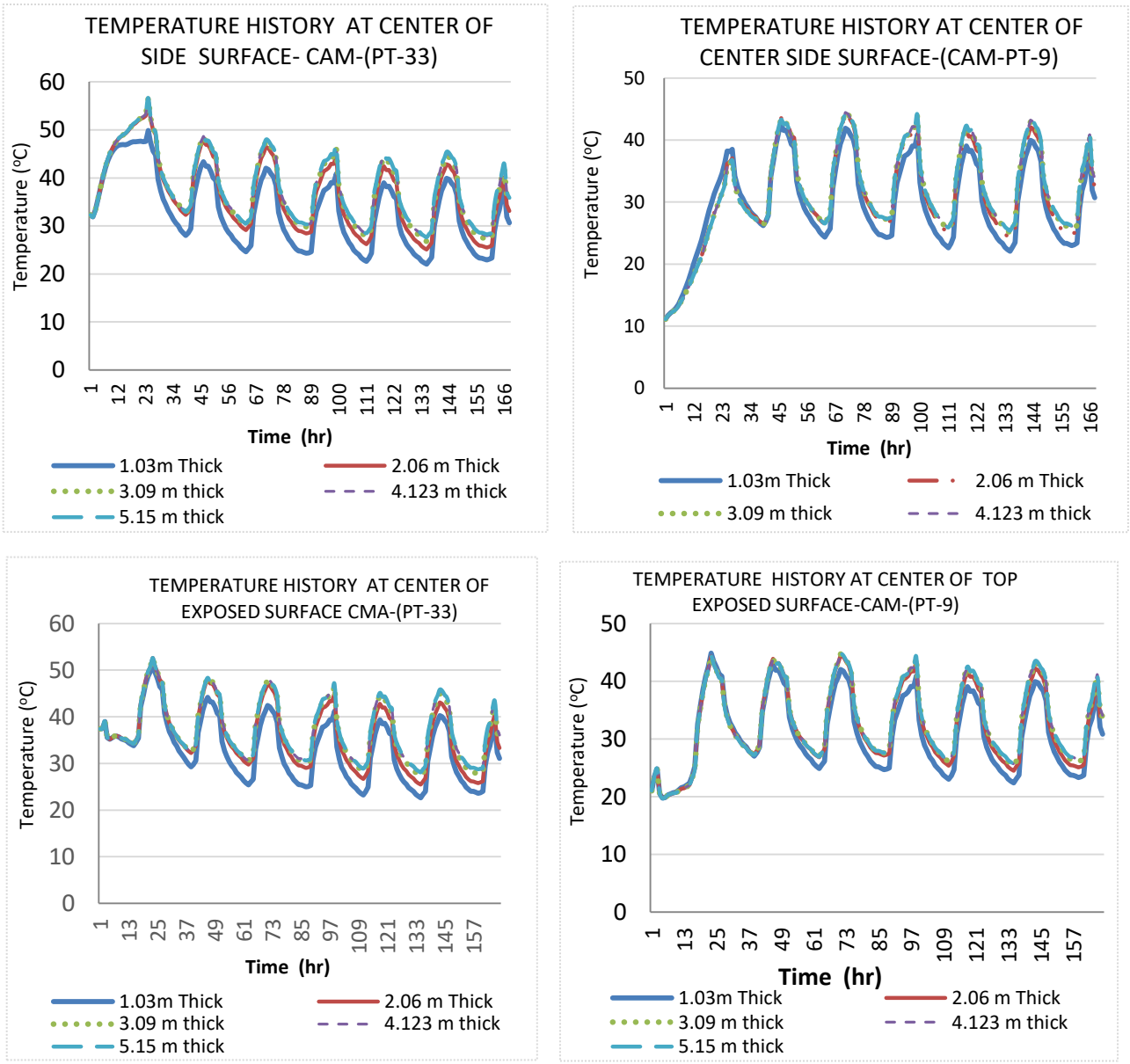

Figure4. 9 Temperature history at center side surface top exposed surface of CAM for early form removal case of PT 33 and 9 ^{o}C

4.2.3 Maximum temperature reduction

Table 4.1 shows relative maximum temperature reductions obtained due to reduction of placement temperature from reference 33 ^{o}C for early form removal case at center of core, top exposed surface, side surface and corner of CAM. The analysis result shows that, size has not significant effect on efficiency of precooling method in reduction of maximum temperature.

(a)	Maximum center side surface Temperature Reduction		
Thickness(m)	**PT-26**	**PT-20**	**PT-9**
1.03	6.7%	12.9%	15.0%
2.06	**9.5%**	**18.5%**	**21.4%**
3.09	**9.7%**	**18.9%**	**21.4%**
4.123	**9.7%**	**18.7%**	**21.5%**
5.15	**9.7%**	**18.7%**	**21.6%**

Maximum Center Core Temperature Reduction			
Thickness(m)	**PT-26**	**PT-20**	**PT-9**
1.03	11.3%	18.9%	27.6%
2.06	**9.9%**	**18.2%**	**31.1%**
3.09	**9.3%**	**17.3%**	**30.8%**
4.123	**9.0%**	**16.6%**	**30.2%**
5.15	**8.7%**	**16.2%**	**30.0%**

(b)	Maximum Center of top exposed surface Temperature Reduction		
Thickness (m)	**PT-26**	**PT-20**	**PT-9**
1.03	**3.0%**	**5.9%**	**12.6%**
2.06	**3.7%**	**7.3%**	**15.4%**
3.09	**3.7%**	**7.3%**	**15.0%**
4.123	**3.7%**	**7.3%**	**15.0%**
5.15	**3.7%**	**7.3%**	**15.0%**

Maximum Corner point Temperature Reduction			
Thickness (m)	**PT-26**	**PT-20**	**PT-9**
1.03	**0.8%**	**0.8%**	**0.7%**
2.06	**0.2%**	**0.4%**	**0.7%**
3.09	**0.2%**	**0.4%**	**0.7%**
4.123	**0.2%**	**0.4%**	**0.7%**
5.15	**0.2%**	**0.4%**	**0.7%**

Table4. 1Maximum temperature reduction by percentage at (a) core and center of side surface (b) center of top exposed surface and top corner –CAM.(Early form removal case)

Significant maximum temperature values change has not seen at top corner edges for reduction of placement temperature from reference (33 ^{o}C), according to the results maximum temperature value of 5.15 m diameter CAM was reduced by 21%, 39%, 73 % at center of side surface temperatures for reduction of PT by 9.7%, 18.7%, 21.6%, respectively. Similarly maximum temperatures value

was reduced by 3.7%, 7.3%, 15.0% at center of top exposed surface, by 0.2%, 0.4%, 0.7%, top corner and by 8.7%, 16.2% 30.0% at the center core for respective placement temperature reduction. In case of 2.5 m thick massive wall maximum temperature values was reduced by 9.6%, 18.6%, 21.7% at center of side surface, by 9.4%, 17.5%, 31.4% at core for respective placement temperature reduction. This result is quite similar with 3.06 m diameter CAM. See table 4.2

Generally, the result shows that 1 ^{o}C reduction of placement temperature reduced the peak temperature by 1.2-1.5 % at center of side and core of the structure and by 0.5-0.6 % at top exposed surface.

Maximum Temperature reduction at center side surface					Maximum Temperature reduction at Center Core			
Thickness(m)	PT-26	PT-20	PT-9		Thicknes s(m)	PT-26	PT-20	PT-9
0.5	7.9%	15.4%	20.8%		0.5	9.6%	17.0%	31.3%
1	9.5%	18.5%	22.2%		1	10.4%	19.3%	34.0%
1.5	9.6%	18.7%	21.7%		1.5	10.2%	19.1%	33.2%
2	9.6%	18.7%	21.7%		2	9.8%	18.2%	32.2%
2.5	9.6%	18.6%	21.7%		2.5	9.4%	17.5%	31.4%

Table4. 2 Maximum temperature reduction by percentage at center core and center of side surface –MW.

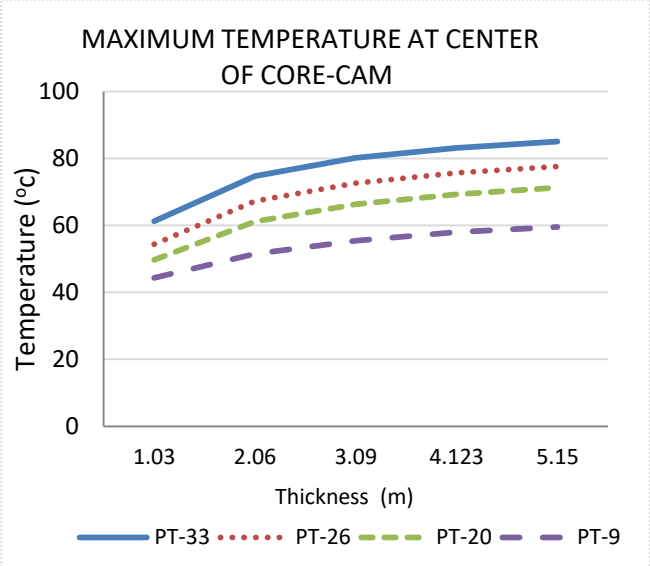

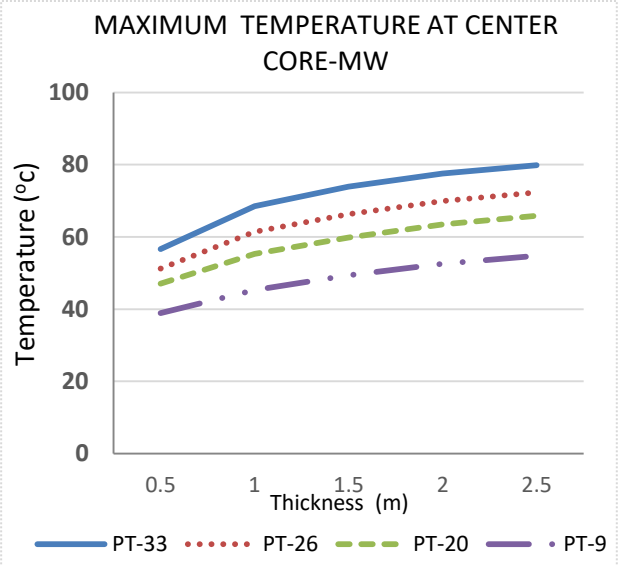

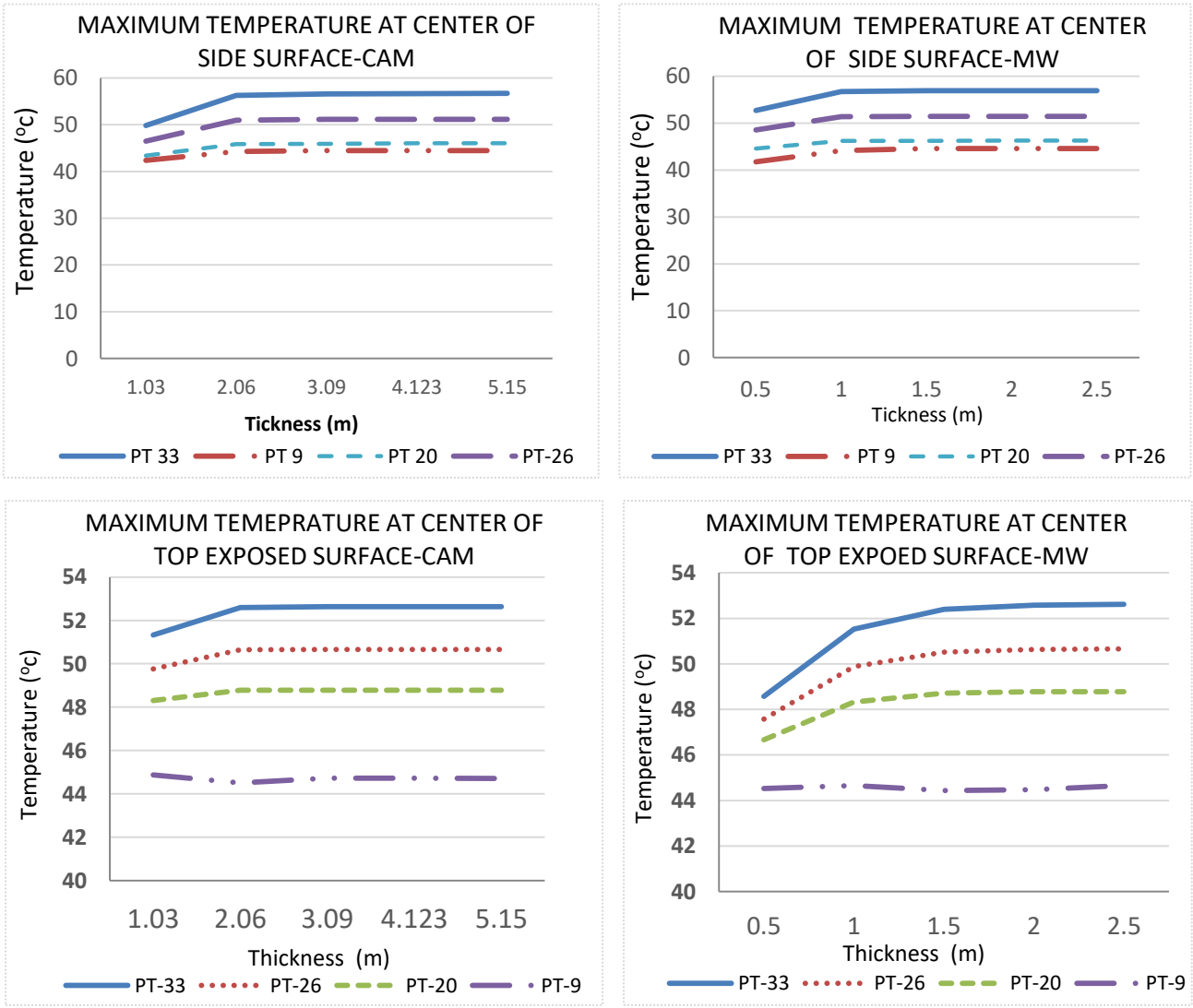

Figure4. 10 Maximum temperature of CAM and MW for early form removal case at center of core, center of side center of top exposed surface.

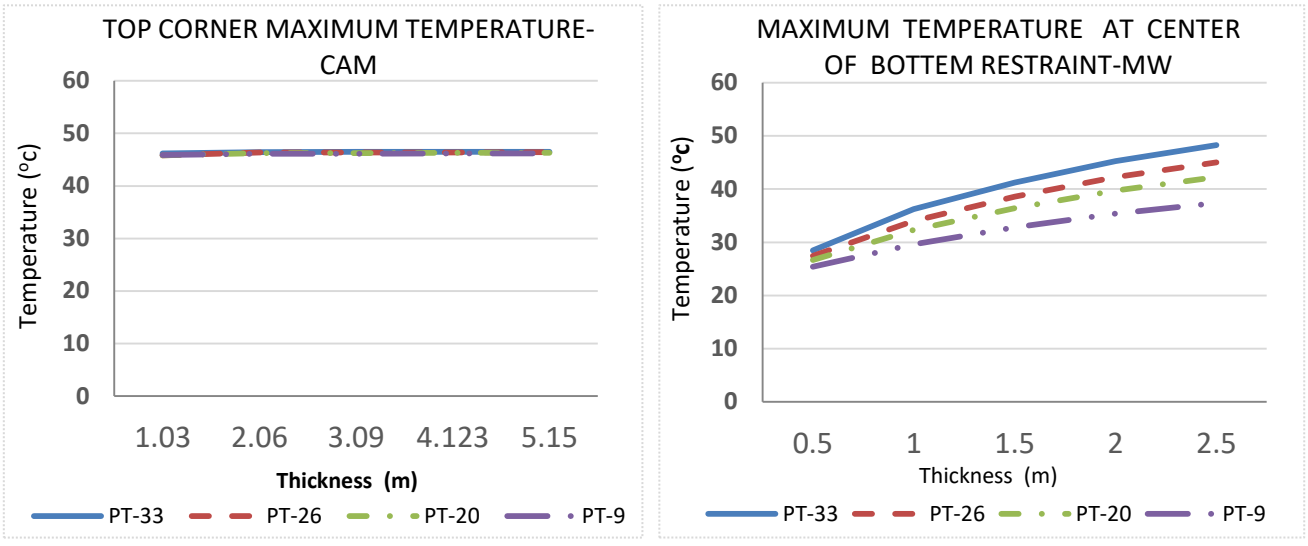

Figure4. 11 Maximum temperature at top corner (CAM) and at center of bottom restraint MW.

4.2.4 Maximum temperature differentials

As it can be seen in figure 4.12 and 4.13, precooling concrete components before the mix significantly reduced the temperature differential (the temperature difference of core and surface), but it was not sufficient to reduce the differential below 20 ^{o}C for large sections. Precooling was more effective and efficient in reduction of temperature differential in thick sections than thin sections.

As per the recommendation of different codes the temperature deferential between the core and the surface is restricted to 35 ^{o} F (19.43 ^{o} C) for any type aggregate. Concerning this limit, precooling was not efficient. But it doesn't mean that temperature differential exceeded this limit initiate cracking, because temperature deferential limit recommendation is not based on performance of concrete. For example, crack was initiated at center of side surface of CAM 1.03 m thick by 10.7 ^{o}C temperature differentials at 86 hr while the top exposed surface cracked by 22.5 ^{o}C during the heating period. This indicates that, the surfaces can crack at higher or lower temperature differentials depending on strength development and the restraint condition.

As shown in figure 4.12 that, the temperature differential has not shown significant change in thin sections for any placement temperature. For example 5.8 ^{o}C temperature differential drops was observed at side surface of 1.03 m diameter CAM for reduction of placement temperature from 33 ^{o}C to 9 ^{o}C while in 5.15 diameter CAM 20 ^{o}C temperature deferential was noticed for the same placement temperature reduction. In other word, temperature deferential drop increase with size and placement temperature. In fact, an increase in size has not significant effect on the magnitude of surface maximum temperature for a given placement temperature. In order to gate full advantage of precooling method and reducing temperature differentials, the core of structures should be casted at low temperature concrete and the side with relatively high.

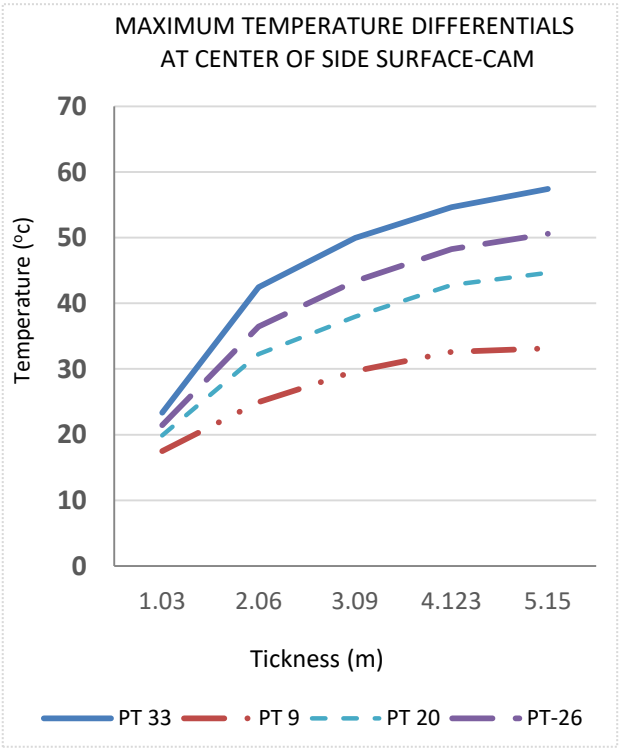

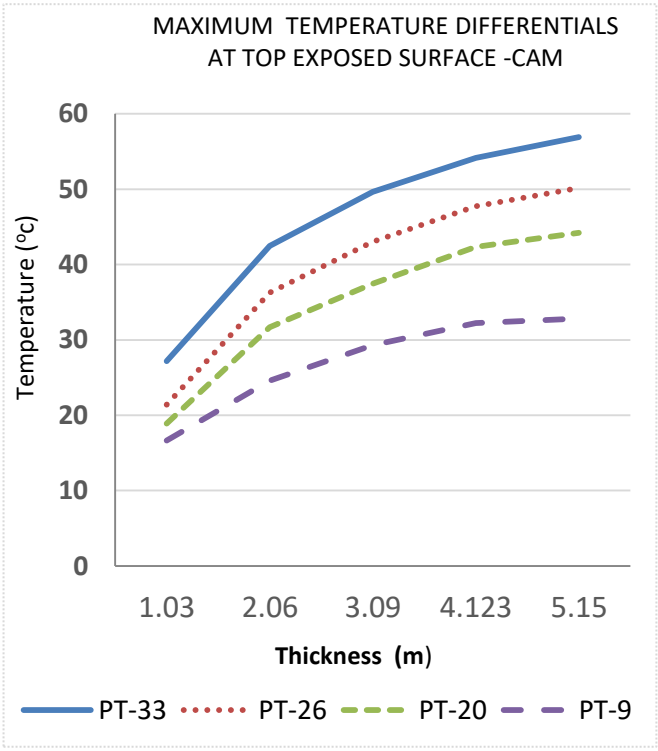

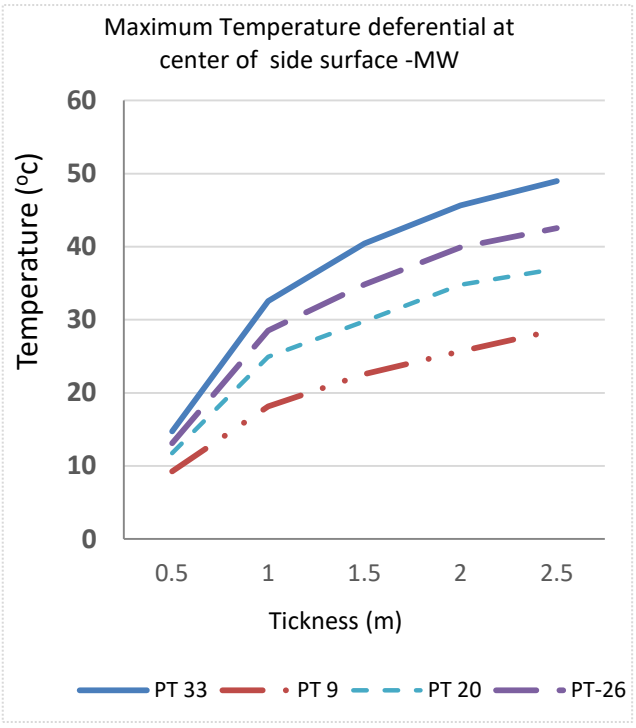

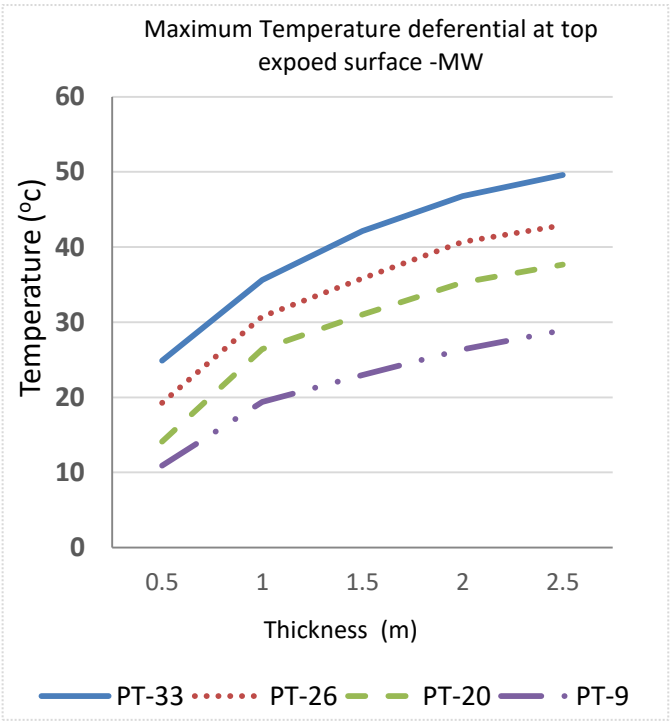

Figure4. 12 Maximum temperature differentials at center of side surface and top exposed surface, of CAM and MW for early form removal case.

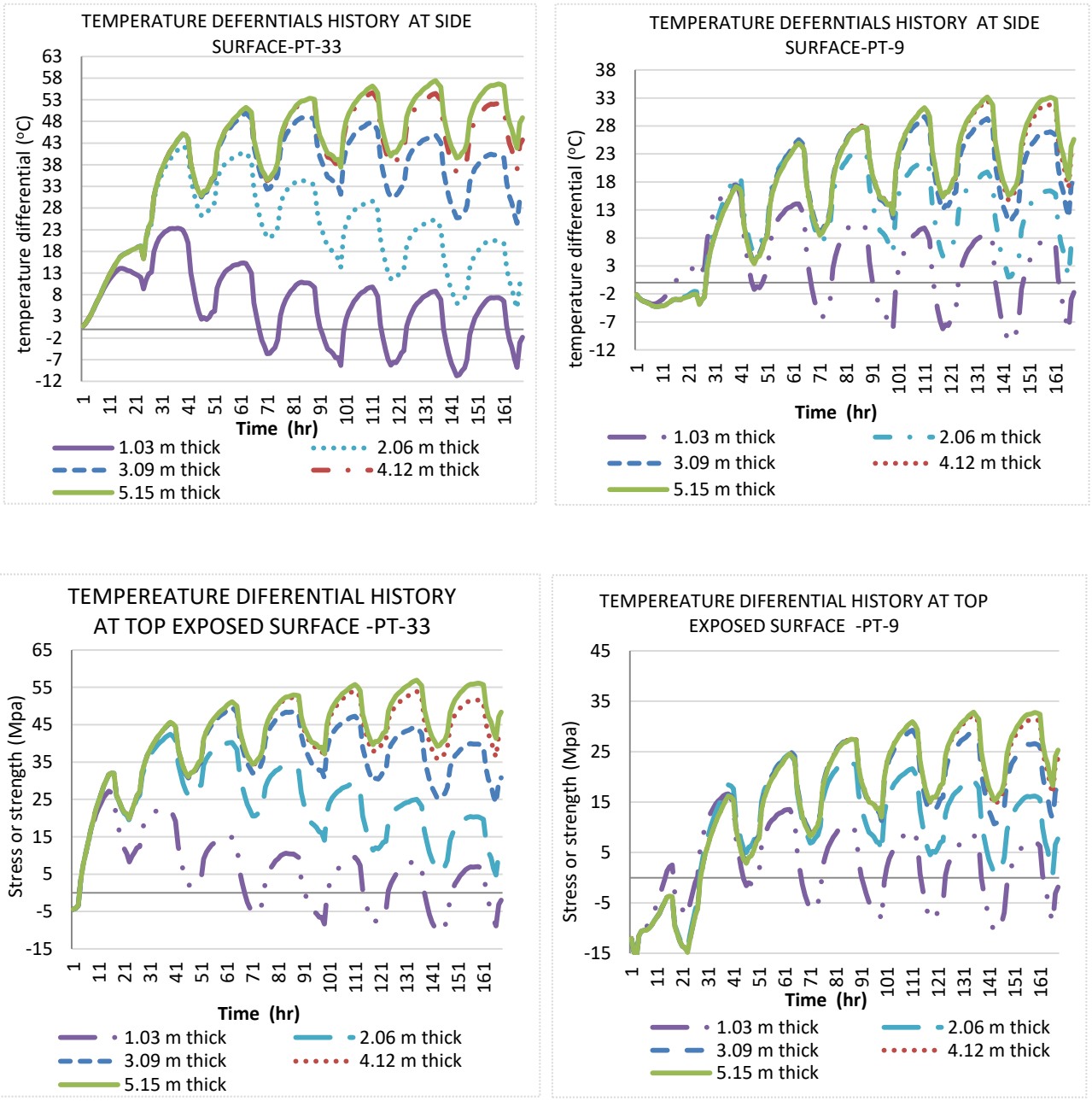

Figure4. 13 Temperature differential history of CAM for early form removal case at center of side surface and top exposed surface for PT 33 ^{o} C and PT 9 ^{o} C.

During large volume concrete pouring work, it is advantageous to cast the core with full effort of cooling and the surface with less effort to gate low temperature deferential drop. This means that, pouring the core with lower placement temperature. Temperature differentials at surface were very high and this means applying precooling method alone was not effective to minimize the temperature deferential. The result also indicates that other methods should combine with precooling method to minimize temperature differentials for thick sections.

Temperature deferential history for low placement temperature case shows negative differential at very early age, this shows that in a casing of low placement in hot weather surfaces concrete hydrated faster at higher rate than the core and absorbed heat from the surrounding this produce negative temperature deferential at surface at very early age.

4.2.5 Maximum Stress history.

Figure 4.14, presents the total stress at the core of CAM with respect to time for different sizes and multiple placement temperature. Stress history results are collected at points of interest which are located at the core, center side surface, center of top exposed surface and top corner of the finite element model. In the analysis of analytical models the worst scenario of form removal at early age (24 hr) and delayed form removal case are considered.

Stress history plot indicates that the surface undergoes tensile (positive) stress as the concrete hydrates and expands, while the core experiences compressive stress. This is consistent with the theory that a faster hydrating central region of a massive concrete structure will be in compression as it tries to expand, but it is restricted by the less mature concrete around it during cooling phase. At early age, form removal cause thermal shock. As shown in the figure 4.14, thermal shock stress which happened immediately after the forms removed was avoided by delaying the form removal time, but the core compression stress decrees and became susceptible for tensile stress. Thin sections (<=2.06 m) were found in tension in cooling phase in both form removal case. Tensile stress at core was developed during cooling phase and the critical time for tensile stress development starts from the point of “zero stress” shortly after the peak temperature.

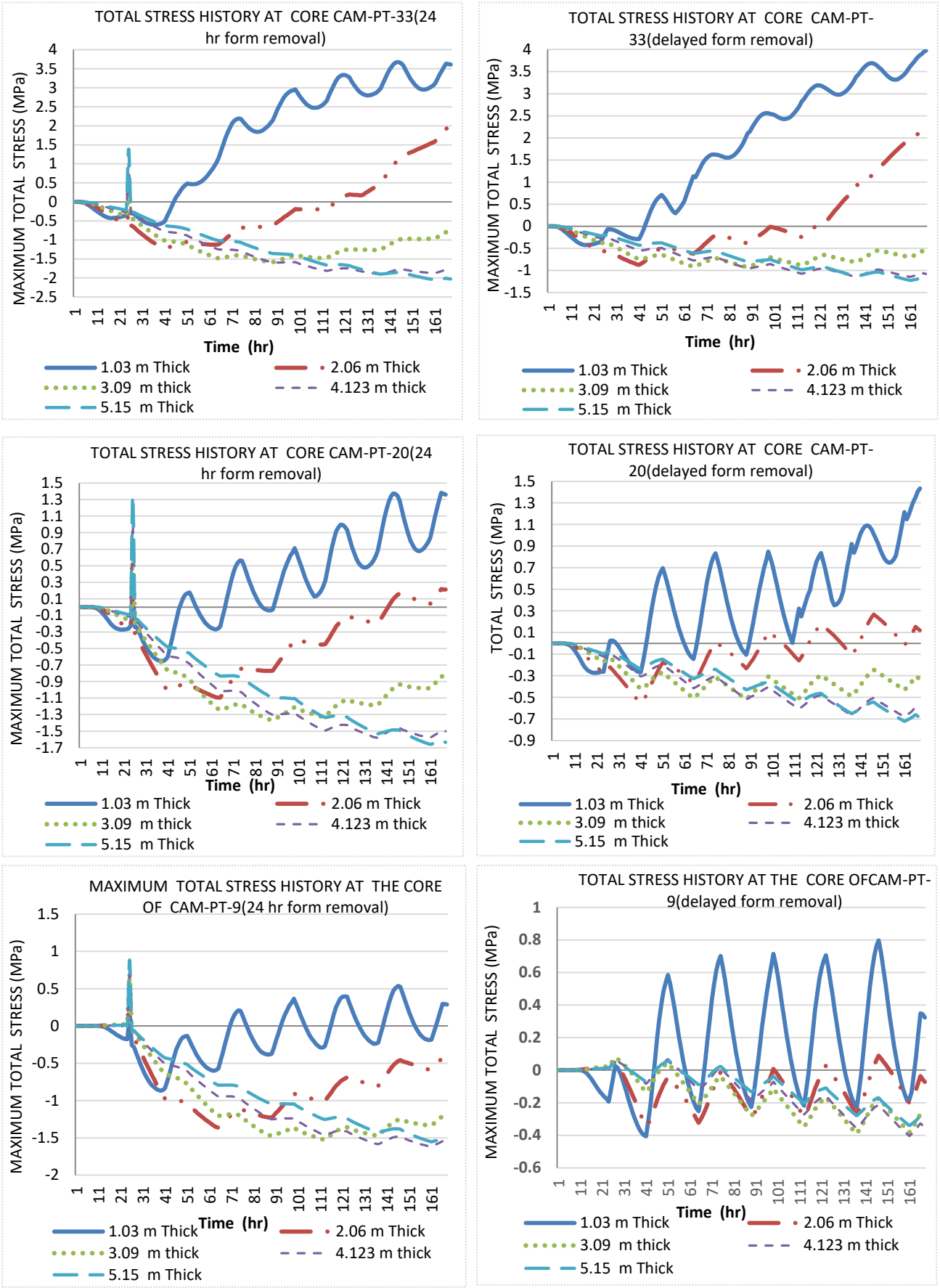

Figure4. 14 Maximum total stress history at center of core of CAM with different PT and form removal case.

The core started to contract due to temperature drop during cooling but the concrete has developed strength and stiffness, and this cause tensile stress to be initiated. Core of thin sections are susceptible for cracking due to high tensile stress as shown in figure 4.14.

The magnitude of tensile stress development at core section of thin sections was very greatly dependent on the placement temperature. For example, 3.98 MPa tensile stresses was developed at the core of 1.03 m diameter CAM for 33 ^{o}C placement temperature and the magnitude diminished to 0.8 MPa when the placement changed to 9 ^{o}C.

The stress development at side surface was high for early form removal case because the surface was exposed to the high cooling rate and temperature differential. The influence of the rate of cooling on stress development of side surface was high for thin sections in a case of delayed form removal. The tensile strength at surface changed to compression when the surface cools, then the tensile stress developed again and increased as shown in figure 4.15. This tensile stress was high in magnitude for thin sections for high placement temperature but in thick sections, high stress magnitude was observed in low placement temperature. This was caused by restraint due to mechanical support.

The stress development of top exposed and side surface was affected by daily temperature difference. The stress at night time reached the peak and diminish to low stress level during the day time. In a case of early form removal thermal shock at top exposed surface was the main cause to produce high tensile stress as shown in figure 4.16. The magnitude of this stress was decreased as the placement temperature was decreased.

During early age tensile stress was developed at top exposed surface after the form removed and became increased as the same fashion of temperature deferential. In case of delayed form removal the stress continuously increased up to 168 hr.

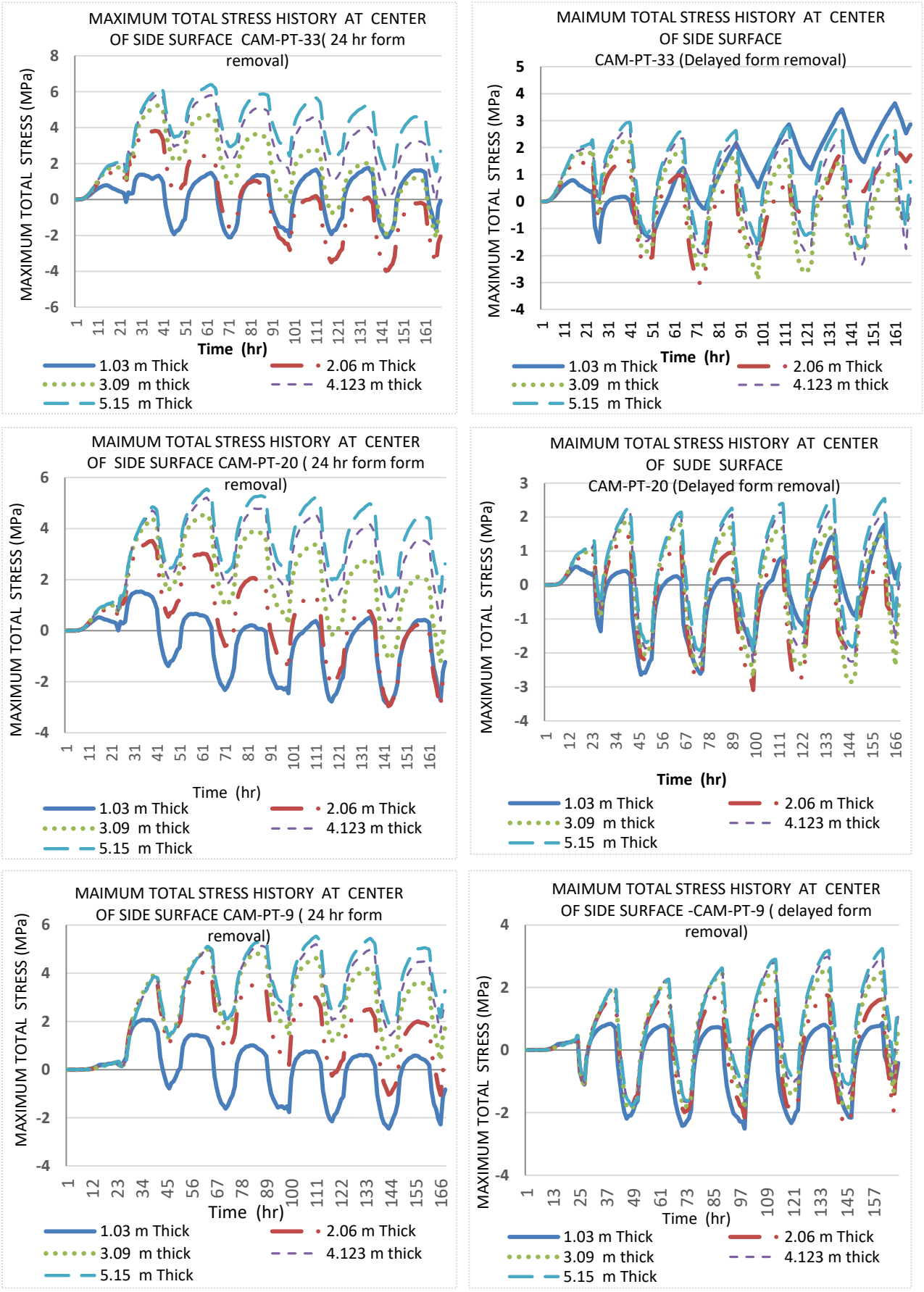

Figure4. 15 Maximum total stress history of CAM at center of side surface for different PT and form removal case.

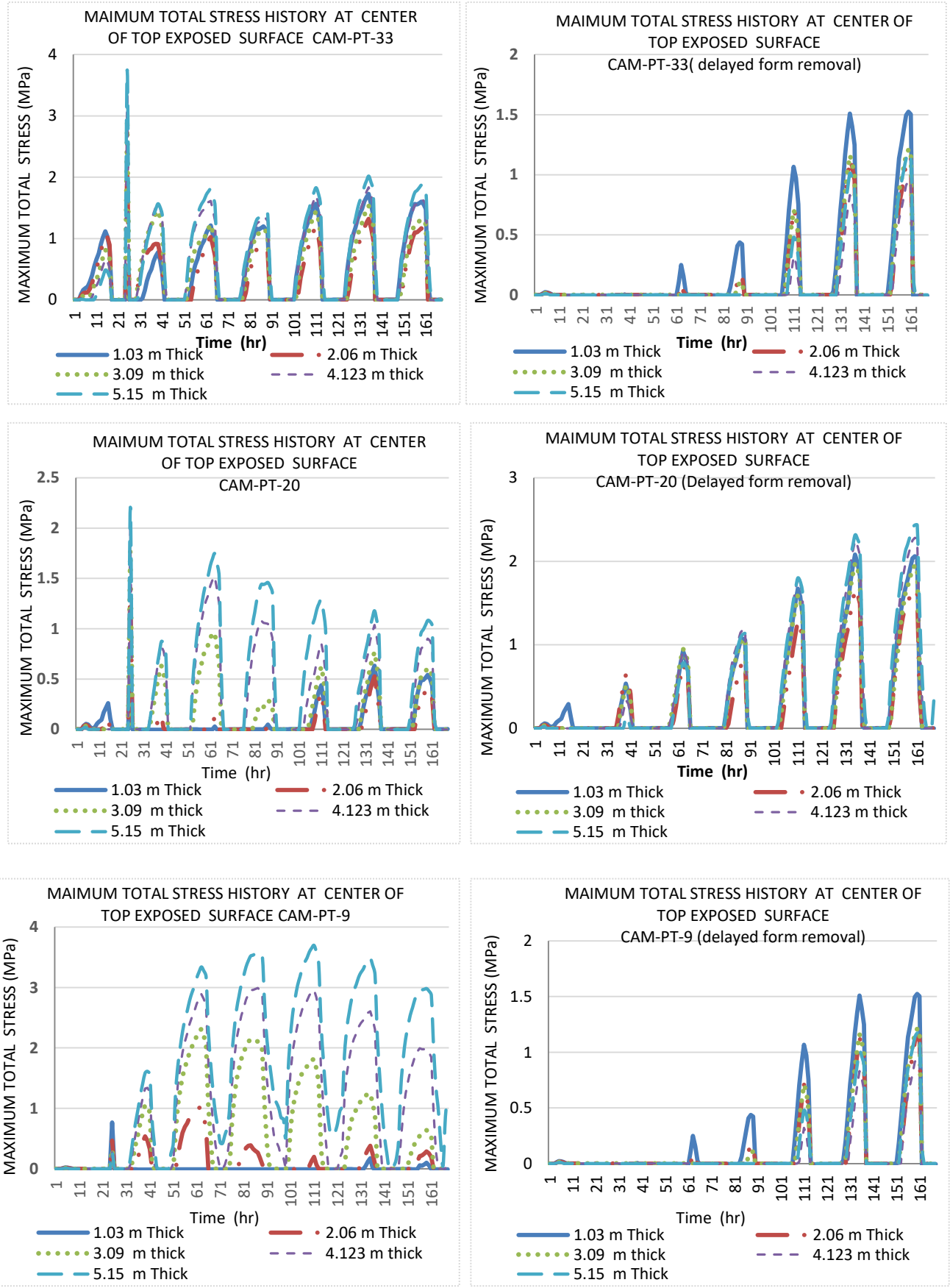

Figure4. 16 Maximum total stress history of CAM at center of top exposed surface for different PT.

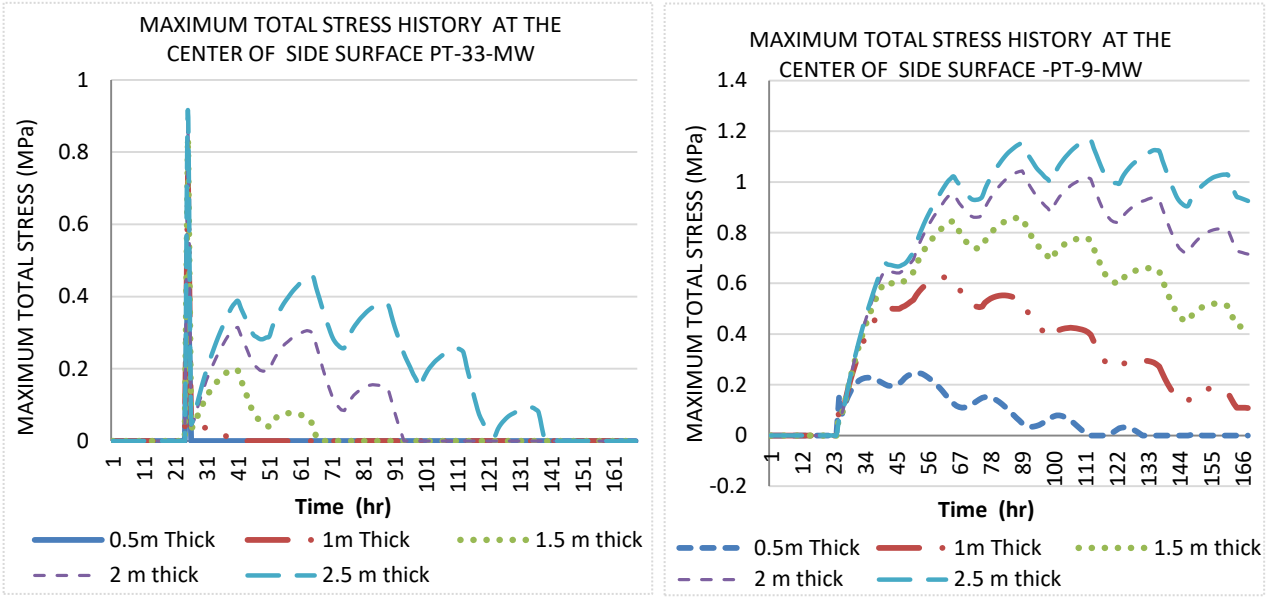

Figure4. 17 Maximum total stress history at center side surface of MW for PT 33 and 9.

Stress analysis result of MW shows that, the center of side surface of MW found to be sensitive for thermal shock. This sensitivity was high at high placement temperature. This sensitivity was related with concrete temperature at time of form removal. The rate of hydration was high at high placement; surface temperature in case of high placement temperature was hotter than low placement surface. This means during form removal the hottest surface was experienced high thermal shock and result in high stress. In case of low placement temperature, the side surface cools at relatively same rate as the core until the form removed. In a case of high placement temperature, while the form removed from the surface, the surface cools relatively faster than the core and this produce high thermal gradient.

The result presented in figure 4.17, for a case of 9 ^{o}C placement temperature, shows that, thick sections experienced higher side surface stress, because the temperature differentials was relatively higher than thin sections.

As it can be seen in figure 4.18 and 4.19, at the bottom restraint thin sections experience high stress in all placement temperature. The stress history at the bottom of restraint shows that the stresses initiate immediately after the form is removed.

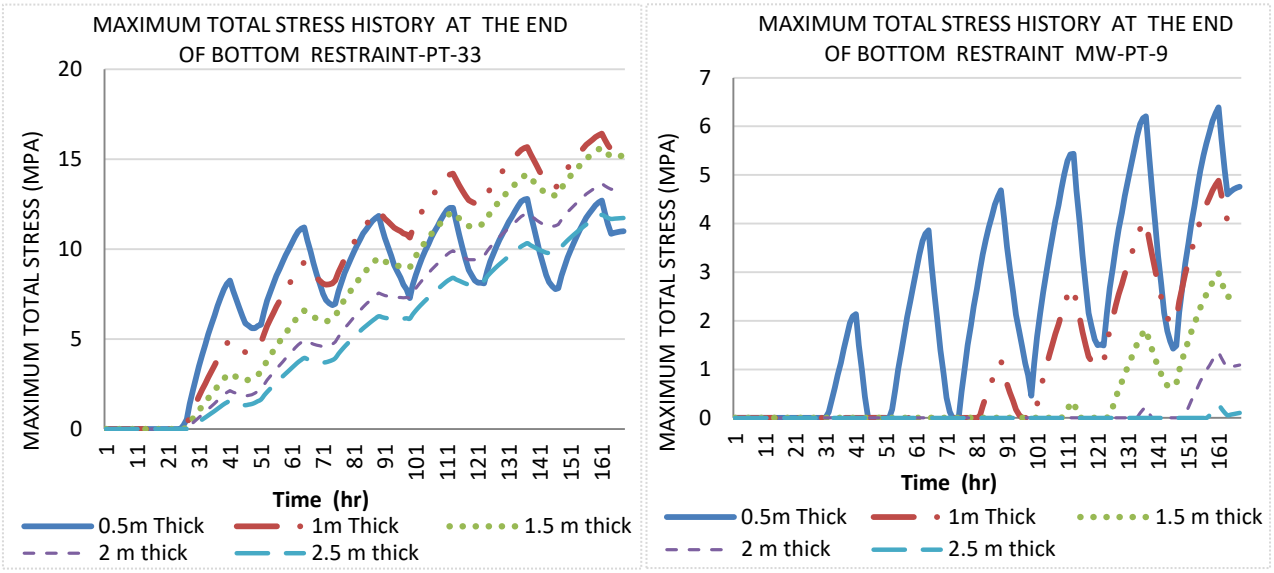

Figure4. 18 Maximum total stress history at End of bottom restraint of MW for PT 33 and 9

High restraint stress reduction was observed for reduction of placement temperature. Thin sections of MW are very sensitive for restraint stress and this can cause through cracks. The stress development was highly affected by the placement temperature, for example, reduction of placement temperature for 0.5m thick section MW by 72 % was reduced the restraint stress by 53 %.

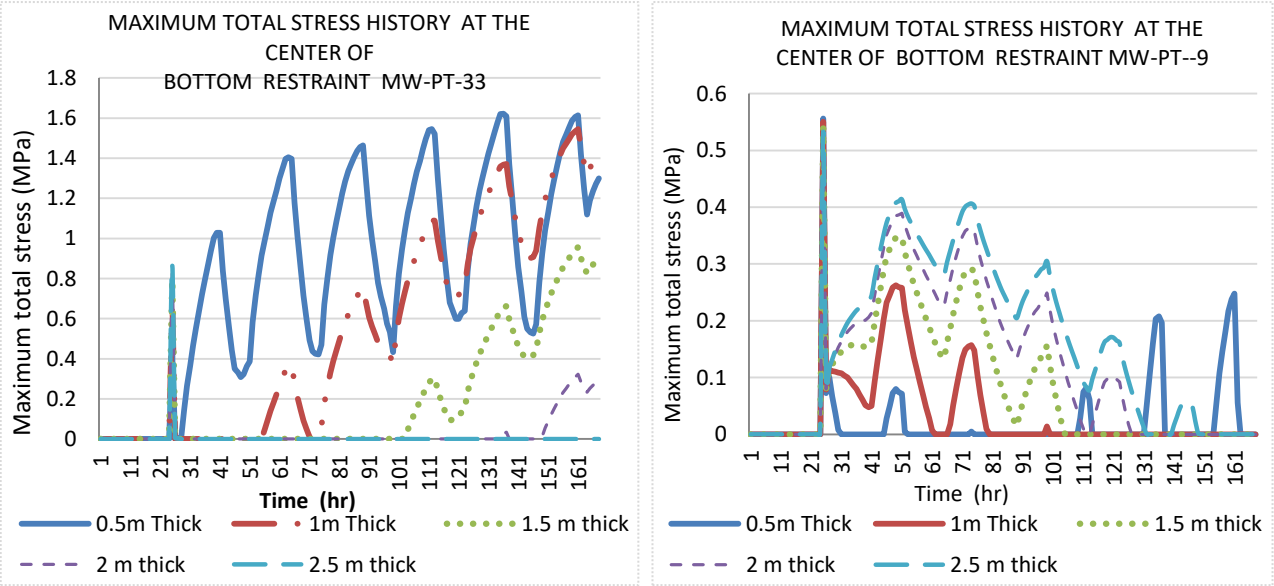

Figure4. 19 Maximum total stress history at center of bottom restraint of MW for PT 33 and 9.

4.2.6 Maximum total stress and stress reduction.

Maximum stress results of all analytical models at top exposed surface, top corner and core with multiple placement temperature are presented in figure 4.19. For early form removal case refers Appendix B.

As shown in the figure 4.20, maximum stress was significantly affected by the size and placement temperature. At side surface, thin sections ware more sensitive for placement temperature and result in higher magnitude of maximum stress. This is true for restraint side surface and core of CAM but in case of top exposed surface. The maximum stress increased when size and placement temperature increased. The maximum stress at top corner of CAM decreased as the size increased for all placement temperature case.

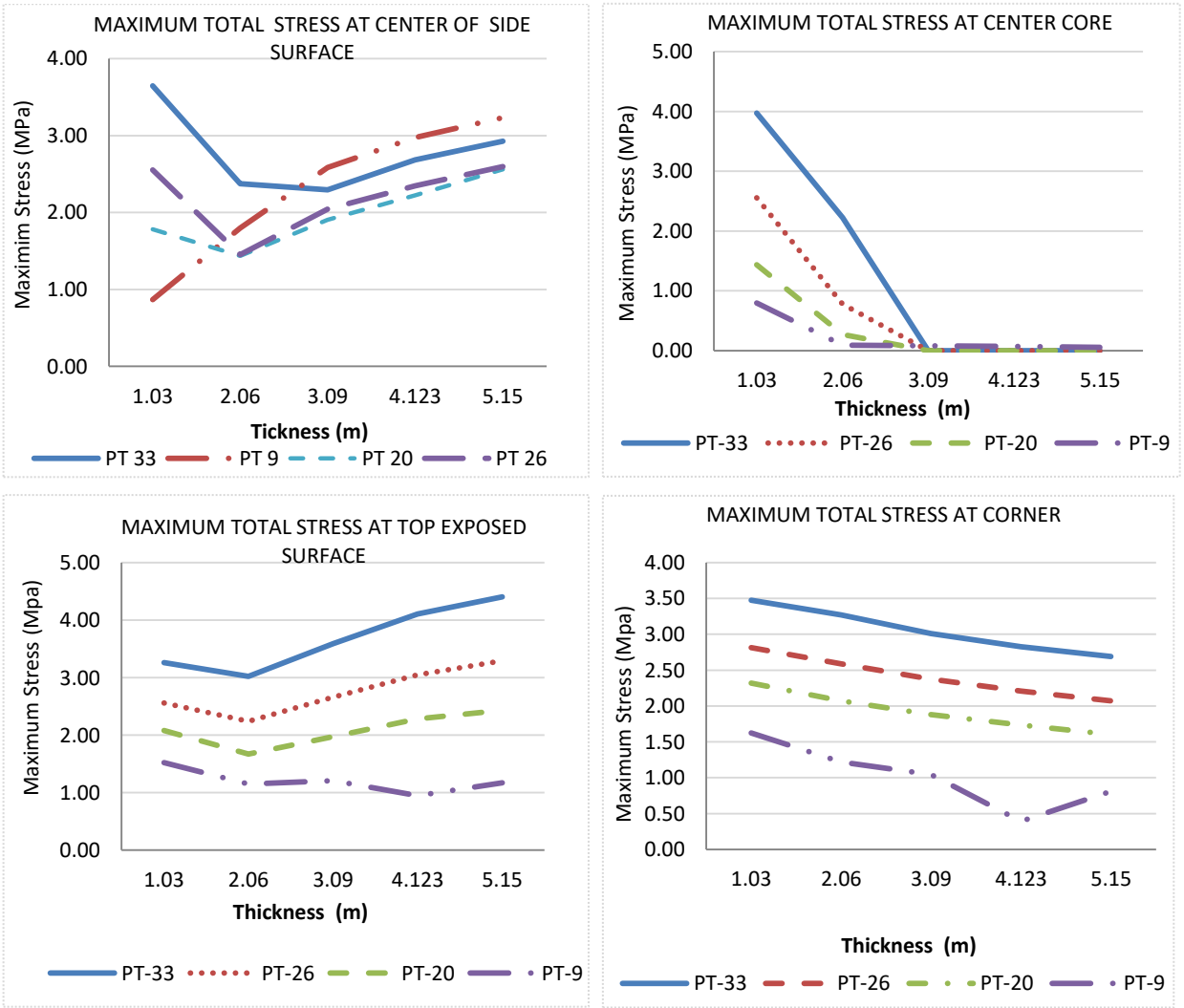

Figure4. 20 Maximum total stress at center core, center of side surface, center of top exposed surface and top corner of CAM (for delayed form removal case)

Similarly, maximum stress of massive wall found significantly reduced in case of low placement temperature. The reduction of placement temperature was reduced the maximum stress below 2 MPa during the early age.

4.2.7 Cracking tendency (stress –Strength ratio).

Stress strength ratio shows the cracking tendency of concrete. Cracking tendency of core, center of top exposed surface, center side surface and top corner of CAM are presented in figure 4.21 and 4.22. Similarly cracking tendency at center of side surface, edge and center of bottom restraint are presented in figure 4.23. If cracking tendency is exceeds 100 % the crack is expected.

The cores of thin sections of CAM have high degree of cracking at early age as shown in both form removal cases. This susceptibility of thin sections for cracking at early age was controlled by 20 ^{o}C and 9 ^{o}C PT; this means precooling method was efficient to reduce the tendency of cracking at early age. In case of early form removal the efficiency was poor to control thermal shock. Similarly by reducing the placement temperature, crack tendency at side surface was not minimized enough to avoid cracks in both case of form removal. The cracking tendency at top exposed surface and top corner was minimized below 100 % by reducing the placement temperature to 9 ^{o}C. Similarly in thick section of massive wall the cracking tendency was minimized below 100 % at bottom restraints by reducing the reference placement temperature (33 ^{o}C) to 26 ^{o}C.

Generally, cracking tendency of early age CAM and MW concrete was greatly affected by thermal shock of early form removal, self-restraint due to temperature differentials, and external restraints.

High cracking risk was seen at the end edge of the bottom restraint as shown in figure and all thickness of massive walls were cracked in case of PT 33 ^{o} C .

As shown in figure 4.23, PT 20 ^{o} C was more efficient than PT 9 ^{o} C in reduction cracking tendency of thick sections (> 1 m) at side surface of MW. In case of reduction of placement temperature to 20 ^{o}C shows the same reduction of cracking risk in the same fashion as seen in temperature deferential reduction.

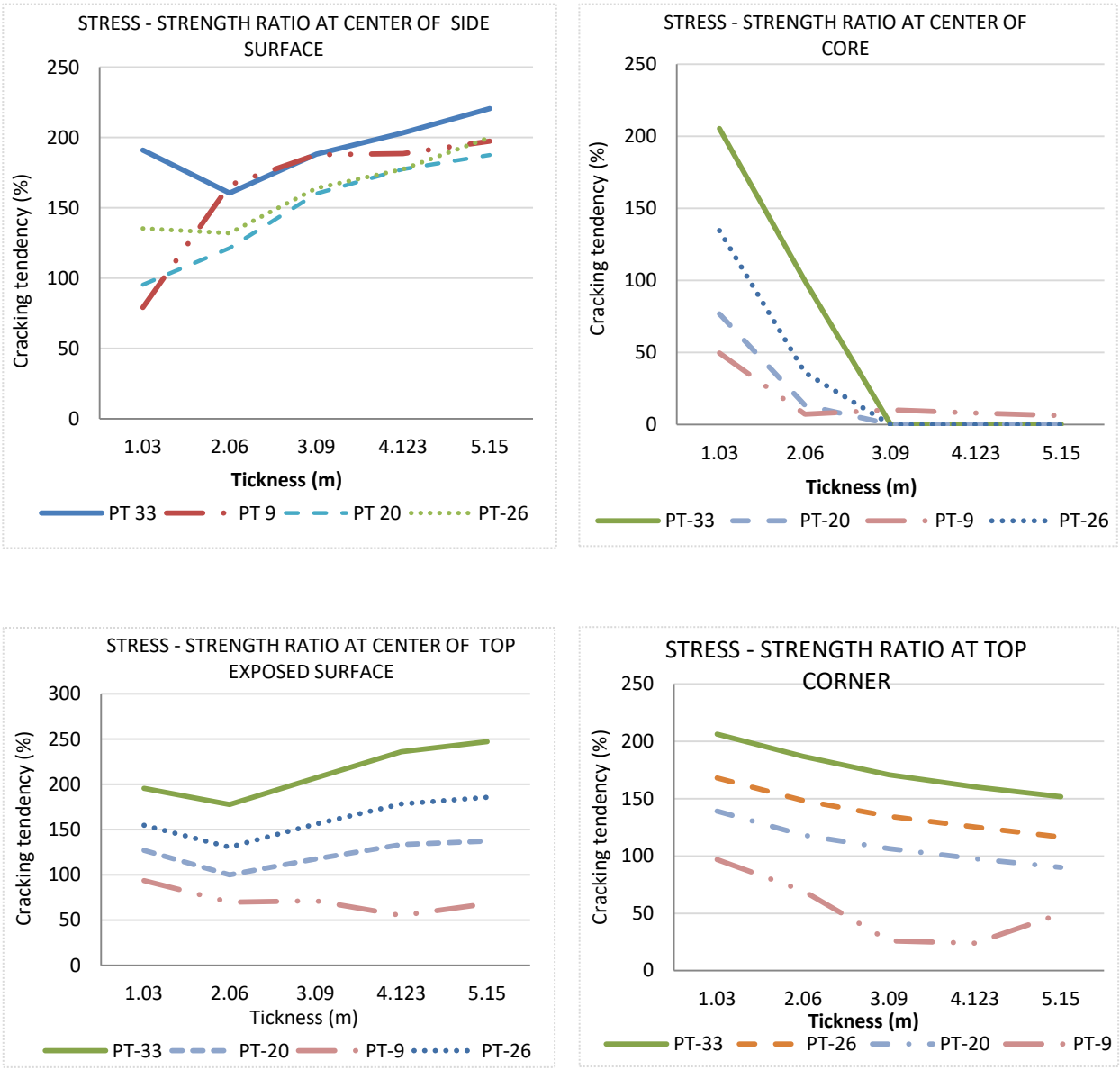

Figure4. 21 Cracking tendency by percentage at center core, center of side surface, center of top exposed surface and top corner of CAM for delayed form removal case.

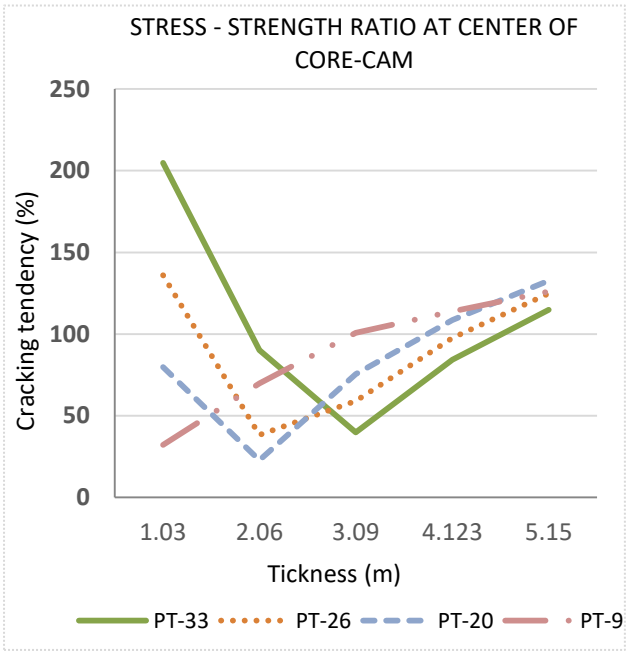

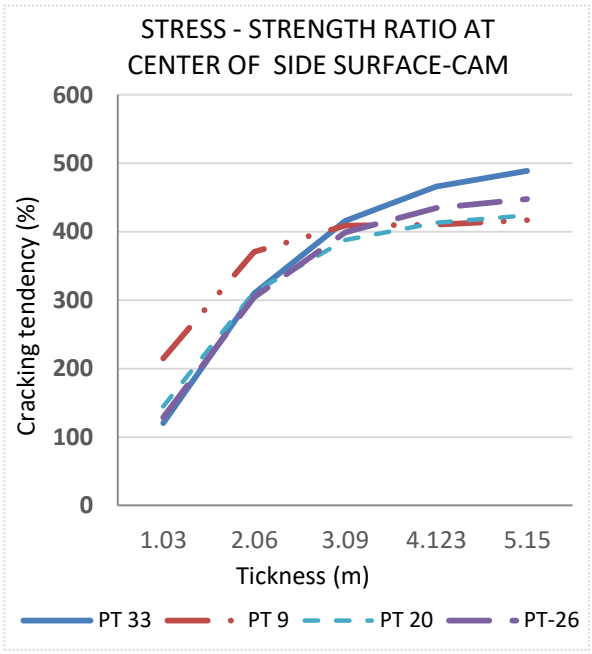

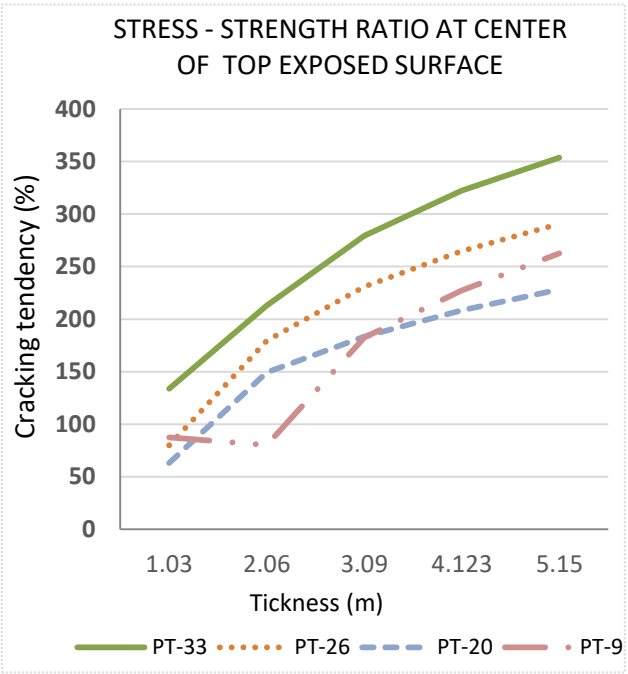

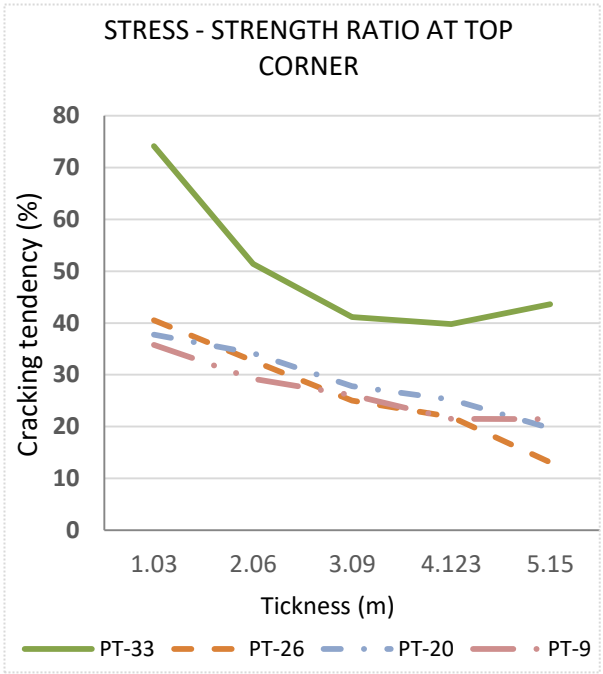

Figure4. 22 cracking tendency by percentage at center core, center of side surface, center of top exposed surface and top corner of CAM for early age form removal case.

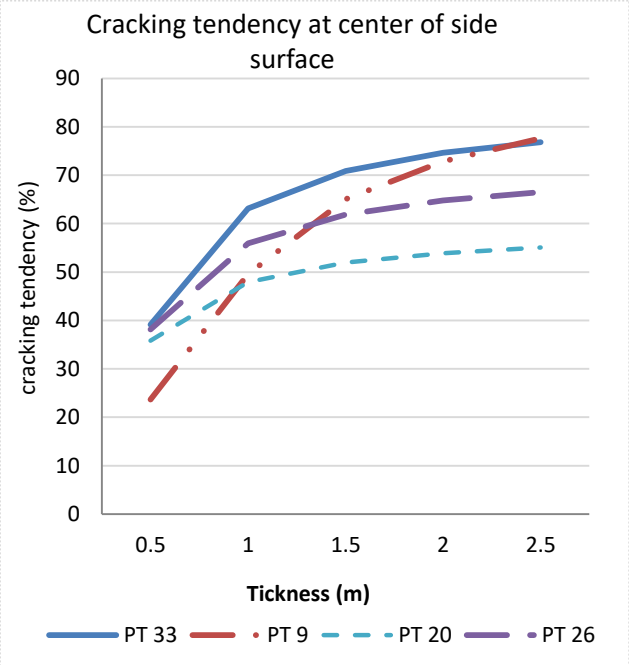

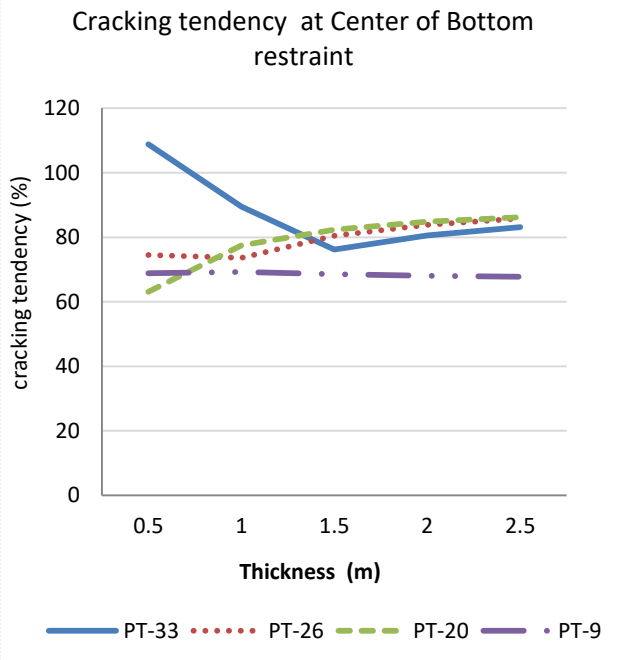

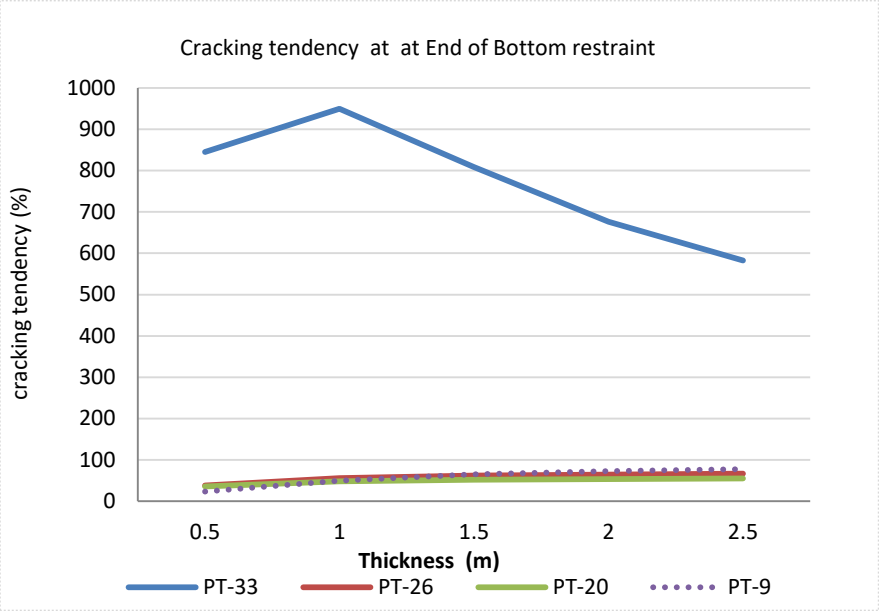

Figure4. 23 Cracking tendency by percentage at center core, center of side surface, center of top exposed surface and top corner of MW.

5. Conclusion and Recommendation

5.1 Conclusion

Surfaces of mass concrete structures are susceptible for cracking at high placement temperature and cracking tendency increase with an increase of placement temperature and size. Surface cracking is inevitable in hot weather unless precooling of concrete components is applied. In thick sections, precooling method should be combined with other temperature deferential controlling method (surface insulation) to significantly minimize surface early age cracking spatially in restraint conditions.

Similarly, thin sections of mass concrete have high tendency of early age cracking at core. This early age cracking tendency can significantly minimized by cooling concrete ingredients and reducing the placement temperature near to average air temperature. This means with very less effort of handling concrete materials at construction site and maintaining their temperatures about average air temperature cracking tendency of concrete at early age can be significantly minimize. In most construction sites, concrete materials are poorly handled and placement of temperature are higher than air temperature at casting by 5 ^{o}C as in a case of placement temperature in site experiment 1. Increasing of placement temperature significantly increase the cracking tendency of thin sections at core in hot weather condition. Generally, the following additional observations are noted:

- ✓ The cores of thin sections are more sensitive to ambient temperature than thick sections and this sensitivity is higher in low placement temperature.
- ✓ Placement temperature increases, both the maximum temperature and the maximum temperature difference increase.
- ✓ Maximum side surface temperatures were independent of thickness for given placement temperature except thin sections which are less than 2 m diameter in the case of Cylindrical axisymmetric and less than 0.5 m thick in the case of massive wall.
- ✓ The results also showed that percentage of temperature reductions were almost independent from the thickness of the structure. This conclusion is however only valid for Cylindrical axisymmetric mass concrete structures

and massive wall, where cases with 1.03 m, 2.06 m ,3.09, 4.12 m , 5.15 m diameter and massive wall case with 0.5 m, 1m, 1.5 m 2 m, 2.5 m were analyzed.

- ✓ Pre cooling method is effective in reduction of temperature differential but it was not effective to limit the maximum temperature differential between cores and surface below 20 ^{o}C in thick sections.
- ✓ The approach that a temperature differential limits (20 ^{o} C) provided by codes to minimize crack is very conservative majority of cases, in other cases it can be an overestimation of the allowable gradient. Because mass concrete can crack at early age by temperature differential below or above 20 ^{o} C based on the tensile strength development.
- ✓ Reduction of concrete placement temperature minimized the thermal shock effect and delayed form removal avoids the thermal shock at surface.

5.2 Recommendations

Concrete materials should be stored properly in shaded area in order to reduce their temperature and this significantly reduces the casting temperature of concrete. For thick sections precooling method should combined with other temperature differential controlling methods (e.g. surface insulation) to significantly minimize surface early age cracking tendency. In addition attention should be given during casting of the core of massive structures than side of structures.

Reference

[1] Concrete Information, " Concrete for Massive Structures ", Portland Cernent Association, 1987]

[2] Sanda Radovanovic, “THERMAL AND STRUCTURAL FINITE ELEMENT ANALYSIS” thesis submitted to University of Manitoba Winnipeg, Manitoba OF EARLY AGE MASS CONCRETE STRUCTURE, (1998)

[3] Bjøntegaard,. Basis for and practical approaches to stress calculations and crack risk estimation in hardening concrete structures – State of the art. (2011)

[4] Zhu Bofang, “Thermal Stresses and Temperature Control of Mass Concrete” China Institute of Water Resources and Hydropower Research and Chinese Academy of Engineering, 2014.

[5] Jan byforse, “Plain Concrete at early age”, Stockholm 1980.

[6] Hacona program for simulation of temperature and stress in hardening concrete, ola dahlblom and jonas lindemann, lund, sweden, may 2000.

[7] AC1 Cornmittee 207, "Mass Concrete ", AC1 207.1R-87 Manual of Concrete Practice, Part1

[8] Cooling and Insulating Systems for Mass Concrete Reported by ACI Committee 207 ACI 207.4R-93 (Reapproved 1998)

[9] Mang Tia, Chrstophor Feraro. Al. final report on “development of design parameters for mass concrete using finite element”.department of civil and costal engineering college of engineering, university of Florida. February 2.

[10] Abdol. R. chini Larry C. Al. “determination of maximum temperature and curing temperature to avoid durability problem and DEF, final report submitted to florida department of transportation. February 2003.

Appendix A

From relation between heat and temperature in adiabatic condition, temperature is given by

$$\text{Tad} = \frac{Qc*C}{\rho c*Cp} \text{.....I}$$

Where

$$Qc = 500\,\frac{kJ}{kg} = heat\ generation$$

$$C = 350\,\frac{kg}{m^3} = \ cement\ content\ per\ m^3$$

$$\rho c = 2400\,\frac{kg}{m^3} = concrete\ density$$

$$Cp = 1\ \frac{KJ}{kg\ o_C} = concrete\ heat\ capacity$$

$$\text{Tad} = \frac{500*350}{2400*1} = 72.9\ ^{o}\text{C}$$

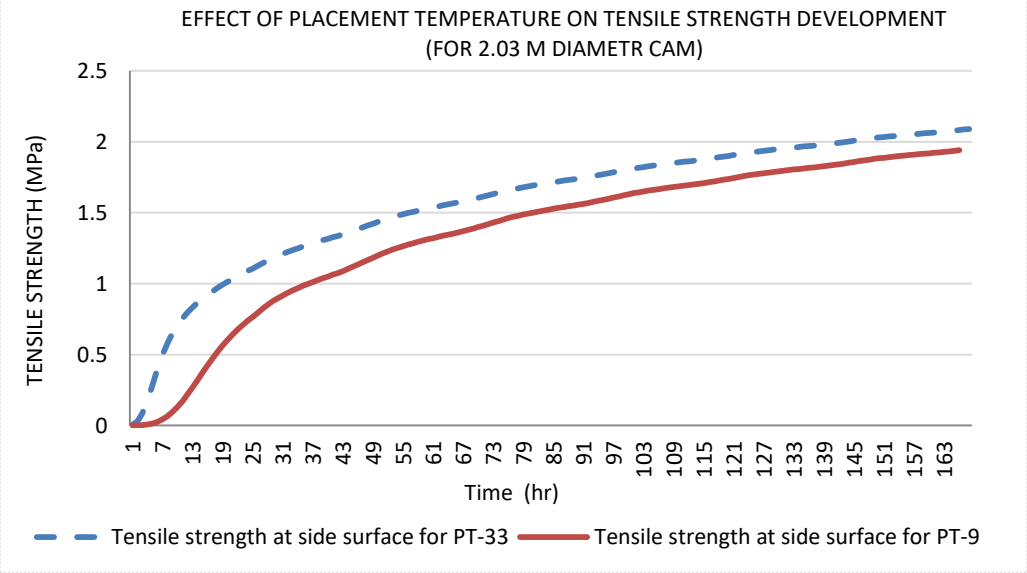

Figure A. 1 Tensile strength at side surface of 2.06 m diameter CAM for PT 33 and 9 ^{o}C

Appendix B

1. Measured temperature history and simulation results of reference field concrete Blocks

RCB -1

1.1 Degree of hydration, and strength **development of** RCB-**1(PT-33**)

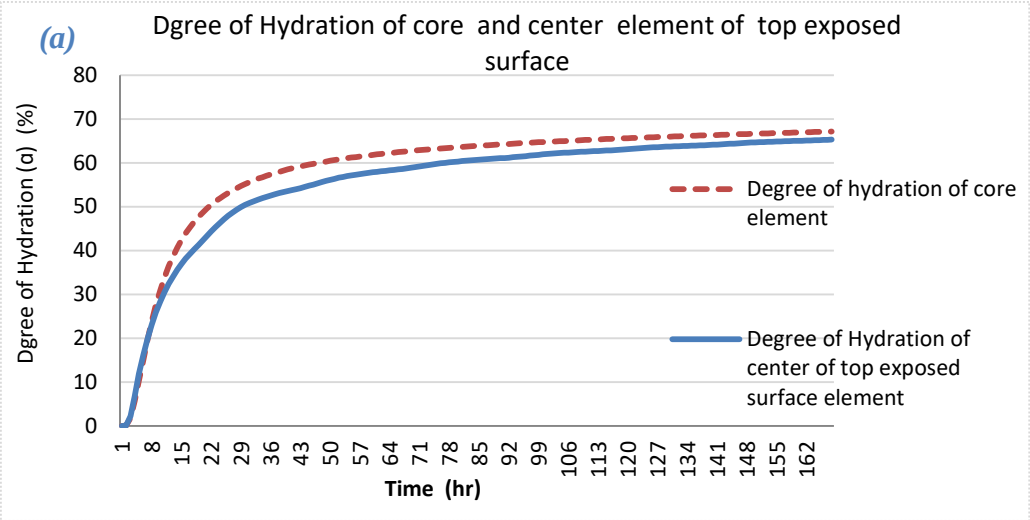

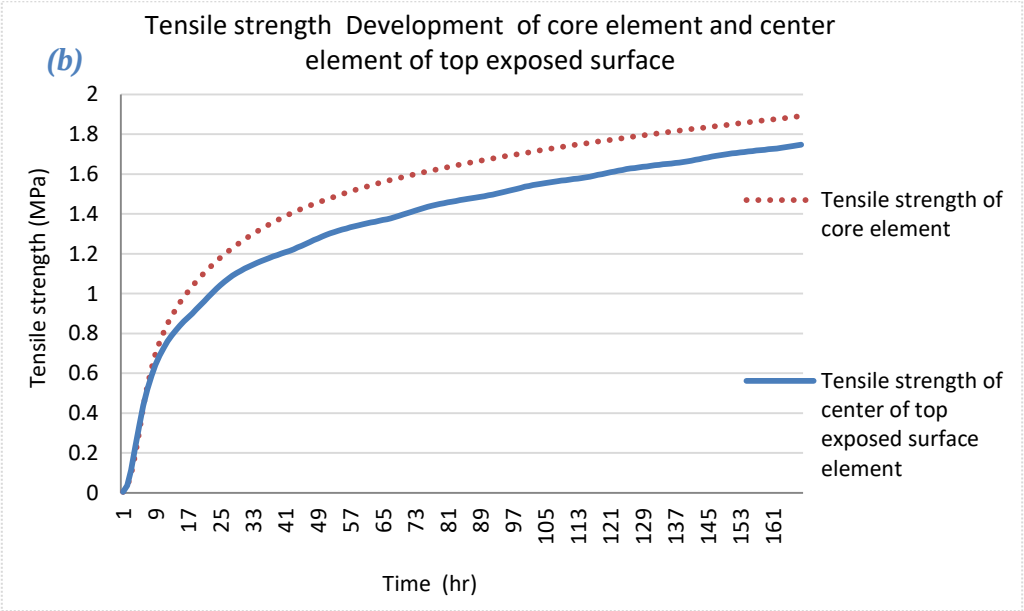

Figure B. 1 (a) Degree of hydration, (b) tensile strength Development of RCB-1 at core and top exposed surface for PT-33

1.2 Stress history

Block 1- Placement temperature (PT- 33 ^{o} C)

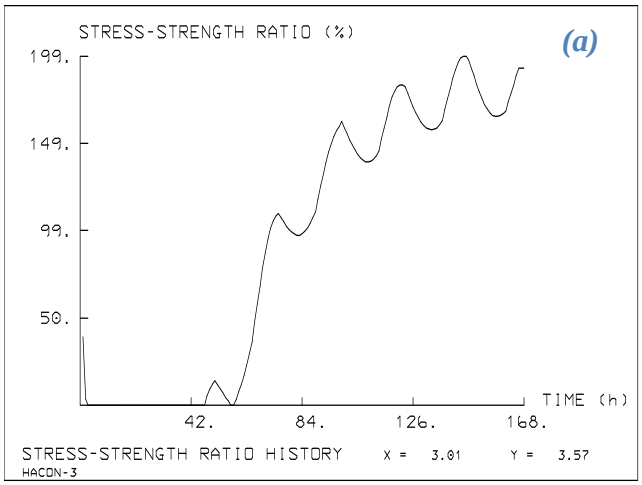

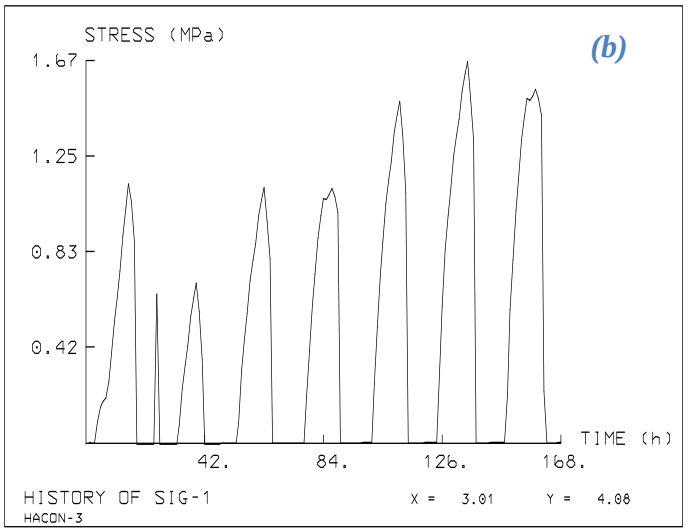

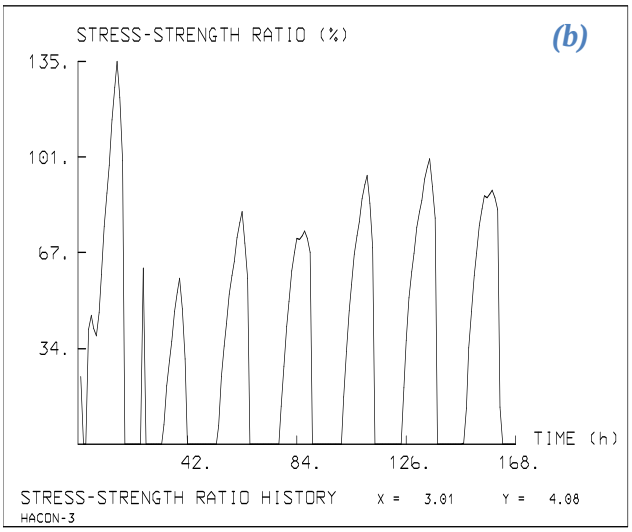

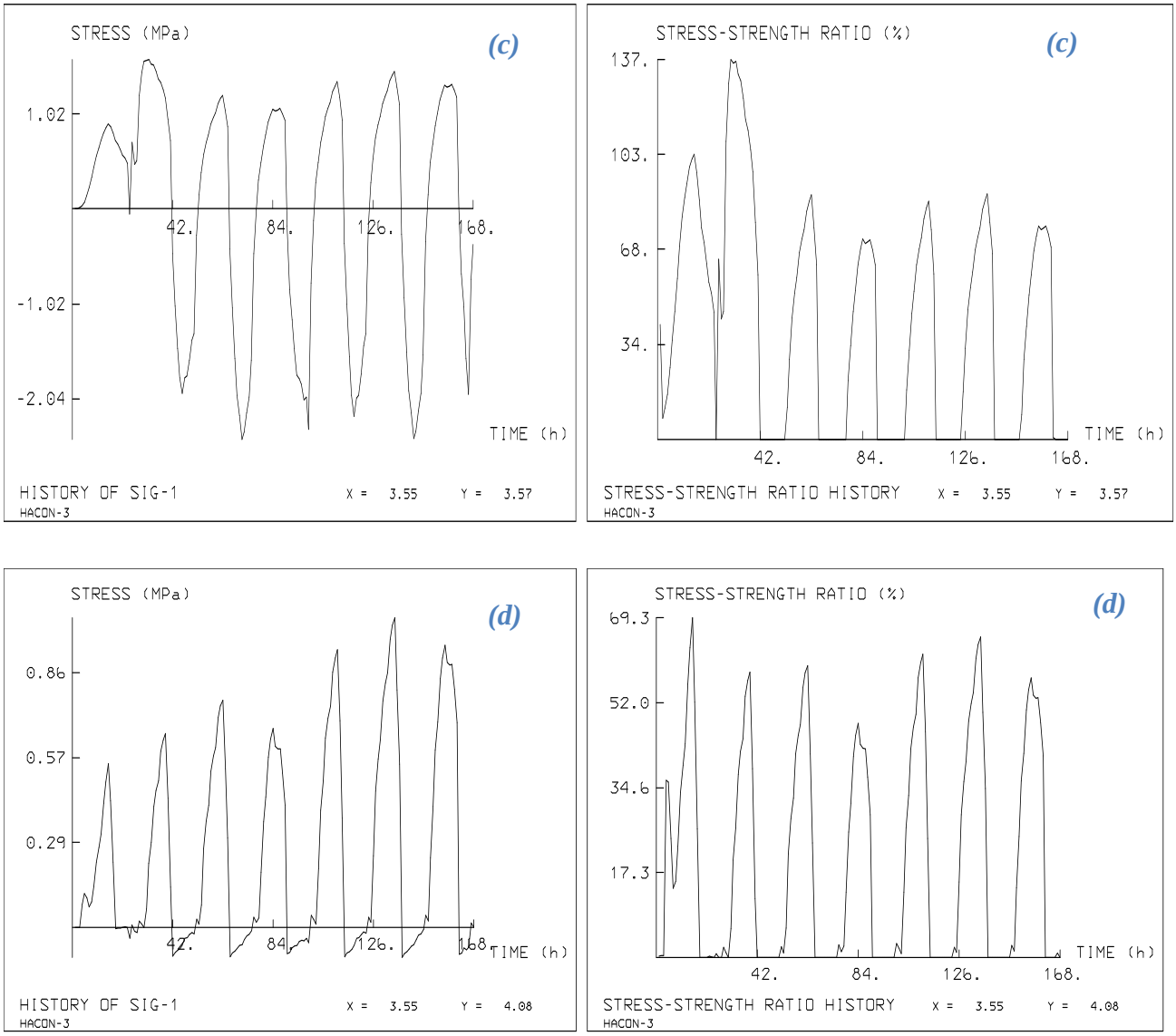

Figure B. 2 Stress history of RCB-1 PT-33 at (a) core, (b) top exposed surface, (c) side surface (d) top corner.

2. Simulated results of analytic models of CAM and MW.

2.1 Maximum temperature of CAM

Diameter (Thickness) (m)	Maximum center of side surface Temperature (^{o} C)				Maximum Center Core Temperature (^{o} C)			
	PT-33	PT-26	PT-20	PT-9	PT-33	PT-26	PT-20	PT-9
1.03	49.85	46.50	43.41	42.38	61.22	54.33	49.67	44.29
2.06	56.27	50.95	45.84	44.24	74.73	67.31	61.15	51.46
3.09	56.59	51.12	45.90	44.48	80.16	72.66	66.29	55.47
4.123	56.64	51.15	46.03	44.46	83.12	75.67	69.28	58.01
5.15	56.68	51.18	46.07	44.46	85.04	77.64	71.27	59.55

Table B. 1 *Maximum Center Core and center of side surface temperature of CAM with different thickness and placement temperature*

(Thickness)(m) Diameter	Maximum Center of top exposed surface Temperature (^{o} C)				Maximum top Corner point Temperature (^{o} C)			
	PT-33	PT-26	PT-20	PT-9	PT-33	PT-26	PT-20	PT-9
1.03	51.33	49.77	48.31	44.88	46.22	45.85	45.85	45.90
2.06	52.60	50.64	48.78	44.51	46.45	46.34	46.26	46.14
3.09	52.63	50.66	48.79	44.72	46.47	46.36	46.28	46.15
4.123	52.63	50.66	48.79	44.72	46.49	46.38	46.29	46.16
5.15	52.63	50.66	48.79	44.72	46.52	46.41	46.32	46.18

Table B. 2 Maximum Center enter of top exposed surface and top Corner point temperature of CAM with different thickness and placement temperature.

2.2 Maximum temperature of MW

(a)	Maximum Temperature at center of side surface (^{o}C)				Maximum Temperature at Center Core (^{o}C)			
Thickness (m)	PT-33	PT-26	PT-20	PT-9	PT-33	PT-26	PT-20	PT-9
0.5	52.69	48.51	44.60	41.74	56.64	51.19	47.03	38.94
1	56.72	51.35	46.22	44.11	68.55	61.44	55.32	45.25
1.5	56.91	51.46	46.25	44.58	73.90	66.34	59.81	49.40
2	56.91	51.46	46.28	44.58	77.54	69.93	63.44	52.56
2.5	56.91	51.46	46.30	44.56	79.89	72.34	65.90	54.81

(b)	Maximum Temperature at Center of top exposed surface (^{o}C)				Maximum Temperature at center of Bottom restraint (^{o}C)			
Thickness (m)	PT-33	PT-26	PT-20	PT-9	PT-33	PT-26	PT-20	PT-9
0.5	48.57	47.58	46.66	44.53	28.48	27.46	26.64	25.42
1	51.53	49.88	48.33	44.65	36.25	34.01	32.32	29.63
1.5	52.40	50.51	48.72	44.44	41.23	38.60	36.40	32.78
2	52.58	50.64	48.78	44.47	45.24	42.27	39.74	35.38
2.5	52.62	50.65	48.78	44.66	48.26	45.03	42.26	37.35

Table B. 3 Maximum Temperature at (a) center of side surface and Center Core;(b) Center of top exposed surface and center of Bottom restrain.

2.3 Maximum temperature differential reduction by percentage

A	maximum temperature deferential reduction at Top exposed Surface			maximum temperature differentials reduction at Top corner			
Thickness(m)	PT-26 ^{o}C	PT-20 ^{o}C	PT-9 ^{o}C	Thickness(m)	PT-26 ^{o}C	PT-20 ^{o}C	PT-9 ^{o}C
1.03	21.3%	30.5%	38.8%	1	12.6%	18.8%	28.5%
2.06	11.8%	20.5%	34.0%	2	13.6%	25.6%	41.1%
3.09	13.3%	24.5%	41.0%	3	12.5%	23.7%	40.1%
4.123	11.8%	21.8%	40.4%	4	11.5%	21.5%	38.9%
5.15	11.9%	22.3%	42.3%	5	11.3%	21.2%	40.2%

B	Maximum temperature deferential reduction at center of Side Surface reduction		
Thickness(m)	PT-26 °C	PT-20 °C	PT-9 °C
1.03	8.2%	14.8%	25.0%
2.06	14.0%	24.0%	41.2%
3.09	13.1%	24.0%	40.6%
4.123	11.7%	21.7%	40.3%
5.15	11.9%	22.3%	42.2%

Table B. 4 Maximum temperature deferential reduction at (a) Top exposed surface and top corner (b) at center side surface.

2.4 Maximum stress for early form removal case of CAM

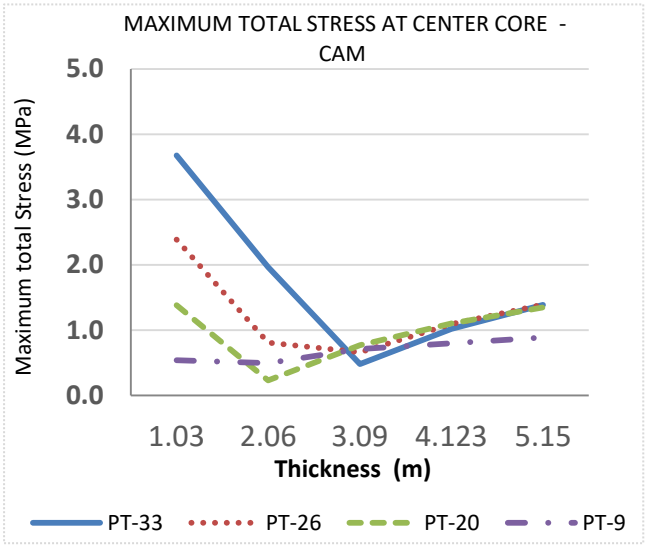

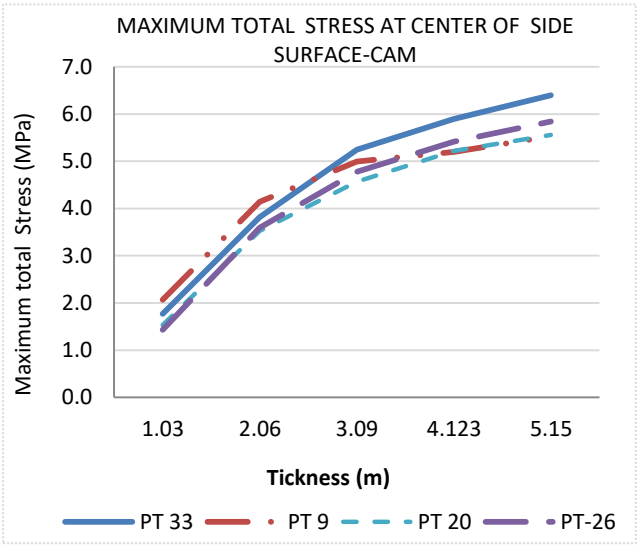

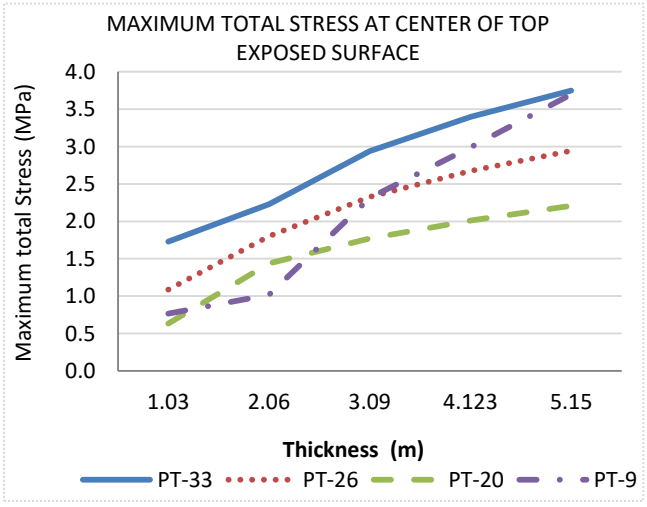

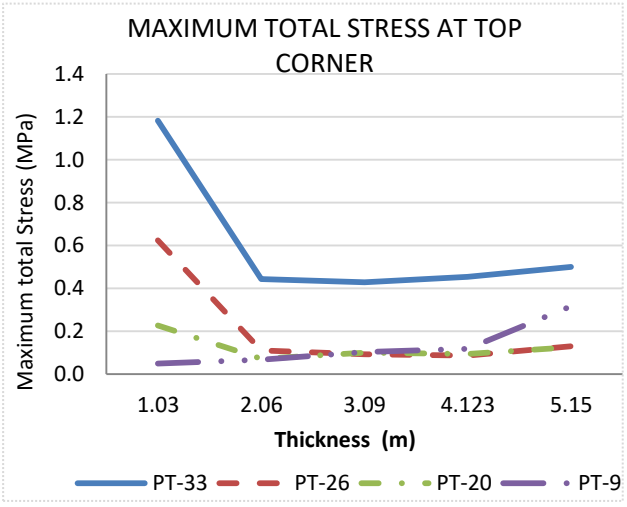

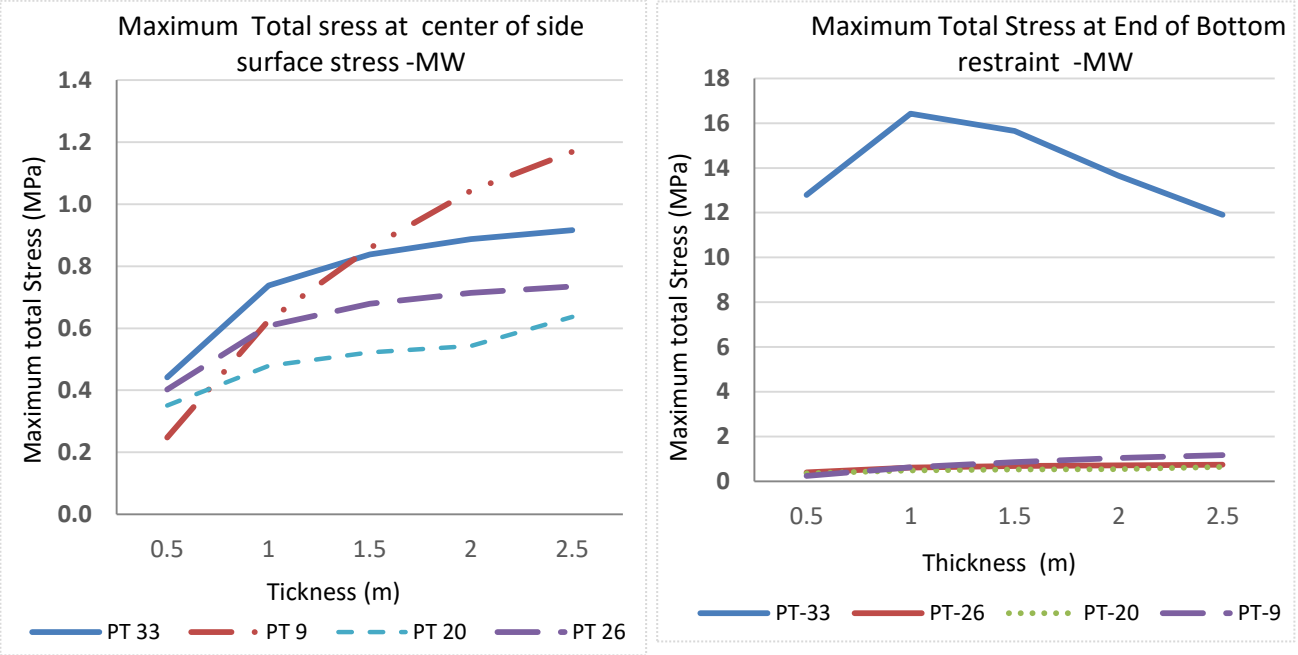

Figure B. 3Maximum total stress at center core, center of side surface, center of top exposed surface and top corner of CAM for early form removal case

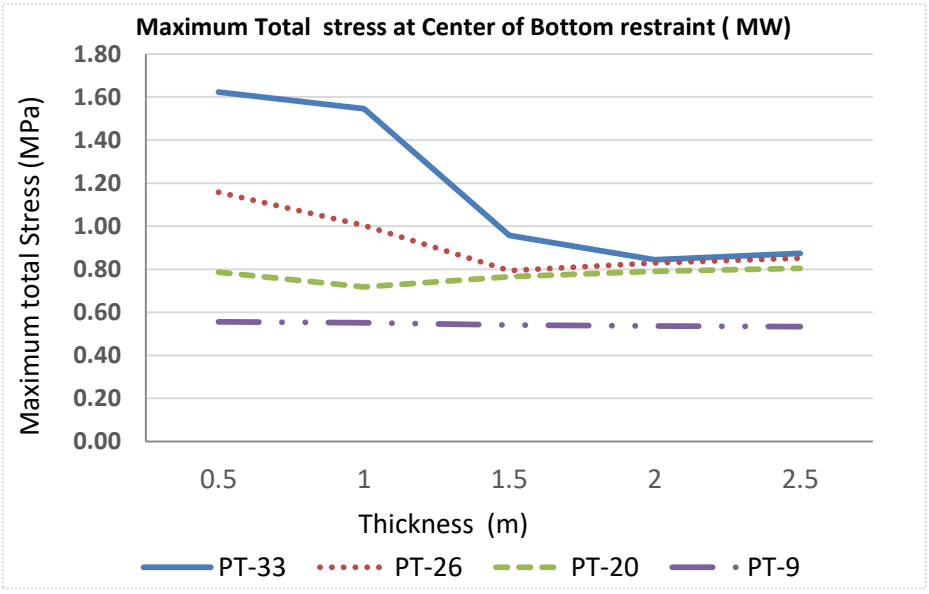

Figure B. 4 *Massive wall Maximum total stress at center of bottom restraint*

2.5 Cracking tendency of CAM for early age form removal case.

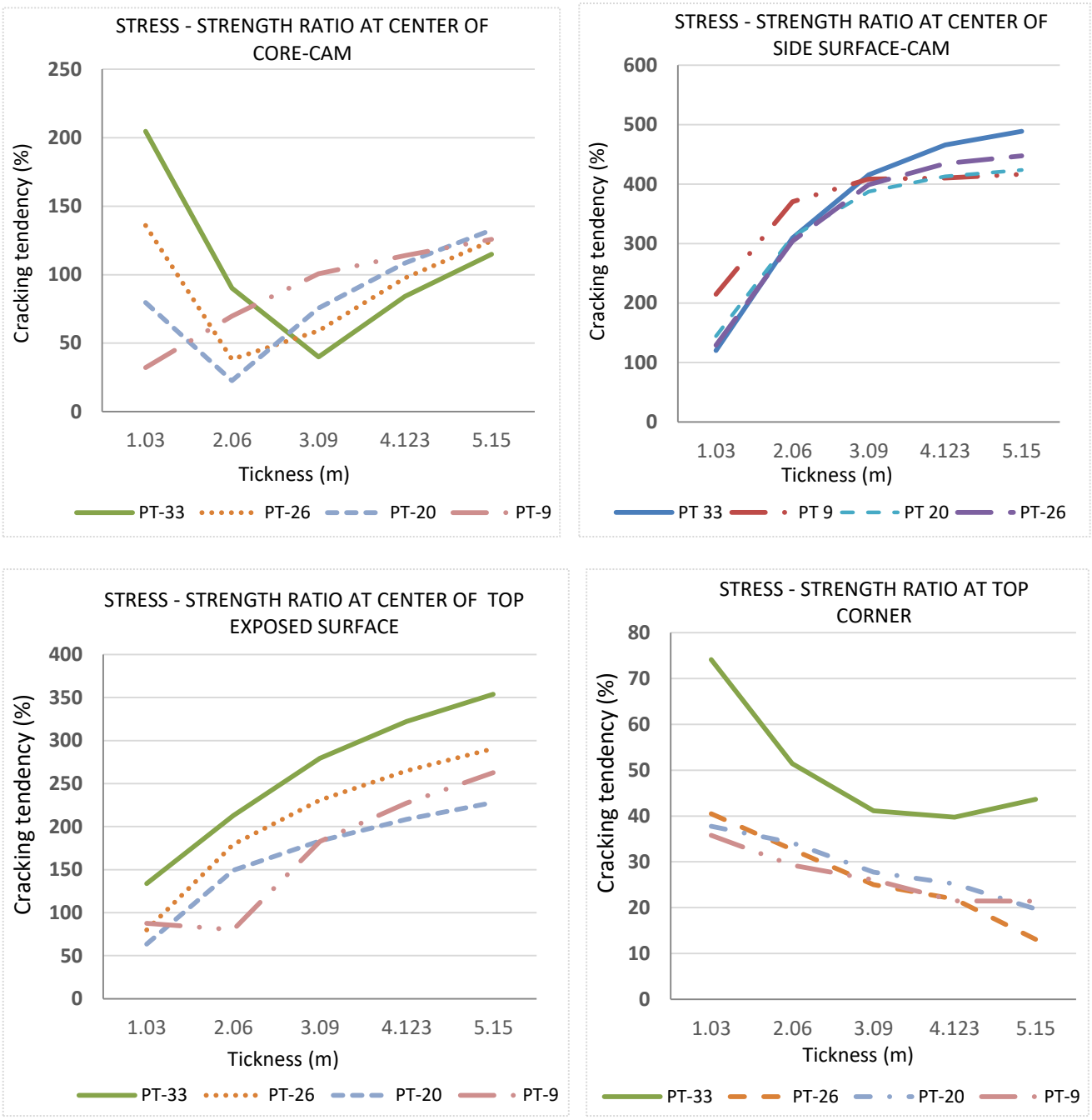

Figure B. 5 Cracking tendency of CAM at center of core, side ,top exposed surface and top corner for early age form removal case.

A	Maximum stress reduction at side Surface				Maximum stress reduction at core			
Thickness(m)	PT-26	PT-20	PT-9		Thickness(m)	PT-26	PT-20	PT-9
1.03	18.9%	13.2%	-16.9%		1	35.1%	62.4%	85.4%
2.06	5.7%	7.6%	-6.9%		2	59.0%	88.3%	74.9%
3.09	9.0%	12.9%	4.8%		3	-36.8%	-59.4%	-46.9%
4.123	8.2%	11.5%	11.8%		4	-7.1%	-8.5%	21.4%
5.15	8.7%	13.2%	13.5%		5	-0.3%	2.9%	36.3%

B	Maximum stress reduction top exposed Surface				Maximum stress reduction at top corner			
Thickness(m)	PT-26	PT-20	PT-9		Thickness(m)	PT-26	PT-20	PT-9
1.03	37.0%	63.5%	55.7%		1	47.2%	80.8%	95.9%
2.06	13.0%	24.0%	36.8%		2	75.2%	83.9%	81.8%
3.09	20.9%	39.8%	21.3%		3	78.3%	76.8%	75.9%
4.123	21.3%	40.8%	12.0%		4	81.1%	79.4%	74.2%
5.15	21.4%	41.1%	1.4%		5	74.1%	75.1%	36.8%

Table B. 5 Maximum stress reduction for early age form removal of CAM at center of core, side ,top exposed surface and top corner

(A)

Maximum stress reduction at center side					Maximum stress reduction at center core			
Thickness(m)	PT-26	PT-20	PT-9		Thickness(m)	PT-26	PT-20	PT-9
1.03	29.6%	22.2%	-20.9%		1	43.8%	73.0%	88.4%
2.06	24.9%	26.5%	-7.5%		2	-125.4%	-81.6%	-401.1%
3.09	27.2%	29.0%	4.9%		3	8.9%	-4.0%	-13.2%
4.123	28.2%	32.2%	10.6%		4	21.4%	22.0%	33.9%
5.15	28.8%	33.6%	32.2%		5	24.6%	28.6%	55.5%

(B)

Maximum stress reduction at center of top exposed surface					Maximum stress reduction at corner point			
Thickness(m)	PT-26	PT-20	PT-9		Thickness(m)	PT-26	PT-20	PT-9
1.03	57.0%	63.4%	49.8%		1	70.1%	95.3%	94.5%
2.06	41.4%	53.8%	58.4%		2	75.0%	83.7%	82.1%
3.09	41.7%	56.3%	27.6%		3	75.1%	73.5%	72.5%
4.123	41.5%	56.7%	4.9%		4	82.4%	80.9%	77.5%
5.15	41.1%	56.6%	26.1%		5	81.8%	80.7%	71.5%

Table B. 6Maximum stress reduction for delayed form removal of CAM at center of core, side, top exposed surface and top corner.